THE ROLE OF FLUORINE IN ENERGETIC MATERIALS, AND ITS IMPACT ON LONG RANGE COUPLING CONSTANTS AND S_N2 – E2 REACTIONS

By

HENRY MARTINEZ

A DISSERTATION PRESENTED TO THE GRADUATE SCHOOL
OF THE UNIVERSITY OF FLORIDA IN PARTIAL FULFILLMENT
OF THE REQUIREMENTS FOR THE DEGREE OF
DOCTOR OF PHILOSOPHY

UNIVERSITY OF FLORIDA

2011

To my family

ACKNOWLEDGMENTS

I would especially like to thank my supervisor, Dr. William R. Dolbier, for not only giving me the opportunity to work with him but also for supporting my ideas. He is a true example of what a great scientist should be – hard worker, honest and a great professor. I hope one day to be half of what he is. I also want to thank all of the committee members for their suggestions, time and kindness.

I want to thank my mom for always being there for me, for believing in me, and for not giving me everything I wanted, but instead, teaching me how to get things myself. Thanks for being the greatest mom ever and caring so much about me. I will work really hard to make you proud every day. Thank you, mom, for bringing into my life my brother Felipe and my sister Veronica; they are one of the reasons why I want to wake up every day; they are the fuel my heart uses to continue running without stopping. I also want to thank my Godparents, Nancy and Efrain, for believing in me and supporting me unconditionally. There is not a way for me to describe how thankful I am for both of you. To Alexander, my brother, thank you for always being there for me; you are the best friend everyone wishes to have. To my grandmother, Stella, thank you for teaching that everything is possible, and I just have to work hard for it. Thank you, grandma, for protecting me the way you did until the last day of your life. To my entire family, my Aunt Rosa, my Uncle Carlos, all my cousins, Erick, Vanessa, Fernanda, Dalhia, Adriana, Juan Carlos and Johanna, and to my Goddaughter, Sofia, thank you all for being part of my life.

To my exceptional wife, Paula, thank you for caring so much about me, for always giving me your best, your understanding, your trust and unconditional love. I am the luckiest guy on earth for having you.

To all my friends, especially Lianhao Zhang, thank you all for the great times, discussions and help. I hope I live enough to return all their kindness and care.

Finally, last but not least, I want to thank God for bringing to my life every person I just mentioned and for giving me everything I needed to complete this journey. Without Him I would not have reached this stage of my life.

TABLE OF CONTENTS

page

LIST OF TABLES

LIST OF FIGURES

LIST OF SCHEMES

Abstract of Dissertation Presented to the Graduate School
of the University of Florida in Partial Fulfillment of the
Requirements for the Degree of Doctor of Philosophy

THE ROLE OF FLUORINE IN ENERGETIC MATERIALS, AND ITS IMPACT ON LONG RANGE COUPLING CONSTANTS AND S_N2 – E2 REACTIONS

By

Henry Martinez

December 2011

Chair: William R. Dolbier, Jr
Major: Chemistry

The role of fluorine has been investigated in three different areas: 1) energetic materials, 2) long range coupling constants and 3) bimolecular substitution and elimination reactions.

High fluorine content can enhance the properties of energetic materials. It was demonstrated that the presence of an SF_5 substituent within energetic compounds serves to increase their density while diminishing their shock sensitivity, which when combined with other favorable properties of aminofurazans produces a new class of high density- high performance energetic materials. Thermogravimetric analyses (DSC/TGA) as well as qualitative sensitivity tests indicated an improvement in the energetic properties of these new materials. The high fluorine content, combined with low hydrogen content and the presence of sulfur may allow these compounds to release “free fluorine” upon detonation, which could allow such high-energy, SF_5-containing furazan derivatives to be useful in combating chemical and biological weapons.

Through space coupling of fluorines comprises an interesting aspect of ^{19}F NMR spectrum. The ^{19}F NMR spectrum of new monosubstituted

perfluoro[2.2]paracyclophanes display unusual ^{19}F-^{19}F coupling patterns (^{4}J and ^{5}J) that suggest a skewed geometry in which the upper deck moves towards or away from the substituent. Quantum chemical calculations were performed at the HF/6-311+G(d,p)//B3LYP/EPR-III level of theory using Gaussian 03, and they shed light on the unusual structures and coupling of F8 and its derivatives. $^{4}J_{FF}$ coupling constants were found to be transmitted through the space by direct contact between the electron cloud of the interacting nuclei, while $^{5}J_{FF}$ coupling constants were also found to be transmitted through the space, but with help of an intermediate moiety that relays the spin polarization from one fluorine to the other.

Finally, a measure of the quantitative effect of proximate fluorine substituents on the rates of S_N2 and E2 reactions has been obtained through a study of reactions on fluorinated *n*-alkyl bromides with a weak base, strong nucleophile azide ion and strong base/nucleophile methoxide ion in the protic solvent methanol and the aprotic solvent, DMSO. The order of reactivity for S_N2 reactions of azide in methanol at 50^{o}C was found to be: *n*-alkyl-Br > *n*-alkyl-CHFBr > *n*-perfluoroalkyl-CH_2CH_2Br >> *n*-perfluoroalkyl-CH_2Br > *n*-alkyl-CF_2Br. The order of reactivity for E2 reactions was found to be: *n*-perfluoroalkyl-CH_2CH_2Br >> *n*-alkyl-CF_2Br > *n*-alkyl-CHFBr > *n*-alkyl-Br. Quantum chemical calculations support and help to understand these orders of reactivity.

CHAPTER 1
INTRODUCTION

An Overview of Fluorine in Organic Chemistry

Over the last few decades, fluorine chemistry has become a well recognized and important field. Nowadays it is not only possible to find books in the general organo-fluorine area, but also in more specialized areas such as medicinal fluorine chemistry, bio-organic fluorine chemistry, fluorine in agrochemicals, and fluorine nuclear magnetic resonance, among others.

The carbon fluorine bond is the shortest single bond involving carbon (D) (~1.47Å) other than C-H and the bond dissociation energy (BDE) is the largest (the CH_3X BDE is 99, 85, 71, 83, 86 and 110 kcal/mol for H, Cl, Br, C, O and F respectively). The inclusion of fluorine within organic molecules enhances the physical, chemical, and biological properties of the resulting organo-fluorine compounds. The small size and high electronegativity of fluorine not only make the C-F bond the strongest bond to carbon, but also create more polarized and hydrophobic molecules than those with a C-H or another C-halogen bond, properties that are important in the medicinal chemistry field.[1,2]

Fluorine, like any other halogen, behaves as an electron withdrawing group, but it is also capable of electron donation by use of its electron lone pairs. The electron withdrawing ability of fluorine occasionally leads to unexpected conformations. For example, the fluorines in 1,2-difluoroethane were expected to be in an anti-periplanar conformation in order to minimize the repulsive interactions between the lone pairs of the fluorines in the gauche conformation (Figure 1-1). Instead the latter conformation is

approximately 1 kcal/mol more stable than the former. Although the repulsive interactions in the gauche conformer must exist, the stabilization by the

Anti-periplanar Gauche

Figure 1-1. Possible conformations for 1,2-difluoromethane.

hyperconjugative interactions between the donor $\sigma_{(CH)}$ and the acceptor $\sigma^*_{(CF)}$ orbitals is greater than the destabilization from the electron-electron repulsive interaction between the fluorines. The hyperconjugative interaction between $\sigma_{(CH)} \rightarrow \sigma^*_{(CF)}$ orbitals also plays an important role in the stabilization of negative charges β to the fluorine(s). In contrast, positive charges are destabilized by fluorines at the β position, but stabilized by α-fluorines due to the electron donation of the lone pairs.[1]

The properties of organo fluorine compounds lead to many different applications (Figure 1-2). One of the most interesting applications of fluorine is found in the medicinal chemistry field, since the introduction of fluorine frequently enhances the biological activity of a substrate. One reason for this derives from the increment on the dipole moment and lipophilicity of the molecule upon introduction of the fluorine.

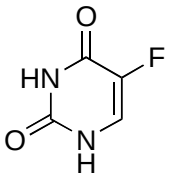

5-Fluorouracil
(Anti-cancer)

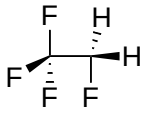

1,1,1,2-Tetrafluoroethane - HFC 134a
(Car air conditioner refrigerant)

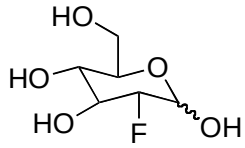

^{18}F-2-Fluorodeoxyglucose
(PET scanning agent)

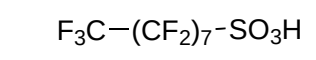

Perfluorooctanesulfonic acid
(Fluorosurfactant)

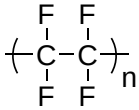

Teflon

Figure 1-2. Examples of organo fluorine compounds in different areas of application.

Polymer chemistry is another area where fluorine plays an important role. Fluoro polymers are greatly benefited by the available electron lone pairs in the fluorine, which produce interesting surface properties that find applicability as water and hydrocarbon repellant. These properties combine with the generally high thermal and chemical stability of the organo-fluorine compounds produce remarkable fluoro polymers such the widely known polytetrafluoroethylene – Teflon.[2]

Despite all the special properties that fluorine can bring to a molecule, the introduction of fluorine into an organic compound it is not only a challenging task, but occasionally can be dangerous as well. Fortunately, the rapid growth of the field of organo fluorine chemistry generally allows the avoidance of reactive and toxic compounds such as F_2, HF or SF_4 for most syntheses. For instance, the addition of fluorine to aromatic rings, double bonds, carbanions and other similar functionalities can be done using commercially available electrophilic fluorinating agents such as *N*-fluoromethansulfonimide (NFOBS) or 1-chloromethyl-4-fluoro-1,4-diazoniabicyclo [2.2.2] octane bis-tetrafluoroborate (Selectfluor), among other electrophilic fluorinated reagents (Figure 1-3).[3]

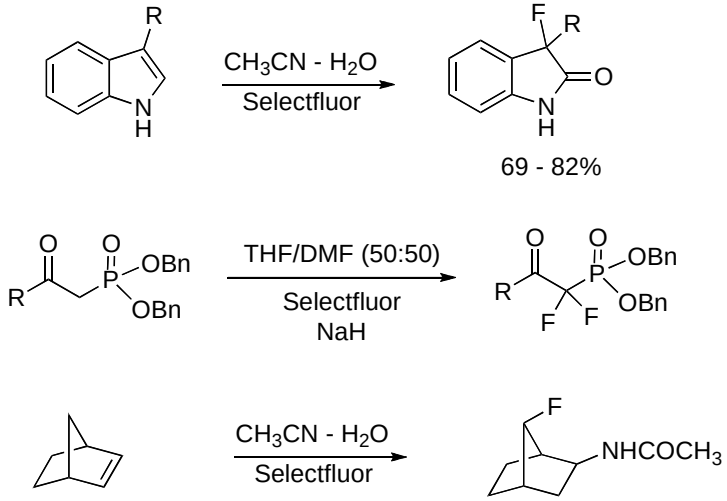

Figure 1-3. Examples of reactions with the electrophilic fluorine reagent, Selectfluor.

Similarly, nucleophilic fluorine is also accessible through different commercially available reagents such as KF, CsF, tetrabutylammonium fluoride (TBAF) or relatively safe solutions (some ionic liquids) such as pyridine-HF, triethylamine-HF, and THF-HF. Anhydrous conditions are always an aspect of importance when nucleophilic fluorine is needed since its nucleophilicity is diminished by the presence of water. Highly anhydrous highly-nucleophilic fluoride can be obtained at -35^{o}C by the reaction between hexafluorobenzene and tetrabutylammonium cyanide, which lets reactions to run at room temperature with short reaction times in contrast to the usually harsh conditions required when using other sources of fluorine (Figure 1-4).[4,5] Any trace of water present in the solvent would react with the cyano groups at the hexafluorocyanide to form other derivatives, making the system highly anhydrous. It is important to mention that fluorine under extremely anhydrous conditions (naked fluorine) can also behave as an excellent base.

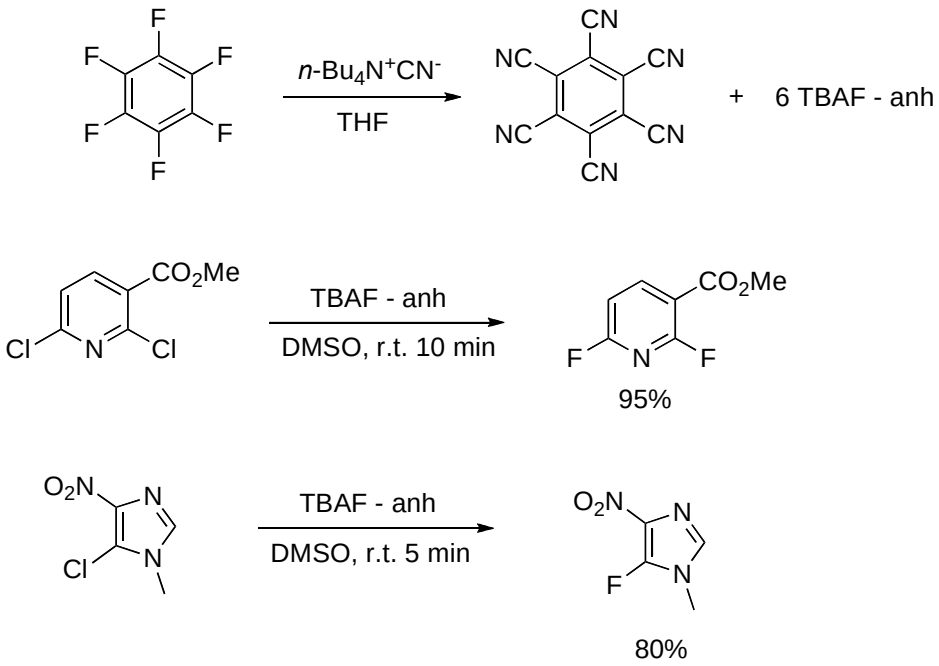

Figure 1-4. Synthesis and reactions of tetrabutylammonium fluoride anhydrous.[5]

The most important fluorinations mediated by transition metals generally involve palladium, silver and copper; however, many of these organo-metallic reactions have proved to be very challenging and are still under study since only very few of these methods use a catalytic amount of the transition metal and are usually limited by the presence of other functional groups (Figure 1-5).[6-9]

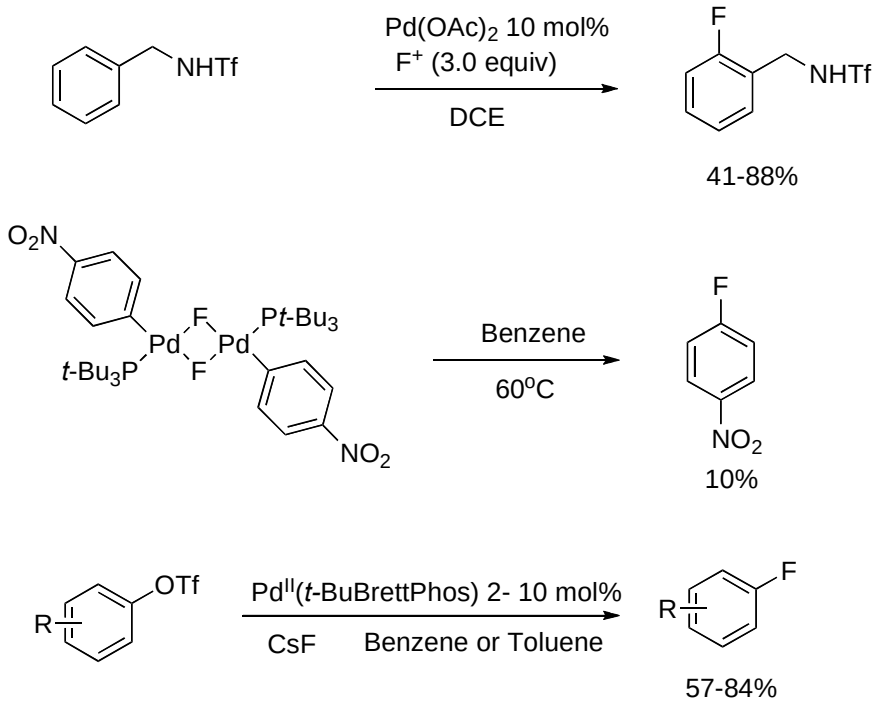

Figure 1-5. Fluorinations mediated by Palladium.[8,9]

Transformation of alcohols, ketone/aldehydes and carboxylic acids to mono-, di-, and trifluoromethyl groups, respectively, has become a common method for the generation of fluoro-organic compounds. The synthesis of such materials can be accomplished by deoxofluorinating reagents such as diethylaminosulfur trifluoride (DAST) and the recently developed 4-tert-butyl-2,6-dimethylphenylsulfur trifluoride (FLUOLEAD) (Figure 1-6). [10]

Although the synthesis of organo fluorine compounds can be a challenging task, new and improved reagents allow the non-fluorine chemist to incorporate fluorine into

their molecules using a large number of safe methodologies, as shown previously. Several other methodologies for the inclusion of fluorine into organic molecules, such as difluorocarbenes, trifluoromethyl anions, perfluororadicals, among others, can be found extensively in the literature and other specialized fluorine synthetic books. The difficulties of those reactions increase with the complexity of the molecule, but most general methodologies are widely described in the literature.

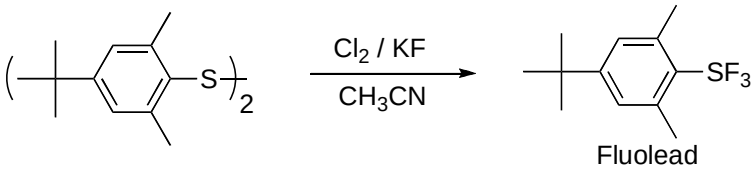

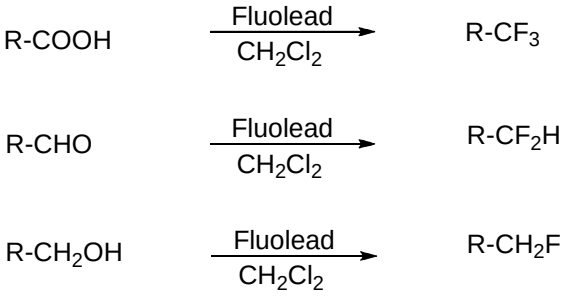

Figure 1-6. Synthesis and reactions of deoxoflorinated reagent, Fluolead.

Fluorine as Pentafluorosulfanyl Group

The pentafluorosulfanyl group has received a lot of recent attention due to its analogy with the trifluoromethyl group. It is considered the "super CF_3" of the millenium. The pentafluorosulfanyl group has two types of fluorine (axial and equatorial, AB4 system) due to the octahedral configuration of the sulfur (Figure 1-7). The S-F bond length (~1.54Å) is almost the same for both the axial and the equatorial fluorines, but generally the axial is slightly shorter than the equatorial and the angle between the two types of fluorines is about 90^o (~89.5^o). The average C-S bond length is 1.73Å when

the carbon has no other fluorine attached. However, if one or more fluorines are attached, the C-S bond length can be as high as 1.91Å.[11]

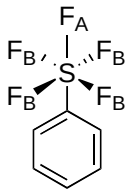

Pentafluorosulfanyl benzene
AB4 System

Figure 1-7. AB4 system in the pentafluorosulfanyl group.

The pentafluorosulfanyl group (SF_5) has a larger size than the CF_3 group (closer to a *tert*-butyl group), but due to the larger amount of fluorines, the SF_5 group is more lipophilic, with the hydrophobic value (π) for the SF_5 being 1.51 vs. 1.09 for the CF_3 group. The higher electron withdrawing ability ($\sigma(SF_5)=0.68$ vs. $\sigma(CF_3)=0.54$) brings a larger dipole moment to the organic molecules.[12] When compared with the CF_3 group or non-fluorinated compounds, the pentafluorosulfanyl group generally introduces a higher chemical and thermal stability to the organic material.[13] All these properties make the pentafluorosulfanyl potentially useful in agrochemicals, pharmaceuticals, liquid crystals, polymers and energetic materials, among others (Figure 1-8).[12,14-18]

The differences in the physical properties of the trifluoromethyl and the pentafluorosulfanyl group result in an improvement in the properties of the material. For example, when the trifluoromethyl is “replaced” by the pentafluorosulfanyl group, the liquid crystal in Figure 1-8 has an increment in the dielectric anisotropy from 13.0 (CF_3) to 14.3 (SF_5). Similar improvement is seen in the energetic material (Figure 1-8), where the pressure of detonation has an increment of 1.67 GPa.[15,18]

Despite all the benefits that the pentafluorosulfanyl group can bring to organic molecules since its first appearance in the literature by Case and co-workers[19] the

introduction of this group has generally been difficult, and the development of new synthetic methods is an active research area.

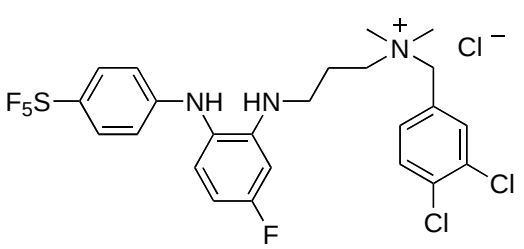

Medicinal chemistry

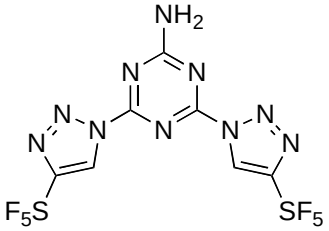

Energetic Material

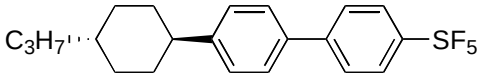

Liquid crystal

Figure 1-8. Examples of SF_5- Organic compounds with different applications.

The synthesis of pentafluorosulfanyl compounds has been accomplished by various approaches. The reaction between thiols or disulfides with CoF_3, AgF_2 or elemental fluorine (F_2) generates the pentafluorosulfanyl group. Relatively milder conditions include the reaction of thiols or disulfides with chlorine and KF; however, the several by-products and generally harsh conditions of these reactions make them impractical.[11]

One of the most common methods for the introduction of the pentafluorosulfanyl group is through the commercially available pentafluorosulfanyl chloride (SF_5-Cl), which can be prepared from SF_4, Cl_2 and CsF in an autoclave.

The reactions of SF_5Cl are limited to free radical chemistry, and its addition to double and triple bonds was initially carried out in an autoclave. In 2002, Dolbier reported the radical addition of SF_5Cl in solution at low temperature using Et_3B as a radical initiator, and high yields were obtained (Figure 1-9). This new methodology is more accessible to regular organic chemists, is regiospecific, works with both double

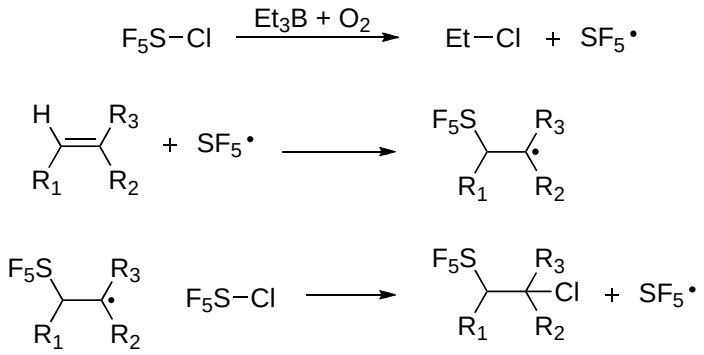

Figure 1-9. Radical addition of SF_5Cl to double bonds using Et_3B at -30^oC.

and triple bonds, reduces the amount of SF_5Cl needed to complete the reaction, allows smaller scale reactions, and decreases the number of by-products.[20] The only limitation presented in this methodology is the addition to α, β- unsaturated carbonyl compounds, where the radical polymerization controls the reaction. This methodology presently remains the most important to generate aliphatic SF_5-building blocks and final molecules (Figure 1-10).[21-23]

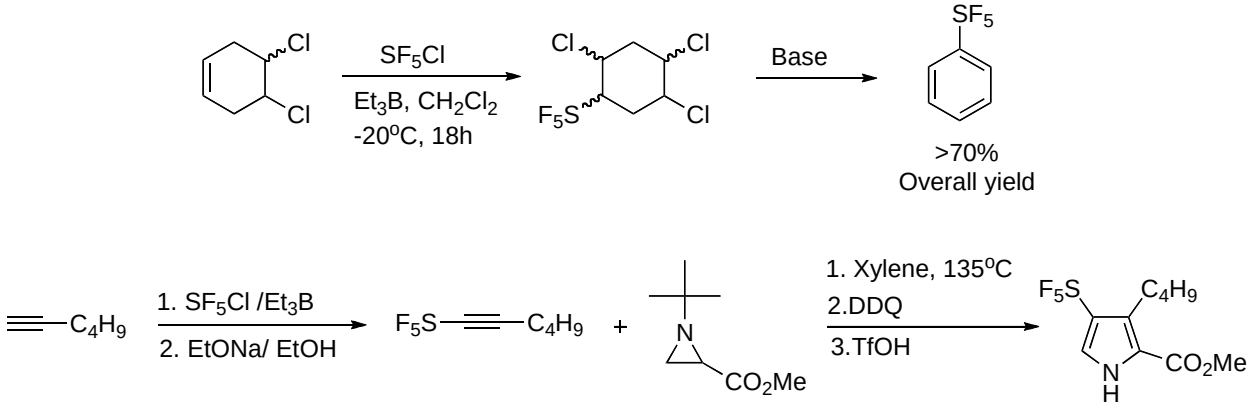

Figure 1-10. Examples of synthesis of SF_5 organic compounds.

Fluorine and Pentafluorosulfanyl Group in Energetic Materials

After the Second World War, research in energetic materials increased substantially. The synthesis, and the chemical and physical properties of such compounds have become better known and understood since then. The continued

increase of chemical and biological weapons (CW/BW) requires the development of new mechanisms of defense.[24]

By definition, an energetic material is a compound or a mixture of compounds that, after an initiation process, undergo very rapid self-propagating decomposition, producing gases at tremendous pressure and with the evolution of a lot of heat. The temperature can reach up to 6000 K and the pressure up to 40 GP.[25]

The performance of an energetic material is mainly evaluated by the type of products formed, the energy released, the pressure and speed of detonation, and the thermal and chemical stability of the material. The carbon-oxygen balance (OB) as well as the density are directly related to the performance. According to the semi-empirical equations developed by Kamlet and Jacobs, the square of the density is directly proportional to the performance of the compound (Equations. 1-1 to 1-3).[26]

$$P_{(CJ)} = 15.58\ \rho^2\ \Phi \qquad (1\text{-}1)$$

$$D = A\ \Phi^{1/2}\ (1+\beta\ \rho) \qquad (1\text{-}2)$$

$$\Phi = N\ M^{1/2}\ Q^{1/2} \qquad (1\text{-}3)$$

P is the detonation pressure (GPa), D is the speed of detonation (m/s), A and B are constants, N is the number of moles of gaseous products of detonation per gram of explosive, M the average molecular weight of the gases, Q is the heat of detonation in calories per gram of explosive and ρ is density. The higher the density is, the better the performance will be. Although the increase of oxygen balance results in a more sensitive material, it also increases the performance due to the “complete” oxidation of all carbons and hydrogens. Most energetic materials, however, are “oxygen-deficient”.[27]

Currently, most new energetic materials are compared to three of the most important known energetic materials: Cyclotrimethylenetrinitramine (RDX),

cyclotetramethylene-tetranitramine (HMX) and trinitrotoluene (TNT). The performances of these three materials are listed in Table 1-1.[24] The development of new energetic materials with better performance than RDX, HMX or TNT constitutes an important area of current active research.

Table 1-1. Performance data of three common energetic materials.

	ρ (g/cm^3)	P (Gpa)	D (m/s)
RDX	1.81	33.8	8750
HMX	1.91	39.3	9100
TNT	1.65	20.0	6900

In order to achieve better performance than RDX or HMX, some new, more advanced energetic materials (CHNO/F) have incorporated fluorine into the system. Fluorinated organic compounds are denser and are intrinsically more chemically and thermally stable than non-fluorinated analogs. In several cases, the introduction of fluorine into energetic materials also enhances its performance.[24,26,27]

During the last few decades, there has been an increased interest regarding the incorporation of the SF_5 group into energetic materials.[14,27-31] It has been previously mentioned that the inclusion of SF_5 generally increases the thermal and chemical stability of organic molecules[13], and in addition to this, it has been demonstrated that the presence of SF_5 also can increase the density,[28] and thus the performance of the energetic material (Figure 1-11).

The high fluorine content along with the presence of hydrogen leads to the formation of hydrogen fluoride (HF) upon detonation, generating a large amount of energy. The S-F Bond Dissociation Energy (BDE) is 79 kcal/mol, while the BDE of H-F is 136 kcal/mol. [14,28,30,31]

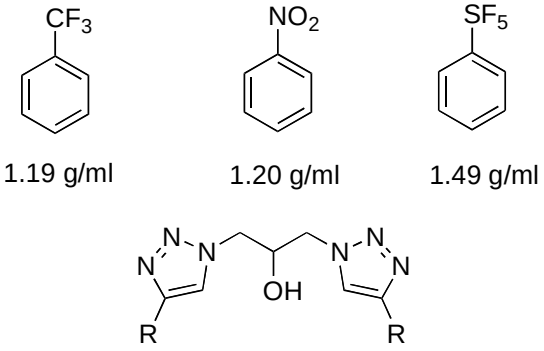

Figure 1-11. Higher density on SF_5 compounds.

The possibility of a higher density, larger energy release, and better thermal and chemical stability without increasing the sensitivity make the SF_5 group attractive in the synthesis of high energy materials (HEM).

Figure 1-12 shows a polynitro-SF_5 energetic material, which upon detonation produces HF as the only product containing fluorine, while the presence of sulfur (S) leads into the formation of COS, inhibiting the formation of COF_2, which is considered a loss of fluorine.[31]

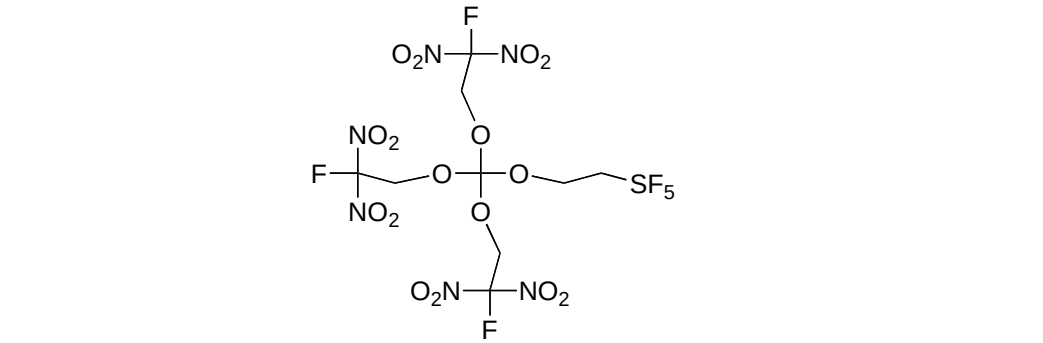

Figure 1-12. Polynitro-SF_5 energetic material.

Fluorine in [2.2]Paracyclophanes

[2.2]Paracyclophane ([2.2]PCP) has two benzene rings face to face that are linked by two ethylene groups in the para position. The proximity of the rings prevents the

rings from rotating freely and produces a repulsive interaction that generates not only unique geometrical structures, but also an interesting chemistry. Due to the repulsive interactions the carbon-carbon bond length in the ethylene bridges is extended from 1.54Å (ethane) to 1.63Å and generates an alteration in the planarity of the benzene rings giving them a bent geometry that looks like a boat (Figure 1-13).

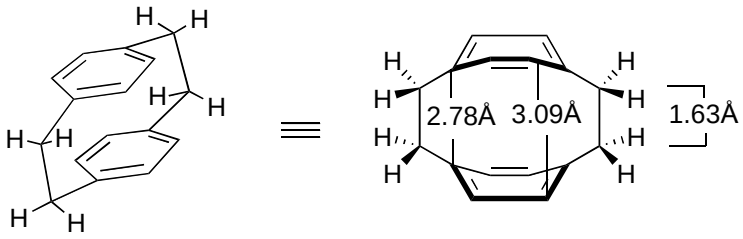

Figure 1-13. Structure of [2.2]paracyclophane.

[2.2]Paracyclophane finds one of its most important applications as a monomer of parylene polymers. This type of polymer is transparent, has a high thermal and chemical resistance and has excellent barriers properties. All of these properties make this polymer useful for coatings in different fields such as electronic, automotive and medical industry.[32,33] Derivatives of [2.2]PCP have found also applications as ligands in asymmetric synthesis,[34-36] biologically active compounds,[37] optoelectronics,[38-40] among others (Figure 1-14).

The interest on [2.2]paracyclophanes has increased considerably in the last 20 years due to their unusual chemistry. [2.2]PCPs present transannular effects, thermal racemizations, faster poly-electrophilic aromatic substitutions than simple aryl systems giving different types of isomers, and several other attractive properties that make their chemistry an active research area.[41,42]

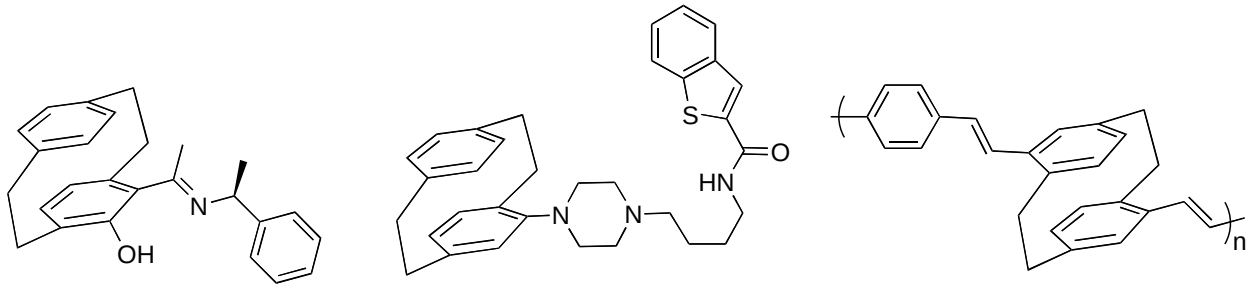

Asymmetric ligand Biologically active compound Conjugated polymers

Figure 1-14. Applications of [2.2]paracyclophane derivatives.

The thermal racemization after the generation of the first optically active derivatives of [2.2]paracyclophane was discussed in detail since three possibilities were considered for the racemization: 1) both of the carbon-carbon bonds at the ethylene bridges could break to generate a *p*-quinodimethane and then dimerized back, 2) only one of the carbon-carbon bonds at the ethylene bridges breaks homolytically to generate a biradical giving free rotation to the ring and 3) one carbon-carbon bond from the benzene ring and the ethylene bridge could break to generate a biradical and then free rotation to the ring as well. Exhaustive work done by Reich in 1968 demonstrated that at 200^{o}C the correct mechanism for racemization of [2.2]paracyclophanes is pathway 2 (Figure 1-15).[43]

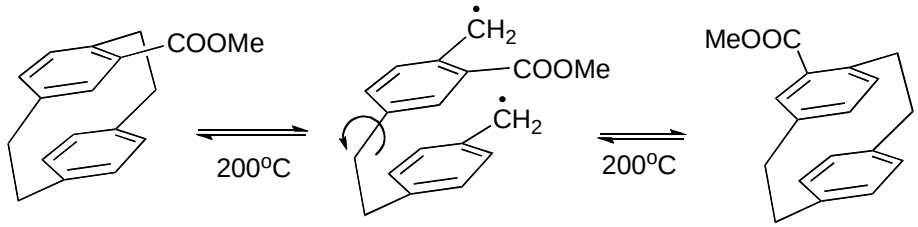

Figure 1-15. Racemization of [2.2]paracyclophane derivatives.

Introduction of fluorine into [2.2]paracyclophanes enhances some of its properties, and generates more interesting chemistry. 1,1,2,2,9,9,10,10-Octafluoro[2.2]paracyclophane (AF4), which is the perfluorination of the ethylene bridges, is one of the most useful parylene polymers. The presence of fluorines

increases the thermal stability and decreases the moisture absorption when compared with its non-fluorinated analogs. These properties along with its low dielectric constant make parylene-AF4 an excellent isolating material.[33] Although the presence of fluorinated methylene groups in the para positions decrease the rates towards electrophilic aromatic substitutions, several derivatives have been reported in good yields.[41]

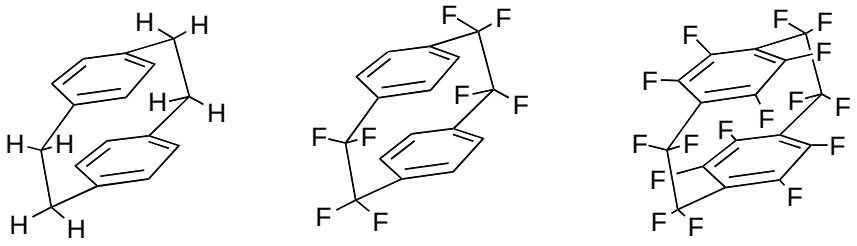

[2.2]PCP AF4 F8

Figure 1-16. [2.2]Paracylophane and the most common fluorinated [2.2]PCPs.

Recently, the chemistry of perfluoro[2.2]paracyclophane (F8) has been studied by Dolbier. The type of chemistry that is observed for this type of perfluorinated material is, in many ways, similar to that of perfluorobenzene and perfluoropyridine.[44,45]

Surprisingly, the chemistry of the 4,5,7,8,12,13,15,16-octafluoro[2.2]paracyclophane, which is the “replacement” of the hydrogens in the benzene rings for fluorines, has hardly been studied. A search on Scifinder for this structure only generates 8 different references with 4 of them between 1965-1989 and the other 4 between 2003-2005, where most of them are dedicated to its synthesis, but not to the study of its chemistry.

All the syntheses of [2.2]paracyclophanes are similar in their last step, which is the elimination of two groups at each methyl substituent to form a *p*-quinodimethane.[32,33,44] Most of the methods that are described before 1998 encounter the problems when the

reactions were scaled up for industrial production, either because the polymerizations lower the yield of the PCP or because of the high cost of the method. Dolbier et al. in 1998 discovered a method that allows the industrial production of AF4 in 60% yield using zinc, and proves to be a general method for the synthesis of other paracyclophanes such as F8.[32,44] Most common methodologies for the synthesis of PCPs are shown in Figure 1-17.

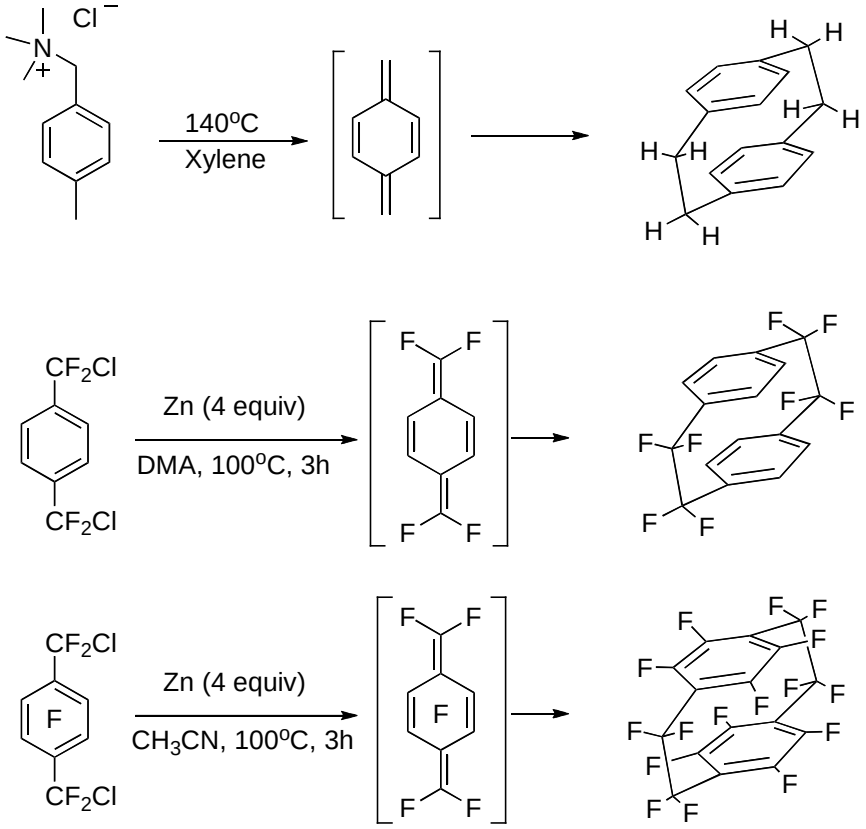

Figure 1-17. Most common methodologies for the synthesis of [2.2]paracyclophanes.

The chemistry of [2.2]paracyclophane and octafluoro[2.2]paracyclophane has been well studied. Derivatives of these two compounds are generally prepared through electrophilic aromatic substitution and further products are usually made after the first substitution (Figure 1-18).

In contrast, the type of chemistry that can be performed on perfluoro[2.2]paracyclophane is through nucleophilic aromatic substitution, and it has only recently been studied by Dolbier et al. (Figure 1-18).[45-49]

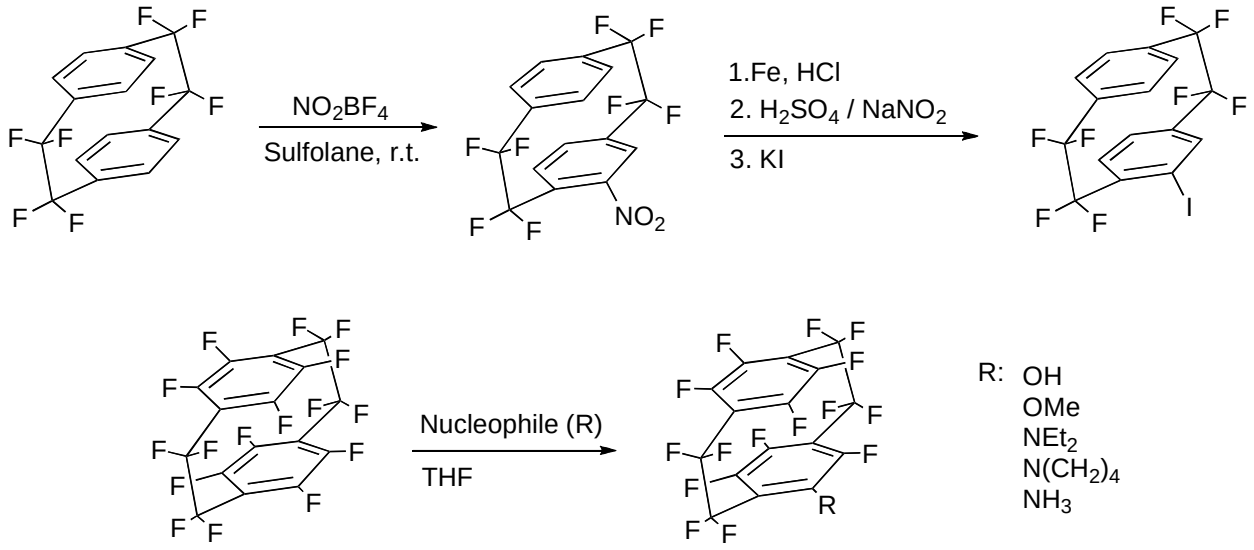

Figure 1-18. Examples of chemical reactions of fluorinated [2.2]paracyclophanes.

Fluorine NMR

Fluorine is probably the third most studied nucleus for nuclear magnetic resonance, after hydrogen and carbon. Fluorine with a spin of ½ and a 100% natural abundance has a similar sensitivity to that of hydrogen. Fluorotrichloromethane ($CFCl_3$) is the most widely use internal reference and has an assigned chemical shift of zero. Most common organo fluorine molecules (aromatic fluorine, fluorines at sp, sp^2 or sp^3 carbons) are generally upfield to the internal reference (negative side), but the range in which fluorine can appear in the spectra goes from +70 to -220 ppm, with only a few exceptions. The fact that most organo fluorine reactions are run in non-fluorinated solvents leads to an easier analysis of the reaction by ^{19}F NMR without need of work up.

Similar to hydrogen, but to a greater extent, fluorine chemical shifts are sensitive to electronic changes around the fluorine nucleus. For instance, Taft has shown

extensively that the fluorine chemical shift of substituted fluorobenzenes depends highly on the electron donor or withdrawing ability of the substituent and the difference between the chemical shifts of fluorobenzene and the substituted fluorobenzene has been correlated with good agreement to the Hammett substituent constant (Equations 1-4 to 1-7) .[50,51]

$$\delta_{m}^{F} = \int_{H}^{m-x} = -7.10\sigma_I + 0.60 \quad (1\text{-}4)$$

$$\delta_{p}^{F} - \delta_{m}^{F} = \int_{m-x}^{p-x} = -29.5\sigma_R \quad (1\text{-}5)$$

$$\sigma_p = 1.25\sigma_I + \sigma_R \quad (1\text{-}6)$$

$$\sigma_m = 1.10\sigma_I + 1.14\sigma_R \quad (1\text{-}7)$$

Where δ_{y}^{F} is the chemical shift difference between fluorobenzene and the meta- or para (y) substituted fluorobenzene; σ_I, σ_R, σ_p and σ_m are the inductive, resonance, para and meta Hammett values respectively.

Hydrogens and fluorines in the proximity of other fluorines will display splitting of its signals due to the coupling between the fluorines and the other nuclei. The spin-spin coupling follows the n+1 rule, as well as the Pascal's triangle for the intensity of the signals.[52]

One of the most important differences between hydrogen and fluorine spin-spin coupling is the ability of fluorine to have a strong through space coupling. This type of coupling can be transmitted through a series of different mechanisms, but all of them will involve an overlap of the orbitals where the fluorine lone pairs are located. As it might be expected, this through space coupling depends on the distance and the angle with which the two nuclei interact (Figure 1-19).[52]

Similar to proton and carbon, 2D NMR techniques using the fluorine nucleus, such as NOESY, COSY, TOCSY, are great tools to determine most, if not all, of the long range coupling that fluorine usually exhibits. This allows the full interpretation of the NMR spectrum without explaining the mechanism of those long range couplings.

$^{6}J_{HF}$=<0.5 Hz
HF(Å)= 2.84

$^{6}J_{HF}$=8.3 Hz
HF(Å)= 1.44

Figure 1-19. Examples of through space spin-spin coupling.

Several publications have reported long-range ^{19}F-^{19}F spin-spin couplings, with a definitive conclusion that those couplings are highly dependent on distance between the interactive nuclei. Nevertheless, there seems to be a lack of complete understanding of the mechanism of some through space couplings.

A simple rule indicates that if two fluorines are coupling through space, the distances between the two interacting fluorines must be less than twice the Van der Waals radii of fluorine (2 x 1.47Å = 2.94Å). This means that if two fluorines are within this distance the transmission is purely through the orbital interactions of the lone pairs of each fluorine. On the other hand, if the coupling fluorines are not within this distance, but are still coupling, the mechanism of "communication" must go through a different pathway. Although Ernst has done a great job identifying long-range ^{19}F-^{19}F spin-spin coupling constants of some fluorinated [2.2]paracyclophanes using different 2D NMR techniques, the mechanism of transmission for those in which the distances between the interacting fluorines is more than twice the Van der Waals radii of fluorine was not discussed (Figure 1-20).[53]

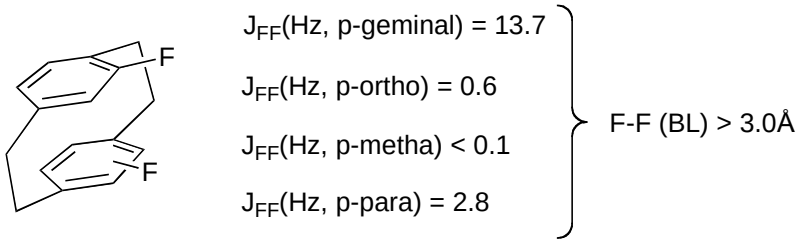

Figure 1-20. Through space coupling identified by Ernst.

Fluorine in S_N2 and E2 Reactions

As can be witnessed by examining any undergraduate textbook, the bimolecular nucleophilic substitution reaction, S_N2, has been studied exhaustively with the result that influences on reactivity such as solvent polarity, leaving group ability, nucleophilicity and steric effects are considered pretty well understood. Each of these effects contributes individually, and sometimes cooperatively, in such a way as to either increase or decrease the reaction barrier.

It is well recognized that nucleophilic aliphatic substitution reactions of primary alkyl substrates proceed via the S_N2 mechanism. It is likewise recognized, although perhaps not so universally, that primary *perfluoroalkyl* substrates will not participate in substitution reactions via the S_N2 mechanism, but rather are capable of undergoing nucleophilic substitution via the $S_{RN}1$ mechanism when the nucleophile can undergo single electron transfer (SET) to initiate the free radical chain process (Figure 1-21).[54]

Indeed, simply the presence of two α-fluorines in substrates with the structure RCH_2CF_2X is understood to severely inhibit, if not prevent, nucleophilic substitution. To our knowledge there are *no* examples of successful S_N2 nucleophilic substitution reactions of such compounds.

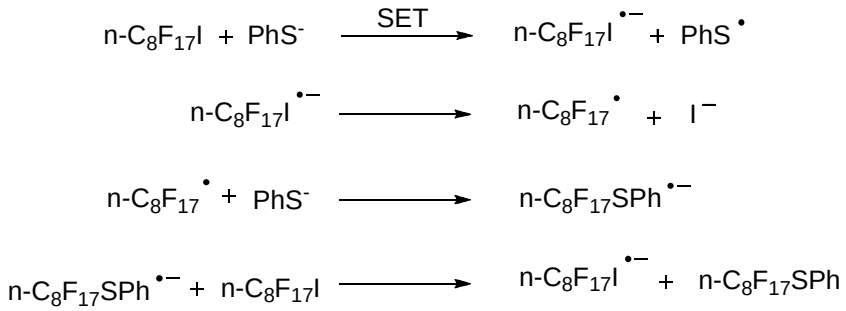

Figure 1-21. $S_{RN}1$ mechanism with perfluoroalkyl iodides.

It is also part of the “lore” of fluorine chemistry that fluorine substituents proximate to the site of nucleophilic substitution will *inhibit* such substitution, and the closer they are, the more impact that they have. In contrast, the elimination reactions are accelerated by the presence of fluorine. This effect is due to the increment in the acidity of the hydrogens in the proximity of the fluorines: the closer they are, the faster the elimination.

CHAPTER 2
DESIGN OF PENTAFLUOROSULFANYL ENERGETIC MATERIALS

Introductory Remarks

Energetic materials can be considered massive controllable energy storage. The design of new materials with higher energy content, better performance, lower cost, less sensitivity to impact and with less danger to synthesize and process keeps this research area active. The synthesis of new materials has been focused on rings with high nitrogen content such as tetrazines, furazans, triazoles and tetrazoles due to the relatively positive heat of formation of these compounds.[25] Recently, the introduction of fluorine to these and other compounds has resulted in a boost in the performance of the energetic materials, mainly due to the increase in the density and thermal and chemical stability. Following this trend, our research focused on the synthesis of a new type of SF_5- furazan type energetic materials.

Furazan Energetic Materials

1,2,5-oxadiazoles (commonly known as furazans) have been included in several publications as great building blocks for the generation of insensitive High Performance Energetic Materials (HEM).[27,55-65] The aromaticity present in the ring increases the thermal stability, while the planarity increases the density. That combined with the positive heat of formation (HOF) make furazans an excellent building block for the generation of HEM.[55]

Since the first synthesis of 3,4-diaminofurazan **1** (DAF) by Coburn in 1968,[66] a vast number of furazan derivatives with good densities and energetic properties have been prepared. The synthesis of aminofurazans generally starts with the synthesis of aminoglyoximes, followed by dehydration under basic conditions. Scheme 2-1 shows

the synthetic pathway applied in this work for the synthesis of some common aminofurazan building blocks.[55,60-63]

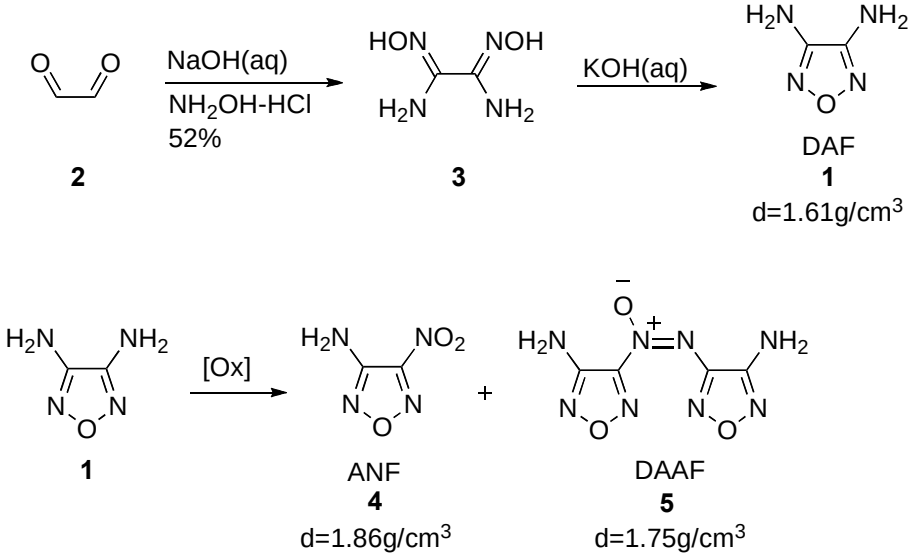

Scheme 2-1. Synthesis of common furazan building blocks.

Although the furazan ring possesses an electron withdrawing ability that makes the amino group(s) in aminofurazans a challenge to derivatize,[67,68] the use of these materials as part of HEM remains of much interest. The majority of the chemistry that can be performed with aminofurazans is done through nucleophilic attack by the amino group, condensation reactions, oxidative reactions, or ring opening of the furazan ring. The last type of these reactions ends up destroying the energetic properties of the material.[67]

Studies on the thermal decomposition of amino furazan derivatives at different temperatures have shown that the major percentages of products are between CO, CO_2, H_2O, HCN, N_2 (when the azo or hydrazine moieties are present) and NO_2 (when present as a nitro group in the molecule). A minor percentage of the products is distributed between HCNO, NH_3, HNO_3 and N_2O. The same studies indicate that most

aminofurazans present a higher thermal stability than the most common energetic materials such as HMX or RDX.[65,69,70]

Alternatively, the high nitrogen content and positive HOF of tetrazole also makes this group a good starting material for the synthesis of HEM. Although tetrazole has a positive HOF, it exhibits good thermal stability.[71-73] Theoretical and experimental studies have shown that the thermal decomposition of 5-aminotetrazole goes through two different retro [3+2] mechanisms with relatively close activation energies. The first mechanism and most favorable generates NH_2CN and HN_3, while the second one produces CH_3N_3 and N_2. However, when the amino group of the aminotetrazole has been functionalized, the second mechanism is the most favorable.[71-75]

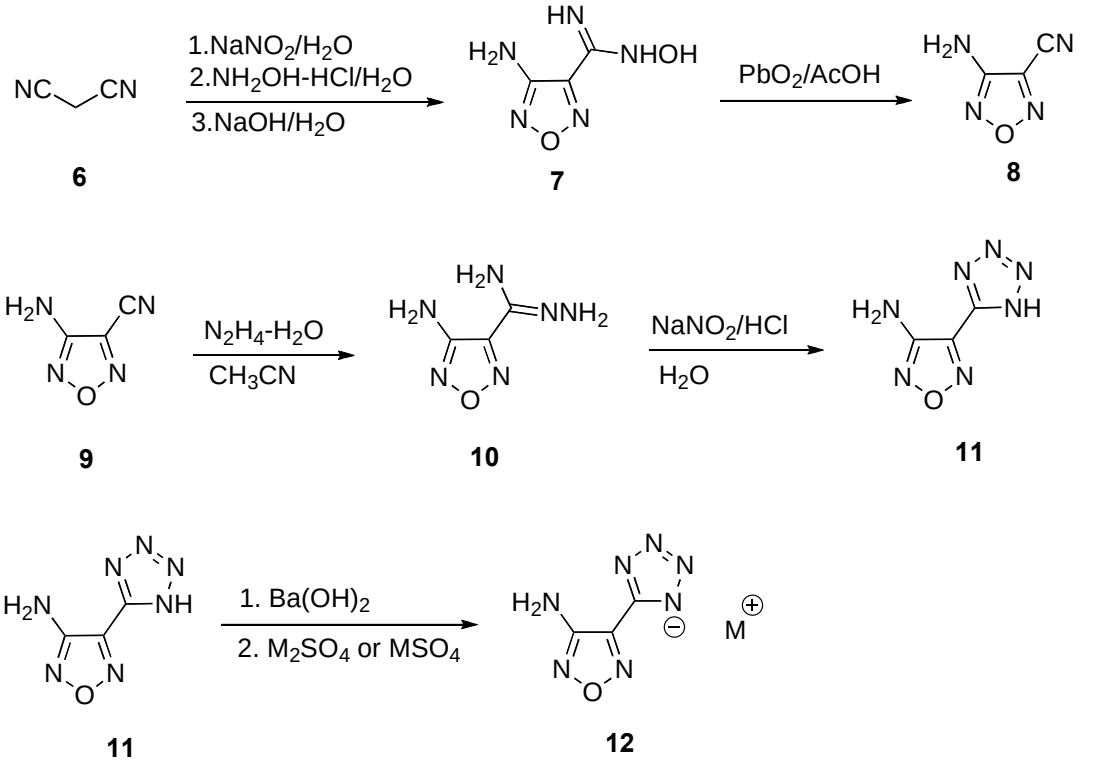

Scheme 2-2. Amino-Furazan-tetrazole synthesis and its derivatives.

The combining of tetrazole and furazan rings have been previously reported,[76] but it was only in 2009 that Shreeve, et al.,[77] reported furazan tetrazolate-based salts as

highly insensitive energetic materials. The high calculated heats of formation and the good densities predicted a good energetic performance. This result, combined with the previously mentioned properties of furazans, makes this group attractive for the preparation of new high-density energetic materials. Scheme 2-2 presents the synthetic pathway applied in this work for the synthesis of amino-furazan-tetrazole and the salts derivatives prepared by Shreeve.[76,77]

Pentafluorosulfanyl (SF_5) as Part of Energetic Materials

During the last few decades, there has been an increased interest regarding the incorporation of the SF_5 group into energetic materials.[14,27-31] It has been demonstrated that the inclusion of the SF_5 group can increase the density,[28] and thus the performance of the energetic material. It is important to remember from Chapter 1 that according to the semi-empirical equations propose by Kamlet and Jacobs (Equations 1-1 to 1-3), an increase in the density will boost the performance of the energetic material.

The formation of C-F, H-F or Al-F bonds, which have a higher bond dissociation energy (BDE) than the S-F bond in the pentafluorosulfanyl group, allows the release of large amounts of energy upon detonation. This combined with the possibility of higher density, higher thermal and chemical stability and low sensitivity makes the pentafluorosulfanyl group very attractive for the synthesis of high performance energetic materials.[13,14,28,30,31]

A large number of SF_5-containing energetic materials have been synthesized where the predicted performance is close to those for HMX, RDX and TNT, but with the benefit of lesser or no impact sensitivity (Figure 2-1).[14,18]

Figure 2-1 shows five SF_5-containing energetic materials having densities around 1.85 g/cm^{-3}, and with predicted pressure and speed of detonation around 17.8 - 20.5 GPa and 6900 - 7100 m/s respectively.

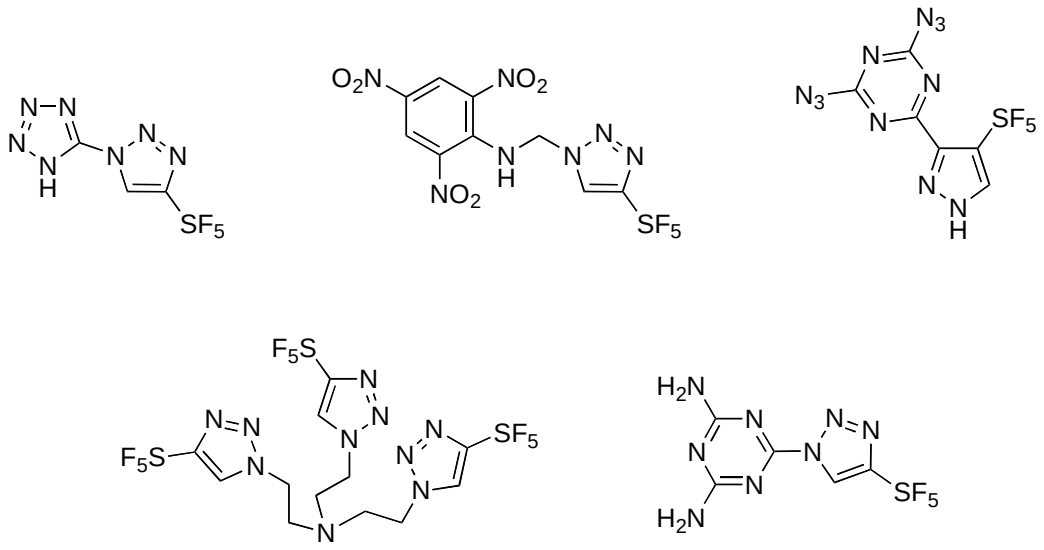

Figure 2-1. Examples of SF_5-containing energetic materials.

Despite all the benefits provided by the SF_5 moiety, the amount of SF_5-containing energetic materials is still limited due to the few ultimate sources of the aliphatic SF_5 group: SF_5Br and SF_5Cl. The chemistry of these two starting materials is limited to free radical chemistry. For this reason, the synthesis of SF_5 building blocks that would allow the “easy” incorporation of this group into HEM remains challenging, and thus provides an incentive and challenge to many research groups.

Figure 1-12 shows a polynitro-SF_5 energetic material, which upon detonation produces HF as the only product containing fluorine. The presence of sulfur (S) as SF_5 inhibited the formation of COF_2, which is considered a loss of fluorine.[31] Then it is considered potentially advantageous to combine the properties of aminofurazans, with those of the SF_5 group, in order to obtain high-performance energetic materials. It is

expected that with high fluorine content and low hydrogen content, such materials might release “free fluorine, F_2” upon detonation.

The goal of this project can be summarized by three points: 1) the synthesis and evaluation of different SF_5- building blocks towards nucleophilic attack by aminofurazans. 2) The synthesis of high-density SF_5-furazan-based energetic materials with low hydrogen content, for the possible release of “free fluorine” upon detonation. 3) Evaluation of the thermal and chemical stability of new energetic materials containing the SF_5 group as well as the possible energetic performance by Cheetah calculations.

Results

Aminofurazan Starting Materials

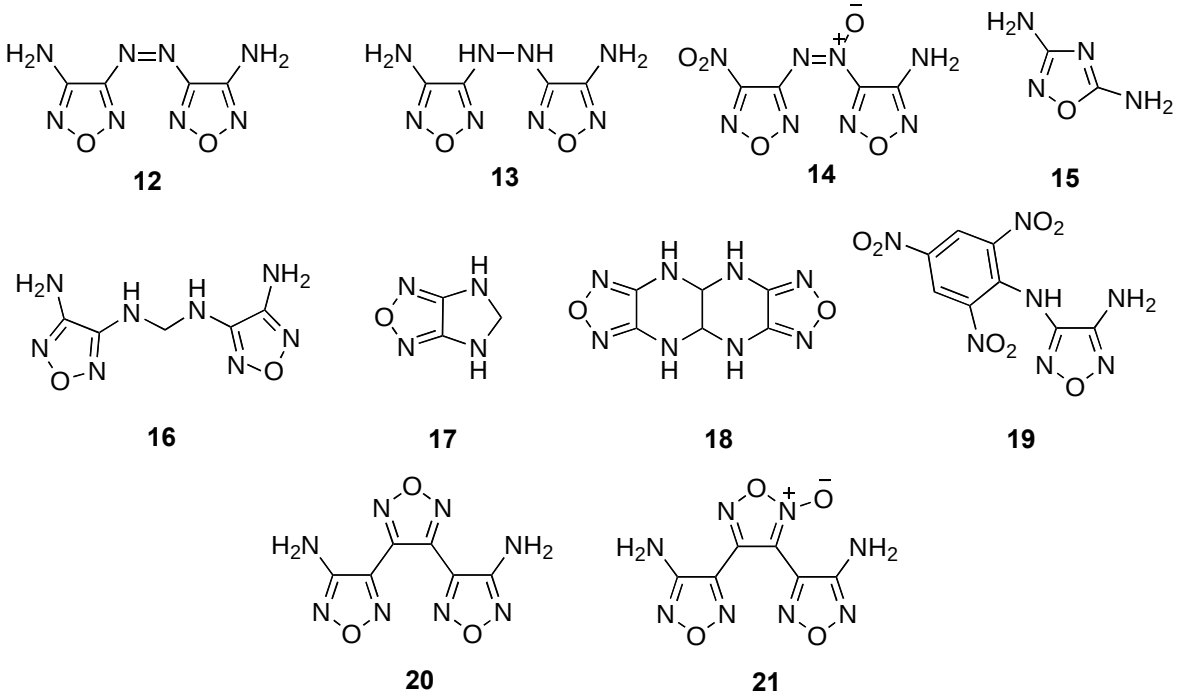

Figure 2-2. Additional synthesized aminofurazans starting materials.

In addition to compounds **1**,**4**,**5** and **11**, a series of aminofurazans were synthesized according to various literature reports (Figure 2-2).[62,76,78-82] Compounds **20** and **21** were provide by the Defense Threat Reduction Agency (DTRA).

Synthesis of SF_5-Furazan-Based Energetic Materials

The SF_5-acetyl building block

In order to achieve an efficient and relatively "easy" incorporation of the SF_5 group into aminofurazans, methyl 2-pentafluorosulfanylacetate **24** was chosen as our initial SF_5-containing building block (Scheme 2-3).[21]

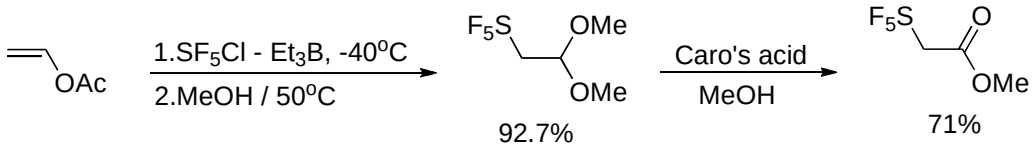

22 **23** **24**

Scheme 2-3. Synthesis of Methyl 2-pentafluorosulfanylacetate **24**.

3,4-diaminofurazan **1** (DAF) was used as our initial starting furazan substrate, to establish conditions for preparation of the SF_5-acetamidofurazan derivatives. Different reaction conditions were attempted using DAF and methyl SF_5-acetate **24**, but these were unsuccessful in obtaining the desired product (Scheme 2-4).

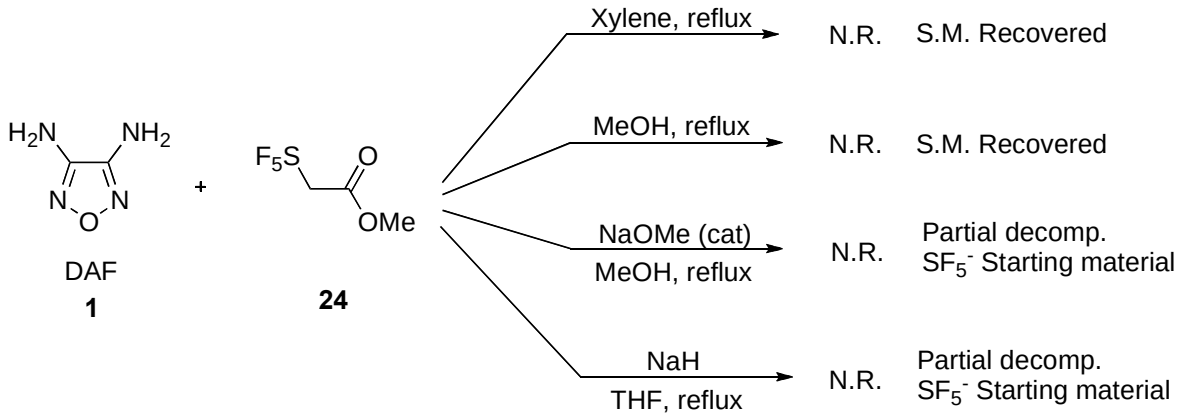

Scheme 2-4. Attempted reactions between DAF **1** and methyl SF_5-acetate **23**.

The lack of nucleophilicity from the DAF thus requires a more reactive SF_5-acetyl building block. Starting from the methyl ester **24**, the SF_5-acetic acid **25** was obtained in 88% yield after optimization, which was then converted to the pentafluorosulfanylacetyl

chloride **26** in 42% yield in a similar methodology to that reported by Sitzmann (Scheme 2-5).[83]

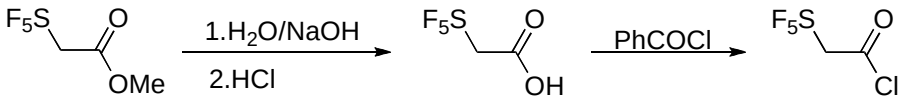

24 88% **25** 42% **26**

Scheme 2-5. Synthesis of pentafluorosulfanylacetyl chloride.

The SF_5-acetyl chloride should be more reactive towards the nucleophilic attack of the aminofurazan, and the reaction between DAF and the SF_5-acetyl chloride is presented in Scheme 2-6.

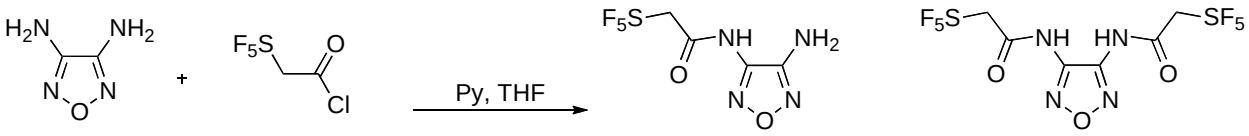

DAF **1** | 1 or 2 equiv. **26** | MASF5-DAF 70% - 1 equiv. **27** | DASF5-DAF 55% - 2 equiv. **28**

Scheme 2-6. Synthesis of pentafluorosulfanylacetamide-furazans.

The syntheses of MASF5-DAF **27** and DASF5-DAF **28** were achieved in decent yields after optimization; however, the low yield in the synthesis of the SF_5-acetyl chloride **26**, encouraged the use of an alternate SF_5-acetyl building block.

The reaction between amines and *N*-acetylbenzotriazole (and derivatives), has been widely use for the synthesis of amides,[84] providing better yields and cleaner reactions than those in the reaction between amines and acyl chlorides.

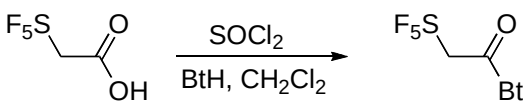

25 95% **29**

Scheme 2-7. Synthesis of the benzotriazole derivative of SF_5-acetic acid.

The reaction between the SF_5-acetic acid with thionyl chloride and benzotriazole provided compound **29** with an excellent yield (Scheme 2-7). Indeed the reaction between DAF and compound **29** proved to be more efficient than the reaction with the ester, but it unfortunately was not better than that obtained when using the acyl chloride (Scheme 2-8).

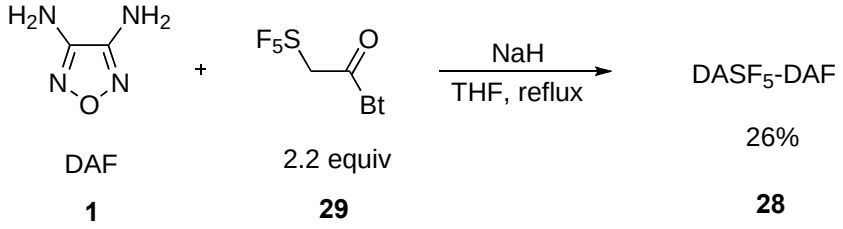

Scheme 2-8. Synthesis of **28** from the benzotriazole derivative of SF_5-acetic acid.

In trying to avoid the low yield synthesis of the SF_5-acetyl chloride **26**, the SF_5-acetic acid **25** was allowed to react with DAF in the presence of a carbodiimide. This type of reaction is well known and typically produces very good results. Various carbodiimides were tried, and the best results were obtained with 1-ethyl-3-(3-dimethylaminopropyl) carbodiimide (EDC) (Scheme 2-9).

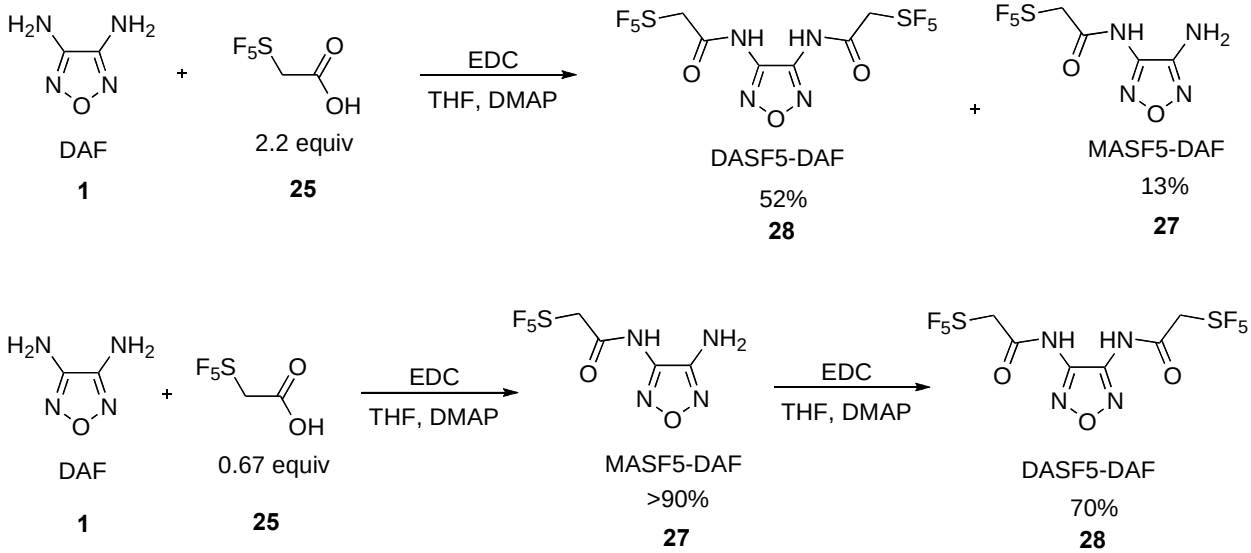

Scheme 2-9. Synthesis of DASF5-DAF from SF_5-acetic acid using EDC.

The reaction with DAF and SF_5-acetic acid using EDC was a more efficient and cleaner reaction, when compared to the reaction with SF_5-acetyl chloride. This method was then used for a series of reactions using various aminofurazans.

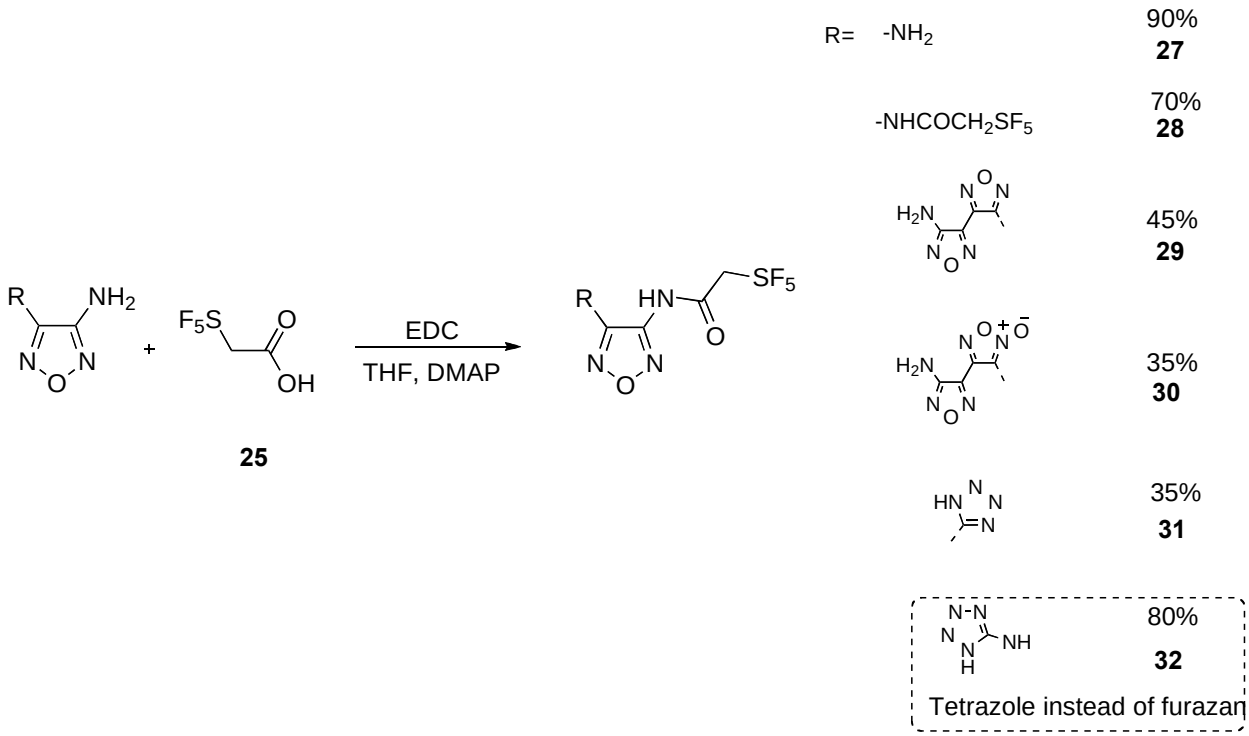

Scheme 2-10. Reaction between different aminofurazans and SF_5-acetic acid in the presence of EDC.

Scheme 2-10 shows all of the reactions that were successful when using the EDC chemistry. All other aminofurazan starting materials failed to yield any product. Compound **32** was prepared with the help of Mr. Zheng, a graduate student in our group. In some cases we returned to the reaction between the aminofurazan and the SF_5-acetyl chloride, when the acid and EDC did not yield any product; however, no product could be obtained from those reactions either. The lack of either nucleophilicity or solubility of the aminofurazan substrates led to products in low yield or no product at all. The two different amino groups in compound **21** result in the formation of two isomers in a 95:5 ratio, where 95 correspond to the amino closest to the $–N=O^-$ moiety.

Compounds **29** and **30** were used in a later reaction to introduce a second SF_5-amide moiety. Compound **29** showed 2% of product (bis-amide) by ^{19}F NMR, but it never reacted to a point where it was possible to isolate the product, while compound **30** never showed the formation of the bis-amide at all.

Pentafluorosulfanylmethyl-dicarbonyl building block

The addition of SF_5Cl to α,β-unsaturated carbonyl compounds under the Et_3B method is not possible due to the electron deficiency of the β-carbon, as well as the possibility of polymerization through the α-carbon. It was thought that the addition of an alkoxy group (RO) to the α-carbon might overcome both problems. Thus a different approach was attempted in order to obtain SF_5-furazan-based energetic materials (Figure 2-3).

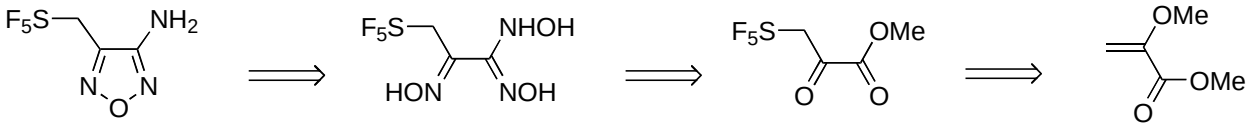

Figure 2-3. Retrosynthetic approach for the synthesis of 3-amino-4-(pentafluorosulfanylmethyl) furazan**.**

Methyl 2-methoxyacrylate **36** was synthesized according to a previous reported method.[85] The reaction between methyl 2-methoxyacrylate **36** and the SF_5Cl using our Et_3B method was shown to be not only possible, but also efficient (Scheme 2-11).

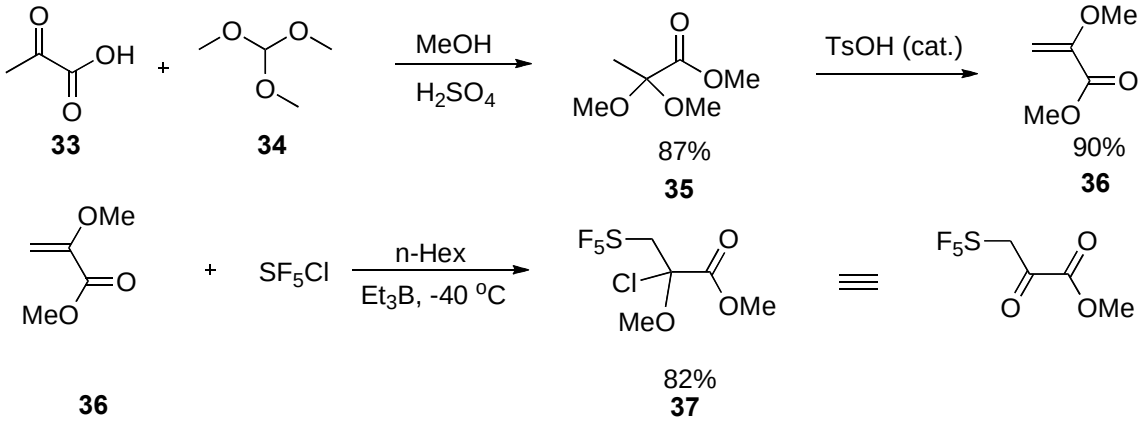

Scheme 2-11. Synthesis and addition of SF_5Cl to methyl 2-methoxyacrylate **36.**

Methyl 3-pentafluorosulfanyl-2-chloro-2-methoxypropanoate **37** is the masked dicarbonyl material and could itself potentially be used directly to obtain SF_5-furazan-based energetic materials; However, various attempts to utilize compound **37** to prepare the desired new furazan were unfortunately not successful (Scheme 2-12).

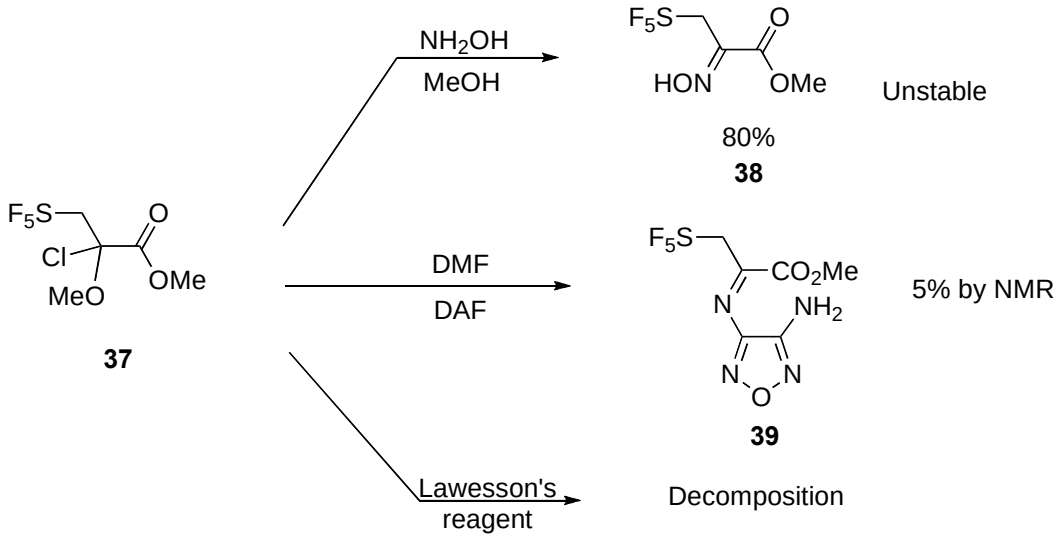

Scheme 2-12. Reactions attempted using compound **37.**

Conversion of **37** to the analogous thiocarbonyl compound, potentially a more reactive substrate, was attempted unsuccessfully under various reaction conditions. In most cases decomposition of the starting material occurred.

Miscellaneous reactions

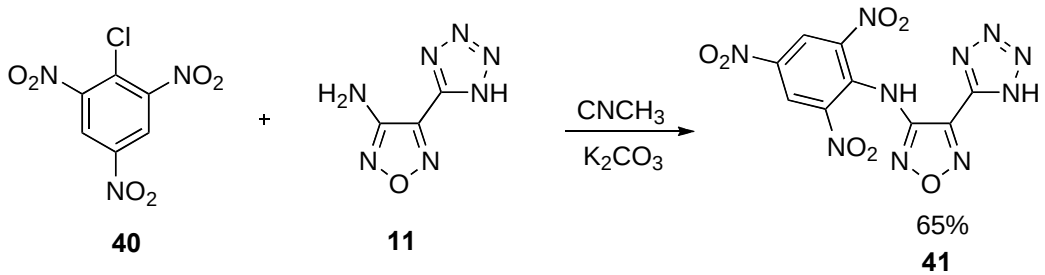

Scheme 2-13. 4-(1H-tetrazol-5-yl)-3-amine-*N*-(2,4,6-trinitrophenyl)furazan **41**

During the course of this project both 3-amino-4-(tetrazo-5-yl)-furazan **11** and picryl chloride **40** were synthesized according to the literature. It was called to our attention that the reaction between these two energetic compounds had not been

reported yet. The product, 4-(1*H*-tetrazol-5-yl)-3-amine-*N*-(2,4,6-trinitrophenyl)furazan **41** was synthetized and could have considerable energetic properties (Scheme 2-13).

2,2-Dinitropropane-1,3-diol **42**, has been also used in the synthesis of energetic materials.[29] The reaction between **42** and SF_5-acetic acid or acetyl chloride was attempted, but no product could be obtained (Scheme 2-14).

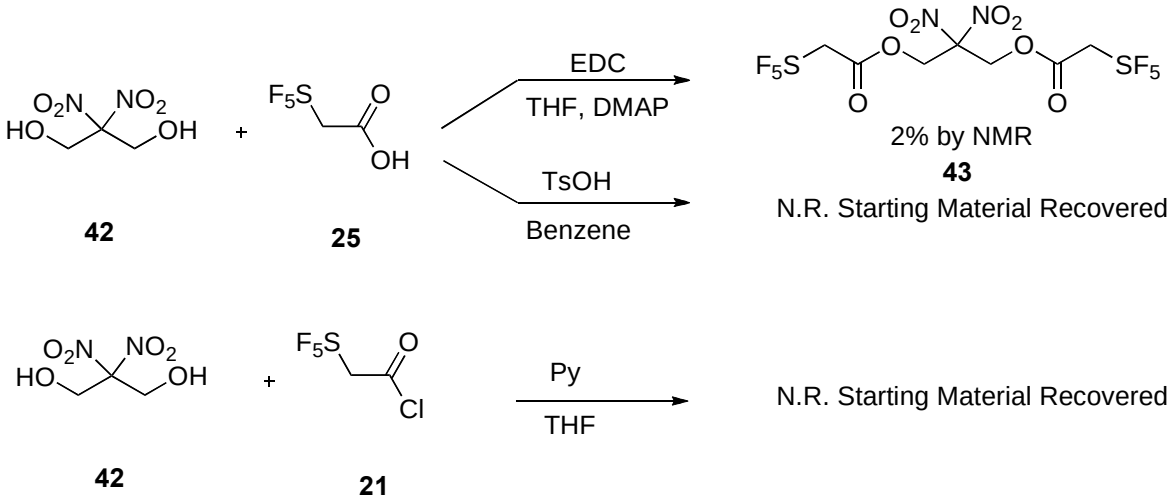

Scheme 2-14. 2,2-Dinitropropane-1,3-diol **42** as the starting material in the reaction with SF_5-acetyl building blocks.

Substitution of hydrogen by fluorine in the SF_5-acetyl group had always been included within the goals of our project, in order to reduce the amount of hydrogen present in the final energetic material. However, previous attempts in the Dolbier group to functionalize the α-carbon of the methyl 2-pentafluorosulfanylacetate **24** by alkaline enolate chemistry resulted in decomposition of the staring material. However, it was possible to prove the deprotonation of the α-carbon by hydrogen-deuterium exchange. On the other hand, Zhang and coworkers in 1998 reported the α-bromination of carboxylic acids using NBS under acidic conditions (Scheme 2-15).[86]

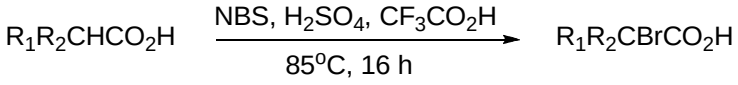

Scheme 2-15. α-Bromination of carboxylic acids.

Using conditions similar to those reported by Zhang, the α-bromination of pentafluorosulfanylacetic acid was not successful. However, the exchange of H_2SO_4 by HSO_3Cl gave the mono-bromo addition in 40% yield (Scheme 2-16). This is the first example in the literature of the α-functionalization of this type of materials. However, further attempts to improve the yield were unsuccessful.

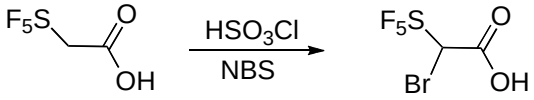

25 **44**

Scheme 2-16. Successful functionalization of the α-carbon in the SF_5-acetic acid.

Realizing the possibility of an enol-isomer in the methyl SF_5-acetate **18**, the reactions with fluorine and Selectfluor were tried. However, interestingly, no product could be obtained, and the starting material was recovered (Scheme 2-17).

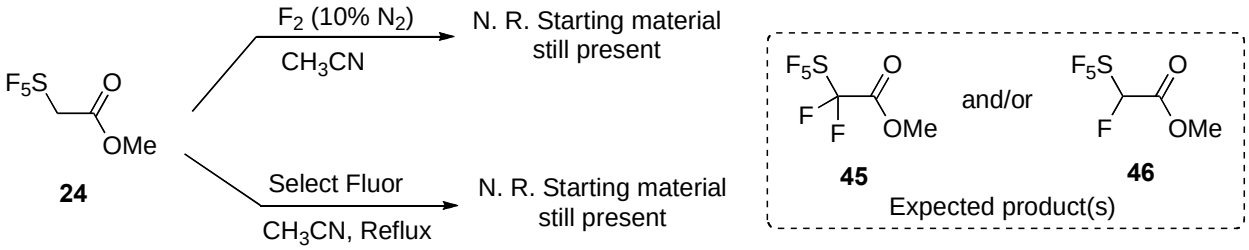

Scheme 2-17. Attempts of fluorination at the CH_2 in the SF_5-acetyl group.

The pentafluorosulfanyl isocynate building block

The high reactivity of SF_5NCO towards several nucleophiles has been already carefully studied,[87,88] including its addition to polynitroalcohols to yield the respective carbamates.[29,89]

Scheme 2-18 shows the synthesis of a bis-SF_5-carbamate previously prepared by Sitzmann,[89] which compound will be used as a baseline material in this project. The SF_5NCO was provided by Dr. Joseph Mannion of National Naval Laboratories at Indian Head.

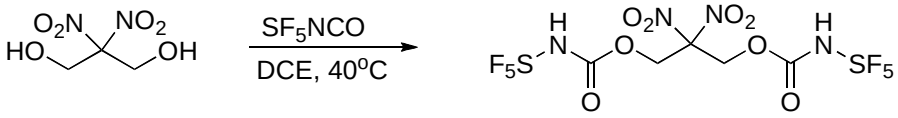

42 **47**

Baseline material

Scheme 2-18. Synthesis of a bis-SF_5-carbamate energetic material.

The high reactivity of SF_5NCO towards nucleophiles makes it a great building block. However, it is this same high reactivity that limits the possible solvents in which it can be used. A solvent screen carried out with SF_5NCO indicated that it reacts with

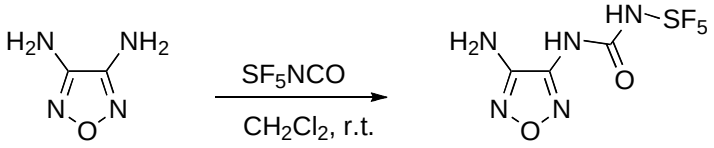

1

DAF

Low solubility

99%

48

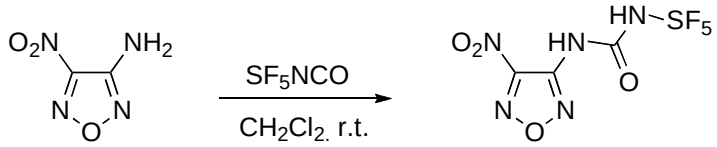

4

ANF

Soluble

20% + 80% ANF

49

Scheme 2-19. Reactions of SF_5NCO with DAF and ANF.

weak nucleophiles such as the enol of acetone (quick reaction), THF (slow) and acetonitrile (slow). In its reaction with the latter two solvents, the products are unknown, but formation of some type of product was clearly seen in each case by ^{19}F NMR. The isocyanate is unreactive with solvents such as dichloromethane and 1,2-dichloroethane. Water, of course, also reacts readily with SF_5NCO, and therefore should be avoided at all times.

Due to the solvent limitation, only two compounds could be obtained from the reaction of SF_5NCO with furazan derivatives (Scheme 2-19). All other aminofurazans were insoluble in either DCM or DCE, even at higher temperatures, and thus could not be used as substrates.

***N*-Nitration and oxidation reactions**

Although the previously synthesized SF_5-furazan-based materials already likely have energetic material properties, an increase in C/O balance might improve their energetic performance. However, all attempts of N-nitration failed. Three mild nitration conditions were used: 1) H_2SO_4 (98%)– HNO_3 (70%) 2) NH_4NO_3 – CF_3CO_2OH (TFAA) – HNO_3 (70%) cat. and 3) NO_2BF_4 – CH_3CN or THF. In all of these cases, the starting material was recovered. Thus, four stronger nitration conditions were used: 1) HNO_3 (>99%) fleshly made. 2) NO_2NO_3 – HNO_3 (>99%). 3) TFAA - HNO_3 (>99%). 4) NO_2BF_4 – NaH or Py – THF. Under these conditions, the starting materials ended up either partially or completely destroyed (Scheme 2-20).

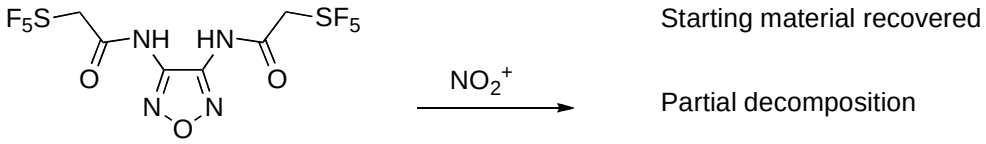

DASF5-DAF

28

Scheme 2-20. Attempts at *N*-nitration of DASF5-DAF **28**.

Another approach to adding additional oxygen to the synthesized SF_5-furazan materials could be through the oxidation of the amino groups to nitro groups, when an amino group is present. The oxidation of MASF5-DAF **27** was successful under three different methods: 1) H_2O_2 (50%) – H_2SO_4 (98%) – Na_2WO_4 in 50% yield. 2) HOF – CH_3CN in 65% yield. 3) H_2O_2 (50%) – H_2SO_4 (98%) in 30% yield. In the last method the

azoxy (-N=N(O)-) moiety was the expected result, but the nitro group was obtained instead. The first method of oxidation was applied by Mr. Zheng on compound **27** with 35% yield, and further optimization yielded 50%. In the particular case of compound **30**, no oxidation was obtained, but a change in the ratios of the two isomers was obtained (Scheme 2-21).

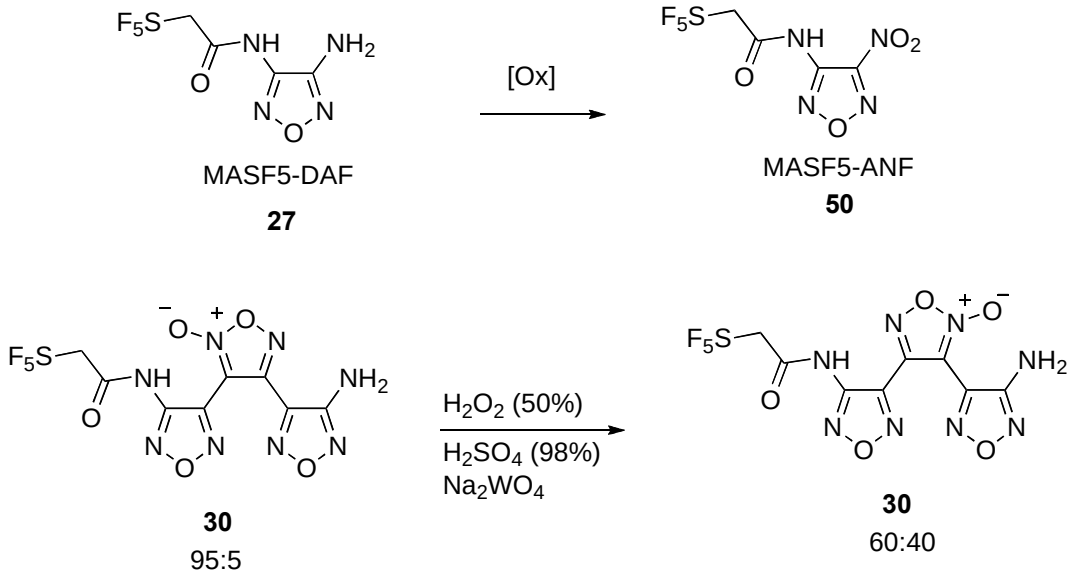

Scheme 2-21. Oxidation reactions of aminofurazans when SF_5-acetamide group present

The oxidation of SF_5-Urea-amino-furazan **48** was attempted using the same three methods previously mentioned for compounds MASF5-DAF **27**, plus a fourth method using $Ph_3PCH_2Ph^+H_2SO_5^-$ - CH_3CN. In all cases the product was the amino nitro furazan **4** (Scheme 2-22).

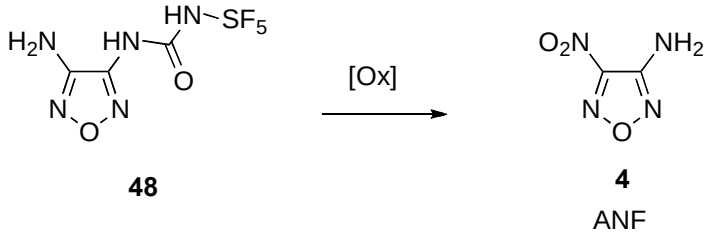

Scheme 2-22. Oxidation reactions of aminofuranzan **41,** when SF_5-urea group present.

The final approach toward improving the performance of these SF_5-furazan-based energetic materials was through the addition of the 2,4,5-trinitrophenyl group (Scheme 2-23).

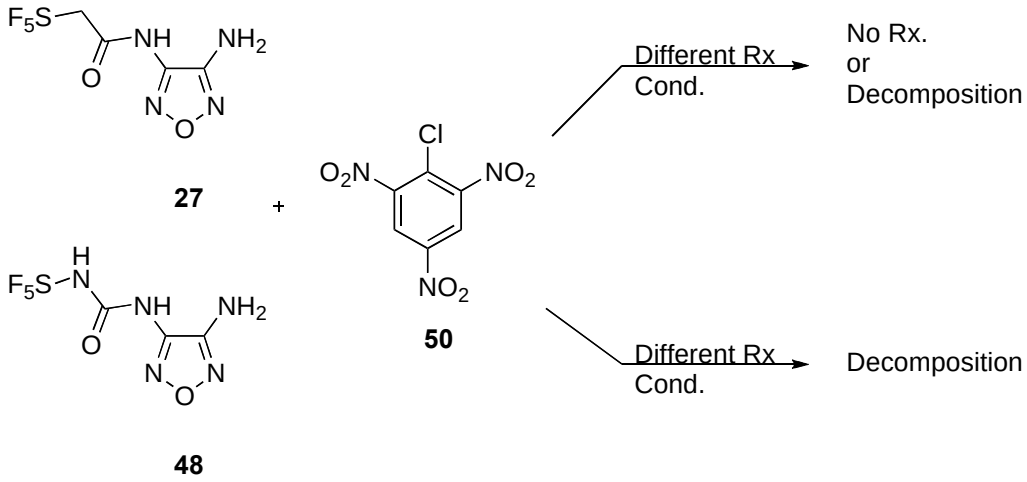

Scheme 2-23. Attempts to add the 2,4,5-trinitrophenyl group to compounds **27** and **48.**

Discussion

Addition of SF_5 Building Blocks

In order to achieve the synthesis of novel SF_5-furazan-based energetic materials, the first step was the synthesis of a reliable SF_5-acetyl building block that would react with amino furazans efficiently. Figure 2-4 presents the four SF_5-acetyl building blocks that were prepared within this project.

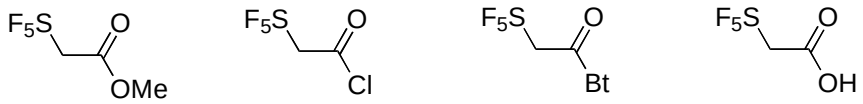

24 **26** **29** **25**

Figure 2-4. SF_5-acetyl building blocks.

The synthesis of methyl 2-pentafluorosulfanylacetate **24**,[21] pentafluorosulfanylacetyl chloride **26**,[90] and pentafluorosulfanylacetic acid **25**,[90,91] have been previously reported. The pentafluorosulfanyacetyl chloride has been synthesized by the addition of SF_5Cl to ketene; however, the possibility of a large-scale production is

limited by the use of ketene and an autoclave. The SF_5-acetic acid **25** was synthesized in high yields from the acetyl chloride **26**, and by the oxidation of the SF_5-acetaldehyde,[91] but only 20% yield is obtained under this method. Then, part of this project was to synthesize each of these materials by a more efficient method.

Scheme 2-3 showed the synthesis of methyl 2-pentafluorosulfanylacetate **24**, which can be done in very good yield according to given method. Scheme 2-5 shows the hydrolysis of **24** to produce the acid in good yield. The acid is then used to prepare the SF_5-acetyl chloride using a method similar to that previously reported by Sitzmann.[83] Lastly, Scheme 2-7 presents the synthesis of the benzotriazole derivative of the SF_5-acetic acid in excellent yield, using a similar methodology to that reported by Katritzky.[84]

We believed that any of these SF_5-acetyl building blocks should be sufficiently reactive regarding a nucleophilic attack by an aromatic amine. However, the lack of nucleophilicity of the aminofurazan derivatives turned out to be a major problem within this project. The p*K*a values (NH_3^+) of some aminofurazan derivatives have been previously reported and the values are presented in Table 2-1.[68]

Table 2-1. p*K*a values of some aminofurazan derivatives.

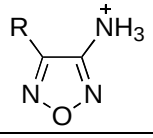

R	pKa
NH_2	-1.94
CH_3	-2.15
OCH_3	-2.51
N_3	-2.88
NO_2	-4.46

The p*K*a values in Table 2-1 indicate the high electron-withdrawing ability of the furazan ring, which diminishes the nucleophilicity of the amino group. A second

approach to support the high electron-withdrawing ability of the furazan ring was done by Fruttero et al. in 1998 on 3-methyl-furazan.[51] In this publication two methods were utlized to obtain the Hammett inductive (σ_I) and resonance (σ_R) values: 1) The meta and para benzoic acid derivatives were prepared and the pKa values were measured; and 2) using correlation and Equations 1-4 to 1-7 proposed by Taft, the meta and para fluorobenzene derivatives were prepared and the fluorine chemical shifts were measured in highly diluted methanol-d_4 (Figure 2-5).

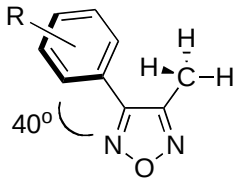

R = COOH, F

Figure 2-5. Methyl-furazan derivatives synthetized by Fruttero.

Although both methods have been criticized, they are still widely used and accepted. Using these two methods the authors concluded that the furazan ring has a strong attractor character similar to that observed for the halogens. The authors included the methyl group in the furazan in order to increase the stability of the compound and claimed that this should not effect their measurements. However, we performed the ground state calculation on the fluorobenzene derivatives and they indicate that due to the vicinal methyl group, the benzene ring in Figure 2-5 is twisted about 40 degrees out from the plane of the furazan ring, which suggest that there is not full conjugation between the benzene and furazan rings and that both the pKa's and the fluorines chemical shifts measurements will not be entirely accurate. The quantum chemical calculation was done at B3LYP/6-31+G(d,p) level of theory using Gaussian 03 Rev E01 software package.[92]

Based on these findings, the reactivity of the SF_5-acetyl group must then be great in order to allow the possibility of a nucleophilic attack. This must be the reason why most of the amide-forming reactions with DAF have required acyl chlorides as acylating agents.[93]

Although the reactivity of the acyl chloride **26** with DAF is good enough to obtain the desired products, the reaction with SF_5-acetic acid in the presence of EDC proved to be not only more efficient, but also cleaner, which made it a more reliable method. Using this methodology we were able to prepare a new series of SF_5-furazan energetic materials (Schemes 2-9 and 2-10).

All synthesized materials exhibited good thermal and chemical stability, with the exception of 3-*N*-pentaflurosulfanylacetamide-4-(1*H*-tetrazol-5-yl)-furazan **31**. This product is chemically stable in the solid state, but easily decomposes in solution. The presence of water (hydrolysis) or any other weak nucleophile leads to attack of the carbonyl group (Scheme 2-24) and destruction of **31**.

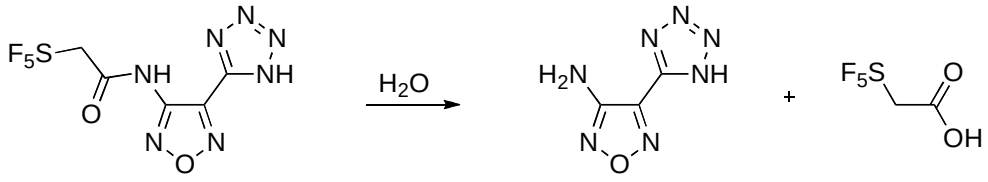

31 **11** **25**

Scheme 2-24. Hydrolysis of compound **31**.

This can be explained the enhancement of the electron-withdrawing ability of the furazan by the presence of the high electron-withdrawing tetrazole, which makes the carbonyl group of **31** more electron deficient. All other aminofurazans were unreactive to either the SF_5-acetyl chloride **26** or the SF_5-acetic acid **25** – EDC method.

There is no significant information related to the reactivity of aminofurazans other than the few reported p*K*a values of some derivatives (Table 2-1) and the Hammett resonance and inductive values. In order to have a better understanding of the lack of reactivity of other aminofurazan derivatives used in this project as starting materials, the ground states of some of these materials were calculated at B3LYP/6-31+G(d,p) level using Gaussian 03 Rev. E.01[92] and the calculated C-NH_2 bond lengths were correlated with the p*K*a values reported by Tselinskii (Table 2-2).[68]

Table 2-2. p*K*a vs C-NH_2 bond distance.

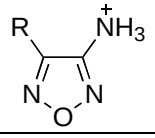

R	pKa	C-NH_2 (Å)
NH_2	-1.94	1.38516
CH_3	-2.15	1.38093
OCH_3	-2.51	1.37397
N_3	-2.88	1.36974
NO_2	-4.46	1.34938

y=71.67±4.9x – 101.11±6.7 - R^2=0.9914.

The equation derived from the plot of was found to be y=71.67x – 101.11, with a correlation coefficient of R^2=0.9914. This correlation coefficient indicates that there is strong correlation between these two parameters. Using the equation from the plot in Table 2-2 and the calculated C- NH_2 bond distances from the ground states of some aminofurazans used in this project, the p*K*a values (NH_3^+) were estimated in order to understand and establish an order of reactivity (Table 2-3).

Combining the experimental results with the calculated p*K*a values, it is possible to see that for any furazan-NH_3^+ that has a p*K*a greater or equal to -3.72 will give a product. This is the case of the 3-amino-4-(tetrazo-5-yl-furazan), which can yield the

desired product, but which is not stable in solution (Scheme 2-24). The high electron-withdrawing ability of the tetrazole in addition to the same effect from the furazan ring pushes the amino group to the limit of its reactivity with respect to nucleophilic attack.

Table 2-3**.** Calculated p*K*a values using the plot from Table 2-2.

R	C-NH_2 (Å)	pKa
1	1.38516	-1.94 [a]
4	1.34938	-4.46 [a]
5[b]	1.35792 [c]	-3.77 [c]
	1.35014 [d]	-4.33 [d]
12	1.35046	-4.31
13[b]	1.37266	-2.71_4 (NH_2)
	1.39755	-0.93_5 (NH)
20	1.3625	-3.44_9
21[b]	1.36186 [c]	-3.49_7 [c]
	1.36957 [d]	-2.94_7 [d]
11	1.35872	-3.72_5

a. Exp. Value Ref.[68]. b. Unsymmetrical amino groups, two values are calculated. c. NH_2 group far from the =N-O^- moiety. d. NH_2 group closer from the =N-O^- moiety

The azoxy-aminofurazan **5** did not yield any product, and it has calculated p*K*a values of -3.77 and -4.33 for its unsymmetrical amino groups. There is a possibility that the desired product is formed, but that it is unstable under the reaction conditions.

Interestingly, the dihydro-azo-diaminofurazan **13** has calculated p*K*a values greater than -3.72 (-2.71 and -0.93), but it did not give products with either the SF_5-acetyl chloride or the SF_5-acetic acid – EDC method. Considering the calculated C-N distances (Table 2-3), it is our belief that the NH from the hydrazine moiety is more reactive than the -NH_2 group and it reacts with the SF_5-acetyl building block, but the product is unstable due to the adjacent NH group.

The reaction of aminofurazans with SF_5-acetic acid in the presence of EDC proved to be the most efficient and cleaner method for preparation of the desired compounds. The only weakness of this methodology is that the intermediate formed from the SF_5-

acetic acid and the EDC, which is rapidly formed after mixing these two reagents, is unstable. This intermediate requires rapid attack by a decent nucleophile (Scheme 2-25); otherwise it will decompose, destroying the SF_5-material in the process.

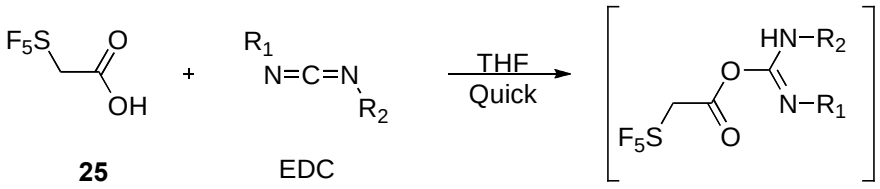

25 EDC

Scheme 2-25. Intermediate between the SF_5-acetic acid and EDC.

The weakness of the SF_5-acetic acid - EDC method takes on more importance when the lack of nucleophilicity of the amino furazans is considered. In order to overcome this problem, the addition of the SF_5-acetic acid was done slowly (drop wise) to the reaction mixture, which contains the aminofurazan and the EDC. In this manner the concentration of the aminofurazan is always high while the intermediate is forming in the reaction mixture.

The synthesis of methyl 2-chloro-3-pentafluorosulfanyl-2-methoxypropanoate **37** from an α,β-unsaturated carbonyl starting material was very efficient under the triethylborane method (Scheme 2-11). As mentioned previously, the addition of SF_5Cl to α,β-unsaturated compounds with Et_3B could not be achieved due to the electron deficiency of the β- carbon and the possible radical polymerization at the α position. Both problems were solved by adding a methoxy group at the α carbon, which led to an 82% yield of SF_5Cl addition. It was thought that this material, as masked version of the dicarbonyl compound, could be used as a building block for the synthesis of SF_5-furazan-based energetic materials. However, the reactivity of the carbonyl (ester) was low and no further functionalization was possible (Scheme 2-12).

The addition of SF_5Cl to fluorinated double bonds is impossible due to the electron deficiency of the carbon where the SF_5 is added. In order to reduce the amount of hydrogens and increase the amount of fluorines, changing the hydrogens at the methylene position of the SF_5 methyl ester **24** was attempted (Scheme 2-17). It is believed that due to the presence of the carbonyl and the SF_5 group there might be an enol equilibrium in this molecule in solution, giving a chance of fluorination at the methylene position by using electrophilic fluorine. Unfortunately this reaction did not yield any fluorination product. The use of different bases to increase the chances of an enolate destroyed the starting material; this last result was expected based on previous experiments done by other group members. Trying to achieve this goal, a stronger reaction conditions was tried. F_2 (10%) in N_2 was bubbled through a solution of acetonitrile containing the SF_5 compound. Interestingly, no fluorinated product was obtained, but neither did the product decompose. This could mean that the expected ketone – enol equilibrium does not exist for this molecule.

The use of 2,2-dinitro-propane-1,3-diol **42** as a building block for energetic materials has been previously reported using SF_5NCO, as well as other polynitroalcohols, to produce biscarbamates (Scheme 2-18).[29,89] Based on these reports we attempted the reaction the reaction between 2,2-dinitro-propane-1,3-diol **42** and SF_5-acetic acid – EDC or SF_5-acetyl chloride under different reaction conditions without any success (Scheme 2-14). The dinitro-diol exhibited very low nucleophilicity, and decomposed when heated. It also decomposed quickly under basic conditions, making it difficult to add the SF_5-acetyl group.

During the process of making new SF_5-energetic materials, it was noted that the synthesis of 4-(1*H*-tetrazol-5-yl)-3-amine-*N*-(2,4,6-trinitrophenyl)furazan **41** had not been reported. We attempted the synthesis of this material and obtained a 65% yield (Scheme 2-13). Due to the high energy that the three rings present on this compound, it was expected that this material should have good energetic properties.

The use of SF_5NCO as a derivatizing reagent was in some ways disappointing. The high reactivity of this material towards the addition of amines or alcohols was thought to make the perfect building block to react with the poorly nucleophilic aminofurazans. However, it was this same high reactivity that limited the solvents that could be used, after which the solubility of the aminofurazans became the problem. Only two solvents were feasible: dichloromethane and 1,2-dichloroethane. Other, similar solvents may also work, but the solvent properties would also be similar.

Although the reactions could be done without the presence of a solvent, the high melting points of some aminofurazans, along with the limited amount of SF_5NCO we had, made this method impractical. The available amount of SF_5NCO forced us to run reactions at milligram scale, so that it would be possible to carry out as many reactions as possible.

The reaction between DAF **1** and SF_5NCO proved to be straightforward. 3,4-Diaminofurazan has a very low solubility in dichloromethane (0.5 mg/10 mL slv), but sufficient to allow the reaction proceed at room temperature. In 4 hours the reaction was almost complete (>90% by ^{19}F NMR), and in 16 hours it was done, 99% yield in a 1:1 DAF:SF_5NCO reaction.

Interestingly, the product 4-amino-3-(3-pentafluorosulfanylurea-1-yl)furazan **48** is insoluble in the dichloromethane and even at higher temperature and more than 2 equivalents of SF_5NCO, the reaction only produces the mono addition product **48**. This compound was observed to be stable as a solid. However it decomposes in the presence of poor nucleophiles such as acetonitrile or water (moisture), as well as under acidic conditions. This is due to the high electron deficiency of the carbonyl group induced by both the SF_5 and furazan moieties.

In a similar manner, the reaction between ANF **4** and SF_5NCO was successful, but only 20% conversion to product could be obtained. It is important to remember that according to Table 2-1, ANF is the worst nucleophile of the whole aminofurazan series. Unlike the other aminofurazans, ANF is highly soluble in DCM. This is why it was concluded that, in this case, it was a problem of reactivity, and not of solubility. Several SF_5NCO equivalents were added (up to 4 equiv.), and long reaction times (up to 15 days) were tried, but the result was the same as when using 1.5 equiv. of SF_5NCO and 24 hours of reaction. A maximum of 20% of product could be obtained. Heating the reaction led to a decrease in the amount of product obtained.

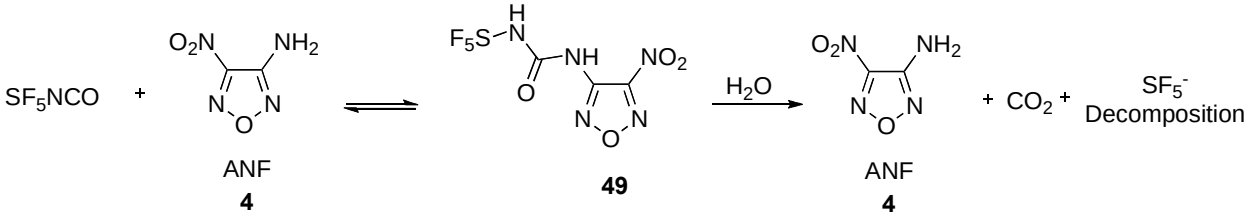

Scheme 2-26. Reaction between ANF **4** and SF_5NCO.

The product 4-nitro-3-(3-pentafluorosulfanylurea-1-yl)furazan **49** proved to be much more unstable to moisture and weak nucleophiles than **48**. Based on the very low nucleophilicity ANF, we believe that there is an equilibrium established under these

reaction conditions, such that, even in the presence of 4 equiv. of SF_5NCO, the reaction will not go significantly further (Scheme 2-26).

Nitration and Oxidation Reactions

It was attempted to improve the performance of our compounds by *N*-nitration of the amide moiety. However, all such reactions failed. When nitration was tried under mild conditions, the starting material was recovered, probably because the lone pair of the nitrogen at the amide function is a relatively poor reducing agent. However, when strong nitration conditions were used, the SF_5-starting material was destroyed. It has been reported by Sheremetev in 2005, that *N*-nitration of 3-acetamide-4-methyl-furazan produces 3-nitramino-4-methylfurazan, which is also be what must be happening in our case (Scheme 2-27).[60]

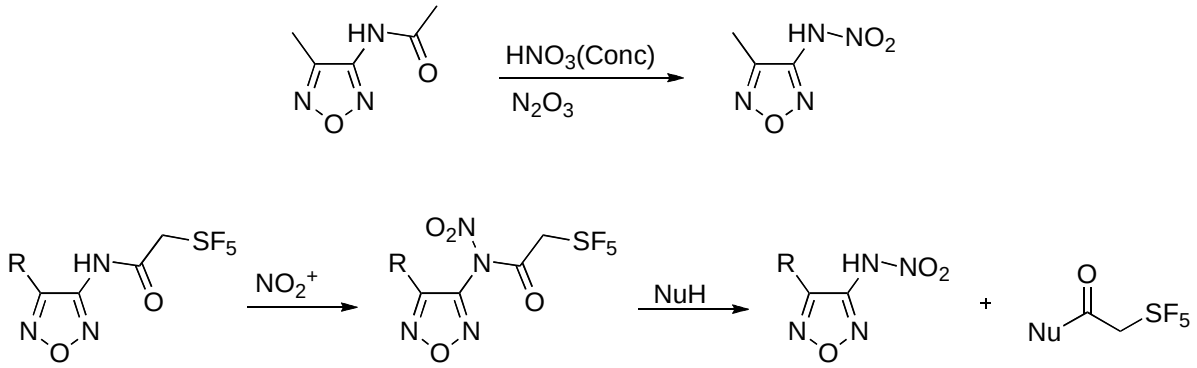

Scheme 2-27. Decomposition of the SF_5-containing energetic material after *N*-nitration.

It is important to mention that no SF_5 product of any kind was seen by ^{19}F NMR after the reaction, which indicates that the SF_5 starting material/product decomposed. The high electron-withdrawing effect from the furazan ring, the nitro group and the pentafluorosulfanyl group increase the electron deficiency of the carbonyl group, making the SF_5-acetyl group an excellent leaving group in the presence of weak nucleophiles such as water or acetonitrile.

The second approach by which we tried to improve the C/O balance was the oxidation of the amino groups (when available) to nitro groups (Schemes 2-21 and 2-22). Three different methods were used to oxidize the amino group in DASF5-DAF **27** to a nitro group. Surprisingly, the H_2O_2 (30%) with H_2SO_4, which was anticipated to give the azoxy derivative, gave the nitro compound, with no presence of the expected product. This might be due to the electron-withdrawing ability of the SF_5-acetamide group. Similar methods were tried with compounds **29** and **30**, but oxidation was not observed for them. Instead, in the case of **30**, the ratio of products was changed (Scheme 2-28).

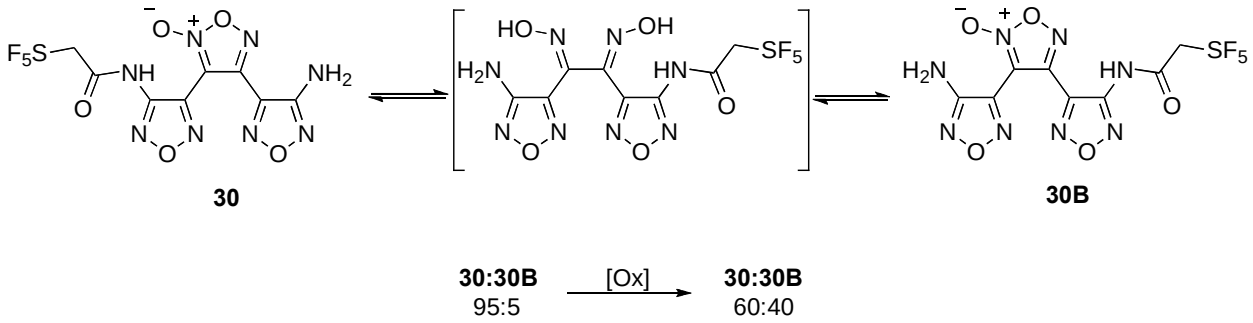

Scheme 2-28. Change in the ratio between **30** and **30B** after oxidation attempt.

The same methods were applied to the 3-amino-4-SF_5-urea-furazan **48**, but in all cases ANF **4** was obtained. As previously mentioned, the urea moiety is sensitive to weak nucleophiles due to the electron withdrawing effect of both the furazan ring and the SF_5 group. The presence of a nitro group ortho to the urea enhances the leaving group ability of the SF_5-urea moiety (Scheme 2-22).

It is important to emphasize that the SF_5 group in the acetamide moiety showed stability under strong oxidizing conditions such as H_2O_2 (50%) or HOF/CH_3CN, which allowed us to obtain compound **50** in good yield (Scheme 2-21).

The third and final attempt to improve the performance of our energetic materials involved the reaction between the available amino groups and picryl chloride (Scheme 2-23). However, we were unable to obtain any condensation product. Under neutral conditions the starting material was recovered and under basic reaction conditions the material was destroyed. Although the picryl chloride is a very reactive material towards nucleophilic attack, the presence of the SF_5-acetamide or SF_5-urea functionality is withdrawing enough to decrease the nucleophilicity of the amino group. On the other hand, the decomposition of the starting material under basic conditions was not a surprise since both the SF_5-acetamide or SF_5-urea contains highly acidic hydrogens that upon deprotonation might lead to the destruction of the SF_5 group.

Properties of the Synthesized SF_5-Furazan-Based Energetic Materials.

Figure 2-6 presents all the new energetic materials that we were able to synthesize within this project. Three different methods were used to characterize these materials: shock sensitivity, thermal stability, and performance using Cheetah calculations.

The impact sensitivity was evaluated qualitatively by placing 5-10 mg of sample in a flat polished area, and hitting the sample with a flat-head hammer. With the exception of compound **41**, all of the synthesized materials exhibited no sensitivity to impact under the conditions of this test. Sample **41** showed partial decomposition. By comparison, when nitroguanidine was tested in the identical manner, detonation occurred. Although there is a more technical procedure to evaluate the impact sensitivity, this particular test exemplifies the intrinsic ability of the SF_5 group to reduce the impact sensitivity of HEM.

In order to evaluate the thermal stability of the new materials, thermogravimetrical analysis (TGA) and Differential Scanning Calorimetry (DSC) were utilized for all

compounds in Figure 2-6 using a TA instrument SDT Q600, TGA/DSC combo instrument, which uses a ventilated system (open-pan). An example of a DSC/TGA thermogram is shown is Figure 2-7 and more detailed information is presented in Table 2-4.

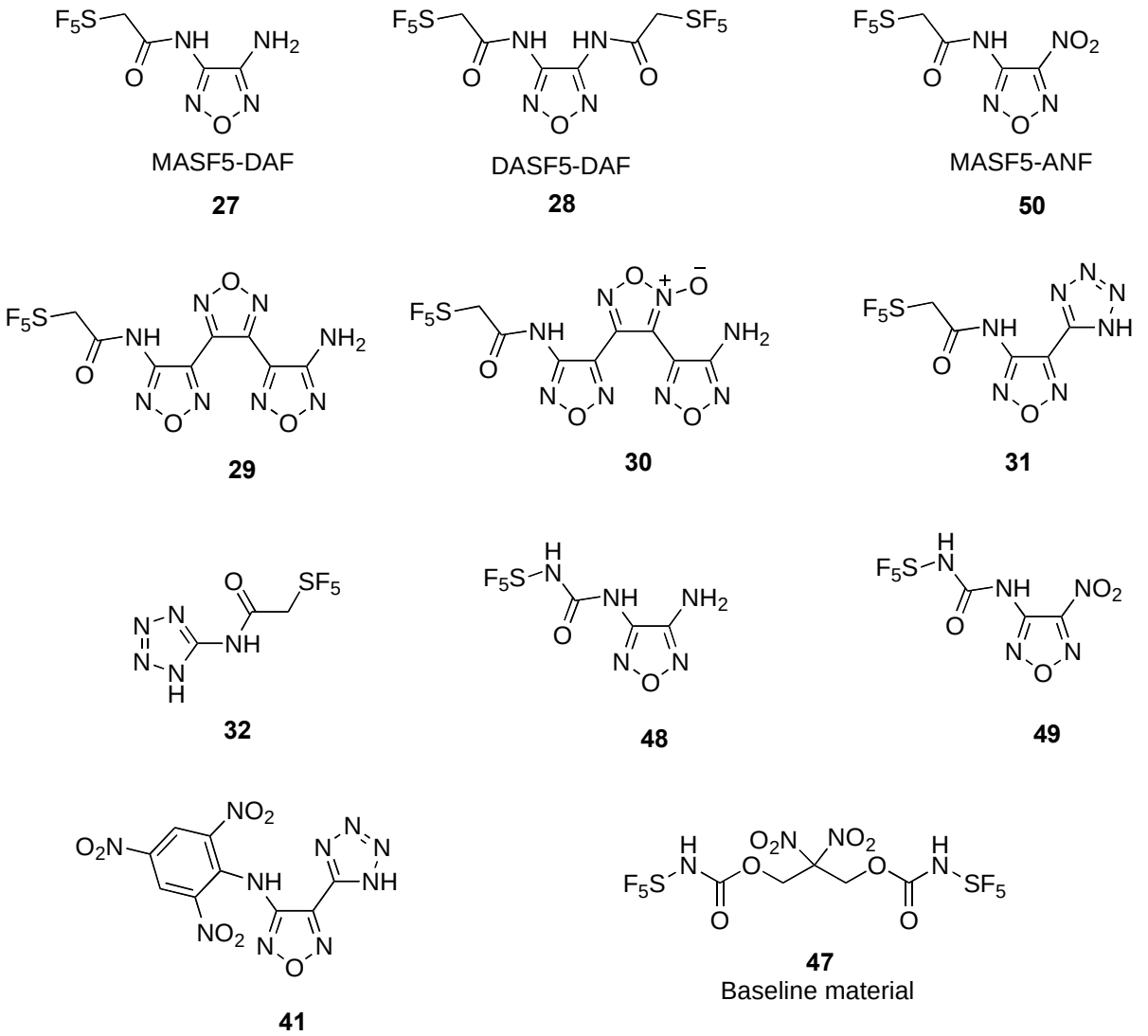

Figure 2-6. New energetic materials synthesized in this project.

Figure 2-7 shows in green the loss of weight vs. the temperature. Compound **28** has a 5% weight loss at 243.73^{o}C which indicates high thermal stability. At 293^{o}C it has

lost almost 80% of its weight and remains the same even at temperature up to 1000^{o}C. This indicates that there is a remaining mass that did not convert into gas. This is probably due to the lack of oxygen in the molecule. This problem is usually addressed in the final explosive material by mixing the desired compound with some oxidizers, which is essentially a material that will provide “oxygen” during the combustion process. The blue line shows the heat flow with an exotherm (energy release) at the maximum point of 282.43^{o}C with an energy release of 247.2 J/g, indicating that this and the other derivatives are promising as energetic materials.

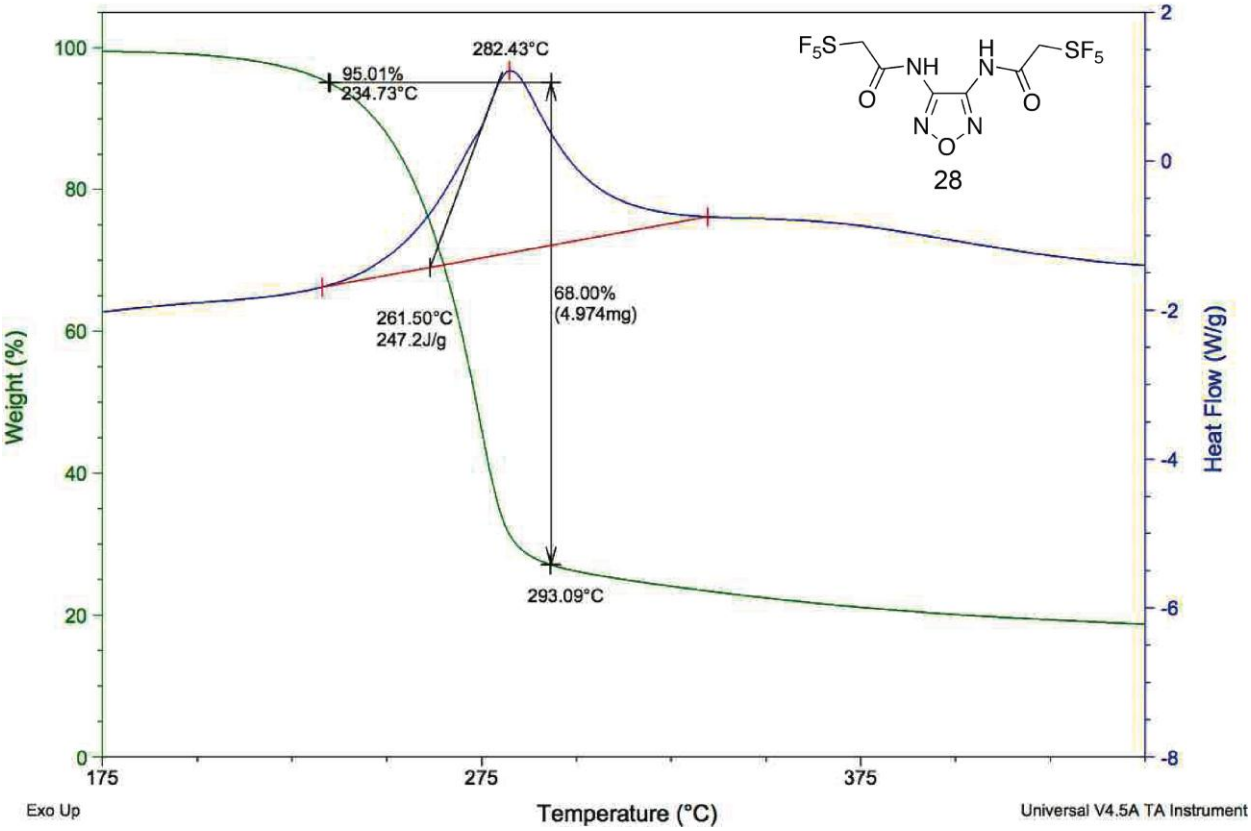

Figure 2-7. DSC/TGA thermogram of compound **28**

Compound **47** was taken as a baseline material. This compound has been previously synthesized,[89] and it exhibited good thermal stability. When compared to **47**, all of our new energetic materials exhibited from good (>100^{o}C) to excellent (>200^{o}C)

thermal stability. Between compounds **27** and **28**, there is a 65^{o}C difference in the starting decomposition temperature, where the bis-acetamide **28** is more stable than the mono-acetamide **27,** indicating that the addition of the SF_5-acetyl group increases the thermal stability of the energetic materials. Another example of this behavior is seen in compound **31**, such that even though its starting decomposition temperature is the second lowest value (100.45^{o}C), its starting material, the 3-amino-4-(tetrazol-5-yl)furazan, starts to decompose at 45.76^{o}C. However, this is not always the case since DAF starts to decompose at 200^{o}C and after the addition of one SF_5-acetyl group it lowers to 169.01^{o}C.

Table 2-4. Thermogram data of the synthesized energetic materials.

Compound	TGA-Temp. of Decomp. (^{o}C)	DSC (^{o}C, __, J/g)
27	169.01 - 245.95	149.79, endo, 76.38
		225.32, endo, 67.15
28	234.73 - 293.09	282.43, exo, -247.20
50	172.06 - 233.88	[161.98, 232.31], endo, 412.10
29	134.10 - 410.88	286.85, exo, -1023
30	214.81 - 382.10	[268.60, 325.27], exo, -1758
31	100.45 - 191.88	175.55, exo, -215.7
32	155.45 - 300.00	198.23, exo, -340.9
48	149.61 - 200.05	[159.28, 196.09], endo, 241.2
49	99.66 - 161.50	[114.46, 146.71], endo, 2481.0
41	141.00 - 201.46	172.58, endo, 55.52
	267.78 - 300.00	294.32, exo, -708.4
	732.75 - 971.64	895.99, endo, 2529
47	158.22 - 204.29	160.56, endo, 128.4

Compound **41** exhibits three stages of decomposition. This is characteristic of compounds that contain the tetrazole group. The retro-1,3-dipolar cycloaddition at the tetrazole group releases nitrogen at the first stage followed by a subsequent unknown decomposition process.

Our baseline material exhibited an endotherm at 160.56^{o}C, even though it was expected to exhibit an exotherm instead. The open-pan system used for this thermogram might not capture the energy liberated when gases are released rapidly. Four other materials also exhibited endotherms, whereas the other six energetic materials exhibited exotherms. The exotherms ranged up as high as -1758 J/g.

After considering its impact sensitivity and thermal stability, the most important way to evaluate these materials is through the density, pressure and speed of detonation. The densities and heats of formation (HOF) were calculated by using the group additive method, while the pressure and speed of detonation, P and D respectively, were calculated using Cheetah software v6 at the Lawrence Livermore National Laboratory (Table 2-5).

Table 2-5. Calculated performance data of the synthesized energetic materials.

Compound	Density (g/cm^3)	HOF (kcal/mol)	P (Gpa)	D(m/s)
27	2.01	-239.05	20.22	6741
28	2.05	-533.70	--	--
50	2.02	-251.56	29.48	7234
29	2.01	-109.65	26.12	7368
30	2.03	-109.17	28.62	7430
31	1.81	-169.13	17.85	7002
32	1.96	-174.52	--	--
48	2.11	-196.85	27.16	8049
49	2.10	-209.36	30.67	6862
41	1.54	147.35	18.25	6788
47	1.99	-623.00	23.73	6263

It is essential to remember that the density is one of the most important properties according to the semiempirical equations suggested by Kamlet and Jacobs.[26] Only two compounds, **28** and **32,** did not converge in the calculations when using the Cheetah software. The way SF_5 affects energetic materials upon detonation is still not fully

understood, and it is unknown why these two molecules did not converge during the calculations and they are still under study.

From Table 2-5 it is possible to see that all of the synthesized materials have from good to excellent densities. When compared with the baseline material, all but three have a greater density, and one of these three does not contain the furazan group (**32**), while another one does not contain an SF_5 group (**41**). This is consistent with the fact that a combination of these two groups has good potential to enhance the properties of energetic materials. Even though compound **41** has a positive HOF, it does not have the SF_5 group, which results then in a low density and relatively poor performance.

Pressure and speed of detonation for most of our materials are better than TNT, but below RDX and HMX. When compared to our baseline material, most compounds have better performance, indicating once more that SF_5 and furazan groups combine to give good energetic properties. When our materials are compared to the SF_5-containing energetic materials synthesized by Shreeve et al. [14,18] (Figure 2-1), where the average pressure and speed of detonation reported by Shreeve were 17.8-20.5 GPa and 6900-7100 m/s respectively, our materials performed much better, particularly in the pressure of detonation. The compounds in Prof. Shreeve's publications have higher heats of formation, but lower densities than our compounds.

Experimental Methods

Instrumentation

All ^{1}H NMR (300 MHz), ^{19}F NMR (282 MHz) and ^{13}C NMR (75 MHz) spectra were recorded in $CDCl_3$m, acetone-d_6 or DMSO- d_6 on VXR 300 spectrophotometer. Chemical shifts were referenced with TMS, $CDCl_3$ and $CFCl_3$. (0 for ^{1}H, 77.23 for ^{13}C and 0 for ^{19}F). Compounds were examined by high-resolution mass spectrometry

(HRMS), Finnegan 4500 gas chromatograph/mass spectrometer using chemical ionization (CI). Thermal analyses were taken in a TA instrument SDT Q600, TGA/DSC combo instrument. See appendix A to see relevant NMR spectra and DSC/TGA thermograms.

General Method for the Syntheses of Pentafluorosulfanylacetamide-Furazans

To a solution of aminofurazan (7.2 mmol, 1.5 equiv.) and 1-ethyl-3-(3-dimethylaminopropyl) carbodiimide (EDC) (9.6 mmol, 2.0 equiv.) in anhydrous THF (30 mL), was added dropwise with stirring in a pressure equalizing dropping funnel over 10 min. pentafluorosulfanylacetic acid (4.8 mmol, 1 equiv.) in anhydrous THF (15 mL) After the addition of the acid, 4-dimathylaminepyridine (DMAP) (0.48 mmol, 0.1 equiv.) was added, and the stirring continue for 16 h. The reaction mixture was then treated with 50 mL of water and extracted with ethyl acetate (3 x 30 mL). The organic solution was then dried over Na_2SO_4, filtrated, and the solvent remove under reduce pressure. The resulting solid (or oil) was purified by column-chromatography (silica gel, 4:1 CH_2Cl_2: Ethyl acetate).

3-Amino-4-N-(2-pentafluorosulfanylacetamide)-1,2,5-oxadiazole (**27**):White solid, 90% yield; mp (DSC) = 133.5^{o}C. ^{1}H NMR (DMSO-d6), δ 4.79 (q, J=9.0 Hz, 2H, CH_2), 6.00 (b, 2H, NH_2), 11.32 (b, 1H, NH); ^{19}F NMR (DMSO-d6), δ_A 83.60 (m, 1F), δ_B 71.30 (d, J_{AB}=149 Hz, 4F); ^{13}C NMR (DMSO-d6), δ 72.2 (m, CH_2), 144.0 (s, C-NH), 156.2 (s, C-NH_2), 160.0 (m, CO); HRMS (M-H, calc): 266.9981, found: 266.9992.

3,4-N,N'-bis-(2-pentafluorosulfanylacetamide)-1,2,5-oxadiazole (**28**): White solid 70% yield; mp (DSC,decomp.) = 234.7^{o}C; ^{1}H NMR (DMSO-d6), δ 4.82 (q, J=9.0 Hz, 4H-CH_2), 11.42 (b, 2H, NH); ^{19}F NMR (DMSO-d6), δ_A 83.57 (m, 1F), δ_B 71.49 (d,

J_{AB}=149 Hz, 4F); ^{13}C NMR (DMSO-d6), δ 71.8 (m, CH_2), 146.4 (s, C-NH), 160.0 (m, CO); HRMS (M+H, calc): 436.9794, found: 436.9796.

4-amine-4''-N-(2-pentafluorosulfanylacetamide)-[3,3':4',3'']-Ter-[1,2,5]-oxadiazole (**29**): Light yellow solid, 45% yield; mp (DSC) = 133.3^{o}C; ^{1}H NMR (DMSO-d6), δ 4.72 (q, J=9.0 Hz, 2H-CH_2), 6.66 (b, 2H, NH_2), 12.44 (b, 1H, NH); ^{19}F NMR (DMSO-d6), δ_A 83.53 (m, 1F), δ_B 71.53 (d, J_{AB}=149 Hz, 4F); HRMS (M+H, calc): 405.0153, found: 405.0161.

4-amine-4''-N-(2-pentafluorosulfanylacetamide)- 2'-oxy- [3,3':4',3'']-Ter-[1,2,5]-oxadiazole (**30**): Light yellow solid, 35% yield; mp (DSC) = 125.2^{o}C; ^{1}H NMR (DMSO-d6), δ 4.73 (q, J=9.0 Hz, 2H-CH_2), 6.67 (b, 2H, NH_2), 12.43 (b, 1H, NH); ^{19}F NMR (DMSO-d6), δ_A 83.51 (m, 1F), δ_B 71.46 (d, J_{AB}=147 Hz, 4F); HRMS (M-H, calc): 418.9951, found: 418.9966.

3-N-(2-pentafluorosulfanylacetamide)-4-(1H-Tetrazo-5-yl)-1,2,5-oxadiazole (**31**): Light yellow solid, 35% yield. m.p (DSC,decomp.) = 100.5^{o}C; ^{1}H NMR (DMSO-d6), δ 4.62 (q, J=9.0 Hz, 2H-CH_2), 11.03 (b, 1H, NH); ^{19}F NMR (DMSO-d6), δ_A 82.32 (m, 1F), δ_B 71.16 (d, J_{AB}=149 Hz, 4F). HRMS (M-H, calc): 319.9995, found: 320.0001.

5-N-(2-pentafluorosulfanylacetamide)-1H-tetrazole (**32**): White Solid, 80% yield; mp (DSC,decomp.) = 155.5^{o}C; ^{1}H NMR (DMSO-d6), δ 4.89 (q, J=9.0 Hz, 2H-CH_2), 12.75 (b, 1H, NH); ^{19}F NMR (DMSO-d6), δ_A 84.00 (m, 1F), δ_B 71.51 (d, J_{AB}=149 Hz, 4F); ^{13}C NMR (DMSO-d6), δ 72.0 (m, CH_2), 149.5 (s, =C-NH), 159.8 (m, CO); HRMS (M-H, calc): 251.9984, found: 251.9982.

Synthesis of 3-N-(2-pentafluorosulfanylacetamide)-4-nitro-1,2,5-oxadiazole (**50**): To a solution of 50% H_2O_2 (1.6 g) and concentrated sulfuric acid (1.1 g) at 0^{o}C,

160 mg of $Na_2WO_4.H_2O$ and 30 mg of 3-amino-4-(pentafluorosulfanylmethyl)furazan **(27)** were added in one portion. The mixture was stirred until the staring material disappears on the TLC (~16 h, 4:1 CH_2Cl_2: Ethyl acetate). The mixture was then treated with 5 mL of water and extracted with ethyl acetate. The solvent was remove under reduce pressure and the resulting oil purified by column-chromatography (silica gel, 4:1 CH_2Cl_2: Ethyl acetate), light yellow solid, 50% yield. m.p (DSC,decomp.) = 172.06^oC. ^1H NMR (DMSO-d6, ppm), δ 5.11 (q, J=9.0 Hz, 2H-CH_2), 11.87 (b, 1H, NH); ^{19}F NMR (DMSO-d6, ppm), δ_A 83.90 (m, 1F), δ_B 71.97 (d, J_{AB}=149 Hz, 4F); ^{13}C NMR (DMSO-d6, ppm), δ 71.6 (m, CH_2), 144.7 (s, C-NH), 158.2 (s, C-NO_2), 160.0 (m, CO). HRMS (M+H, calc): 298.9873, found: 266.9902.

General Method for the Syntheses of Pentafluorosulfanylurea-Furazans

To 30 ml of anhydrous DCM in a Glass Heavy Wall Pressure Vessel, closed with a septa at -40^oC, 7.8 mmol of pentafluorosulfanyl isocyanate was bubbled. Then, the septa was remove and quickly 7.8 mmol of aminofurazan were added, the septa is now replace by the sealed cap. The cold bath was removed and the reaction mixture was stirred for 24 h. After that the Vessel was open and the solvent evaporated under reduced pressure.

3-amino-4-N-(3-pentafluorosulfanylurea)-1,2,5-oxadiazole (**48**): White solid, 99% yield; mp (DSC,decomp.) = 149.61^oC; ^1H NMR (Acetone-d6), δ 10.55 (b, 1H, NH-SF_5), 8.83 (b, 1H, NH-CO), 5.57 (b, 2H, NH_2); ^{19}F NMR (Acetone-d6), δ_A 77.44 (m, 1F), δ_B 72.40 (d, J_{AB}=149 Hz, 4F); ^{13}C NMR (Acetone-d6), δ 145.0 (S, C-NH_2), 148.7 (s, C-NH), 153.0 (m, CO); HRMS (M-H, calc): 267.9933, found: 267.9941.

3-N-(3-pentafluorosulfanylurea)-4-nitro-1,2,5-oxadiazole (**49**): Yellow Solid, 20% NMR yield; mp (DSC,decomp.) = 99.7°C; ^{1}H NMR (Acetone-d6), δ 11.18 (b, 1H, NH-SF_5), 9.19 (b, 1H, NH-CO); ^{19}F NMR (Acetone-d6), δ_A 76.78 (m, 1F), δ_B 72.13 (d, J_{AB}=155 Hz, 4F); HRMS (M-H, calc): 297.9575, found: 297.9678.

Synthesis of 3-amine-N-(2,4,6-trinitrophenyl)-4-(1H-tetrazol-5-yl)-furazan (**41**): To a solution of 3-amino-4-(1H-tetrazol-5-yl)-furazan (153 mg, 1mmol) and K_2CO_3 (2 mmol, 2 equiv.) in acetonitrile (10 ml), was added picryl chloride in one portion (371 mg, 1.5mmol, 1.5 equiv.). The reaction mixture was stirred overnight, and the precipitate was filtrated and washed with acetonitrile. The solid was recrystallized form Acetonitrile: Yellow solid, 65% yield; mp (DSC,decomp.) = 141.2°C. ^{1}H NMR (acetone-d6), δ 8.56 (s, 2H, =CH), 6.53 (b, 1H, NH); HRMS (calc): 387.0157, found: 387.0155.

Synthesis of 1-(1H-benzotriazolyl)-2-pentaflurosulfanylethanone (**29**)

To a solution of SF_5-acetic acid (50 mg, 0.27mmol) in CH_2Cl_2 (1 mL) was added dropwise a mixture of $SOCl_2$ (22 μL, 0.29 mmol, 1.1 equiv.) and 1H-benzotriazole (96 mg, 3 equiv.) in CH_2Cl_2 (1.5 mL) and stirred for 4 h at r.t. the white precipitate was filtered off and the organic solution evaporated under reduce pressure. The resulting oil was purified by flash colum-chromatography (silica gel, CH_2Cl_2), recollecting 73.31 mg of product (95% yield): ^{1}H NMR ($CDCl_3$), δ 5.43 (q, J=7.2 Hz, 2H), 8.30 (d, J=8.2 Hz, 1H), 8.12 (d, J=8 8.2 Hz, 1H), 7.75 (t, J= 8.4 Hz, 1H), 7.60 (t, J= 8.4 Hz, 1H); ^{19}F NMR ($CDCl_3$), δ_A 77.0 (m, 1F), δ_B 71.6 (d, J_{AB}=151 Hz, 4F). HRMS (calc M-H^+): 288.0230, found: 288.0243.

Synthesis of methyl 2-chloro-3-pentafluorosulfanyl-2-methoxypropanoate (**37**) : To a three-necked flask equipped with a dry ice reflux condenser 5 g (43 mmol) of

2-methoxypropenoate **36** and 215 mL of hexane were added and cooled to -40^{o}C. 10.5 g (64.6 mmol, 1.5 eq) of SF_5Cl were added slowly and the solution stirred for 5 min before the addition of 6.46 ml (6.46 mmol, 0.15 eq) of Et_3B 1M in hexane. The solution was stirred for 2h at -30^{o}C and then allows warming to r.t. The mixture was hydrolyzed with aqueous $NaHCO_3$ (10%), and the organic layer dried over $MgSO_4$. The solvent was remove under reduce pressure, resulting in 11.96 g (82% yield) of product: colorless liquid; ^{1}H NMR ($CDCl_3$), δ 3.79 (s, 3H, OCH_3), 3.90 (s, 3H, CO_2CH_3), 4.29 (m, 1H, $CHSF_5$), 4.59 (m, 1H, $CHSF_5$); ^{19}F NMR ($CDCl_3$), δ_A 80.4 (m, 1F), δ_B 67.9 (d, J_{AB}=145 Hz, 4F). HRMS (calc M-H^{+}): 278.9881, found: 278.9882.

CHAPTER 3
CONFORMATIONAL AND 19F-19F COUPLING PATTERNS ANALYSIS IN MONO-SUBSTITUTED-PERFLUORO-[2,2]-PARACYCLOPHANES BY COMPUTATIONAL CALCULATIONS

Introductory Remarks

The chemistry of perfluoro[2.2]paracylophane (F8) was introduced in Chapter 1. During the course of studying the reactivity of F8 by Dolbier et al.,[45] new mono-substituted-F8 derivatives were synthesized. The new compounds display unusual ^{19}F-^{19}F coupling patterns (^{4}J and ^{5}J) that suggest a skewed geometry in which the upper deck moves towards or away from the substituent (Figure 3-1). Neither the different configurations (towards or away) nor the unusual ^{19}F-^{19}F coupling patterns could be explained with traditional theory.[1]

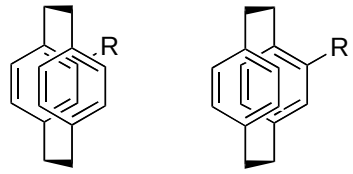

Figure 3-1. Towards and away upper deck orientations

Quantum chemical calculations were performed at the HF/6-311+G(d,p)/ /B3LYP/EPR-III level of theory using Gaussian 03,[92] and they shed light on the unusual structures and coupling of F8 and its derivatives. However, before I get into the results and discussion of this project, some important background must be mentioned.

Calculated spin-spin coupling constants include the four isotropic Ramsey terms, Fermi contact (FC), spin-dipolar (SD), paramagnetic spin orbit (PSO), and diamagnetic spin orbit (DSO) contributions. It is the sum of these four contributions that gives value

[1] Reproduce in part with the permission from *Magn. Reson. Chem*. **2011**, 49 (3), 93-105. License Number: 2730251383944

to the final coupling constant. Although final value is the one that can be seen experimentally, the four contributions can be calculated to help understand the mechanism of the coupling and also hints at the electronic structure of the molecule.[94,95]

A spinning nucleus could simply be considered as a moving charged particle. Any particle that is moving with a charge simultaneously generates an electric current and a magnetic field. The magnetic field of a nucleus will induce both of the following local effects: 1) Electron spin polarization and 2) orbital ring currents. Since the molecule is connected via bonds that are made by electrons, and the electrons “communicate” using Coulombic interactions, the mechanism by which the coupling will be transmitted is an extension of the local effects. The FC and the SD terms are part of mechanism 1 and the PSO and DSO terms are part of mechanism 2. The FC mechanism takes place in both interacting nuclei when the electron spin is at the site of the nuclear spin. This requires that the electron has a non zero probability of being at the same position as the interacting nucleus (tunnel effect). The SD has a similar interaction but the electron is not at the coupling nuclei position; this phenomena is similar to the interaction of two small magnets averaged in space and time. The PSO and DSO mechanisms are the interactions between the electronic spin and its motion around the generated nuclei orbital current. This interaction could be either paramagnetic or diamagnetic.[94-98]

Short range couplings (bonds (n) ≤ 3) can be understood simply as exchange interactions present in the bonds, which have contributions from all four isotropic Ramsey terms, with a major contribution from the FC term, followed by the PSO and DSO terms. Long range coupling (n ≥ 4) could be transmitted through bonds, which requires hyperconjugative interactions, or through space (TS), which could be

transmitted by 1) “contact” of the interacting nucleus, 2) hyperconjugative interactions or 3) both “contact” and hyperconjugation.[95,98]

Long range couplings transmitted through bonds in saturated systems have hyperconjugative interactions that are categorized as “negative”, and are of the type LP→σ* and σ→σ*. In the case of unsaturated systems they are categorized as “positive”, have higher values and are of the type LP→π*, π→π*and σ→π*. In both of these cases the FC term is the main contributor to the coupling and the value of the coupling constant depends on the efficiency with which the hyperconjugation is transmitted.[95,98]

The through space (TS) mechanism by “contact” generally involves the superposition of the electronic clouds of the interacting nuclei, sometimes with the help of an intermediate moiety that connects both coupling nucleus. As it might be expected, the TS mechanism depends mainly on the distance and angle by which both atoms are interacting to each other. In the particular case of fluorine-fluorine coupling interactions, it is generally accepted that the coupling goes through the “contact” interaction of their lone pairs.[96-98]

On the other hand, TS coupling due to hyperconjugation depends on the interaction of occupied and vacant molecular orbitals (“mix” functions). These long range couplings could also be expressed in terms of the molecular orbitals. Specifically, the canonical molecular orbitals (CMOs) are expanded in terms of the natural bond orbitals (NBOs), which helps to explain the Fermi Contact Coupling Pathways by analyzing the CMOs (FCCP-CMOs).[95] The FCCP-CMO analysis shows that there is at least one common atom between the occupied and virtual molecular orbitals that will

transmit the spin polarization and generate the coupling. The efficiency of the coupling is then limited to the energy gap for the transition between the occupied and virtual orbitals that participate in the coupling.

The following expanded theoretical explanation of the long range transmission mechanism has been contributed by Dr. Contreras and Dr. Tormena, both of them whom collaborated with us in the theoretical aspects of this research project.

It may be recalled that CMOs satisfy the Pauli exclusion principle and, therefore, the Fermi hole spans the whole spatial region of each CMO. Since it is known that the FC term is transmitted like the Fermi hole,[99,100] the spin information corresponding to the FC term also spans that spatial region. Therefore, the studied coupling constants ${}^{n}J^{FC}_{F,F'}$ are expressed in terms of CMOs, where n stands for the number of formal bonds separating the coupling fluorine nuclei (Equation 3-1). To identify relevant CMOs for a given coupling, its expression in terms of the polarization propagator approach, PP, at the RPA (Random Phase Approximation) is employed (Equation 3-2).

$$ {}^{n}J^{FC}_{F,F'} = \sum_{ia,jb} {}^{n}J^{FC}_{ia,jb}(F,F') \qquad (3\text{-}1) $$

Where, *i* and *j* stand for occupied CMOs, while *a* and *b* stand for vacant CMOs, and each sum term in Equation 3-1 can be written as in Equation 3-2.[101]

$$ {}^{n}J^{FC}_{ia,jb}(F,F') = {}^{3}W_{ia,jb}[U^{FC}_{ia,F}U^{FC}_{jb,F'} + U^{FC}_{ia,F'}U^{FC}_{jb,F}] \qquad (3\text{-}2) $$

Where $U_{ia,F}$ ($U_{jb,F}$) are the so-called “perturbators”, i.e. the matrix elements $U^{FC}_{ia,X} = \langle i|\delta(\vec{r}_X)|a\rangle$ of the FC operator, $\delta(\vec{r}_X)$, i.e. the Dirac’s delta function, between the occupied *i* (*j*) and vacant *a* (*b*) CMOs evaluated at the sites of the F (F’) coupling nuclei.

$$ {}^{3}W_{ia,jb} = ({}^{3}A - {}^{3}B)^{-1}_{ia,jb} \quad (3\text{-}3) $$

Equation 3-3 shows the elements of the triplet PP matrix, and they can be expressed in terms of orbital energies, □□□and molecular orbital integrals (Equation 3-4).

$$ {}^{3}A_{ia,jb} = (\varepsilon_a - \varepsilon_i)\delta_{ab}\delta_{ij} - \langle aj|bi\rangle \text{ and } {}^{3}B_{ia,jb} = \langle ab|ji\rangle \quad (3\text{-}4) $$

Each sum term in Equation 3-1 ${}^{n}J^{FC}_{ia,jb}(XY)$, is dubbed an FCCP, and depends on both the ${}^{3}W_{ia,jb}$ matrix element and on the "perturbators", $U_{ia,F}$ ($U_{jb,F}$), i.e., a given FCCP is non-negligible whenever both types of terms are simultaneously significant. Therefore here is described very briefly under which conditions those types of terms are significant.

The ${}^{3}W_{ia,jb}$ diagonal matrix elements, i.e. those satisfying *i* = *j* and *a* = *b*, are larger than non-diagonal terms. They depend explicitly and strongly on the energy gap between the vacant *a* and the occupied *i* CMO; □$_{a,i}$ = □$_a$ – □$_i$: they decrease when □$_{a,I}$ increases and vice versa. However, it is important to point out that, for a given coupling constant, many diagonal elements of the PP matrix are also negligibly small.

"Perturbator" $U_{ia,F}$ terms are important whenever there is a substantial overlap between *i* = *j* and *a* = *b* orbitals at the positions of both coupling nuclei. For a significant diagonal PP matrix element one occupied and one vacant CMO determine an efficient FCCP; those orbitals can be spotted when observing their respective NBO expansions. In fact, to have an efficient FCCP, the occupied CMO should be contributed by □-bonds or lone-pairs (excluding those of pure □ character) containing the coupling nuclei, and the unoccupied CMO should be contributed by antibonding □-orbitals containing the

coupling nuclei. It is also recalled that only the diagonal ${}^{3}W_{ia,jb}$ matrix elements depend solely upon the virtual-occupied orbital energy gap, $\Delta_{a,i}$ ($\varepsilon_a - \varepsilon_i$). With this in mind it is easy to identify the CMOs that could constitute efficient FCCPs for a given coupling constant.

Results and Discussion

Ground State Calculations

The ^{19}F NMR spectra of the new mono-substituted perfluoro[2.2]paracyclophanes (F8) displayed unusual ^{19}F-^{19}F coupling patterns (^{4}J and ^{5}J) that suggested a skewed geometry in which the upper deck can move either towards or away from the substituent (Figure 3-1). In order to understand this unusual behavior the first step of the characterization process was to calculate the ground state for two different substituted compounds that display different NMR patterns, for example R=OMe (**51**) and R=NEt_2 (**52**) (Figure 3-1).

Table 3-1. Relative energies (kcal/mol) for the conformational isomers of **51** and **52**.

	OMe(kcal/mol)	NEt_2 (kcal/mol)
Toward	0	+4.99
Away	+2.13	0

The ground state calculation for each compound was carried out for the two possible conformations at the HF/6-311+G(d,p) level of theory using Gaussian 03 Rev. E01.[92] It was found that the towards conformation was the more stable for the OMe substituent, while the away was the more stable for the NEt_2 substituent. These results are consistent with the assumptions that were made in rationalizing the experimental ${}^{n}J_{FF}$ SSCCs. The more stable conformation of each compound was used to calculate the corresponding F-F coupling constants. In all cases the SSCC calculations included

the four isotropic Ramsey terms, Fermi contact (FC), spin-dipolar (SD), paramagnetic spin orbit (PSO), and diamagnetic spin orbit (DSO) contributions calculated at the B3LYP/EPR-III level using Gaussian 03. The numbering used in the following analysis is presented in Figure 3-2.

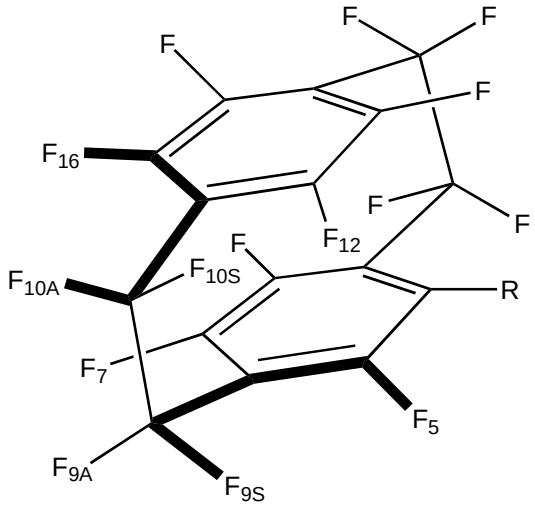

Figure 3-2. Monosubstituted F8, where R= OMe (**51**), NEt_2 (**52**).

$^4J(F_mF_n)$ Coupling Constants

All SSCCs displayed in Table 3-2 derive from a coupling pathway that could be classified as the "U type" (Figure 3-3). The "U type" coupling pathway can transmit through-space via the FC term of the $^4J_{FF}$, and it depends strongly on the F-F distance.

Table 3-2. Calculated $^4J(F_mF_n)$ coupling constants and F-F distance for compound **51** (R=OMe).[a-c]

F_m	F_n	J^{FC}	J^{SD}	J^{PSO}	J^{DSO}	J_{total}	J_{exp}	$d(F_n\text{-}F_m)$
F10A	F16	26.35	0.75	-8.83	1.77	20.04	32	2.71
F9S	F5	27.16	0.86	-9.27	1.82	20.57	33	2.70
F9A	F7	79.03	3.53	-8.42	2.04	76.18	66	2.54
F10S	F12	79.21	3.56	-7.93	2.05	76.89	66	2.54

a. All Values are in Hz. b. Distances in Å. c. See Figure 3-2 for numbering of the atoms.

The calculated values compare well with the experimental ones. Interestingly, from Table 3-2 it is possible to see that both the smaller and larger SSCCs are diagonal to each other (see the bonds selected in bold in Figure 3-2). Although all $^4J_{FF}$ SSCC

have the same type of connections, two of them have a much higher coupling than the other two. In the same Table it is observed that, while the FC terms in $^4J_{F9A,F7}$ and in $^4J_{F10S,F12}$ are about three times larger than in $^4J_{F9S,F5}$ and in $^4J_{F10A,F16}$, the PSO term does not change along the same series. These observations suggest that the much larger FC terms in $^4J_{F9A,F7}$ and $^4J_{F10S,F12}$ SSCCs originate mainly due to an increase in the FC term transmitted through space. To support this assumption, the respective optimized F-F distances are also shown in Table 3-2.

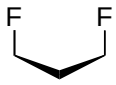

Figure 3-3. “U type” coupling pathway.

The distances reported in Table 3-2 are shorter than twice the F Van der Waals radius, (2 x 1.47) Å, which means that the FC term can be transmitted TS due to the overlap of fluorine lone pair orbitals. It is known that the overlap of proximate lone pairs is an efficient pathway for transmitting the FC interaction, regardless of whether or not it is an attractive or repulsive interaction. The dependence of the FC term on the F-F distances is clearly seen in the Table as the larger coupling values correspond to the smaller F-F distance, while the smaller coupling values correspond to the larger F-F distance. These results are in good agreement with similar data discussed, among other authors, for example by Arnold and co-workers.[102]

Table 3-3. Calculated $^4J(F_mF_n)$ coupling constants and F-F distance for compound **52** (R=NEt_2).[a-c]

F_m	F_n	J^{FC}	J^{SD}	J^{PSO}	J^{DSO}	J_{total}	J_{exp}	$d(F_n\text{-}F_m)$
F10A	F16	77.23	3.383	-8.64	2.04	74.46	67	2.54
F9S	F5	77.43	3.87	-8.02	2.04	75.32	75	2.52
F9A	F7	27.12	0.81	-8.99	1.84	20.78	33	2.70
F10S	F12	28.21	0.85	-9.43	1.91	21.54	35	2.68

a. All Values are in Hz. b. Distances in Å. c. See Figure 3-2 for numbering of the atoms.

Similar behavior is observed for analogous SSCCs in **52** (Table 3-3), with the exception that the larger SSCCs of **51** become the smaller ones of **52**, and vice versa. This data supports not only the assumption made above about the relationship FC term vs. distance, but also the initial hypothesis of the different upper deck position for the two substituents (Figure 3-4).

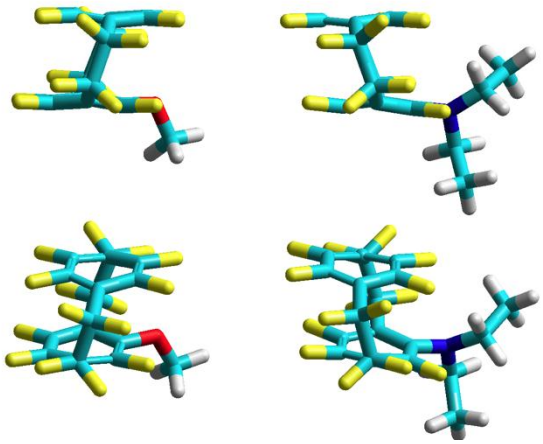

Figure 3-4. Calculated most stable conformations for compounds **51** (left) and **52** (right).

$^{5}J(F_mF_n)$ Coupling Constants

In Table 3-4 the calculated and experimental values for 4 different $^{5}J_{FF}$ SSCCs in compound **51** are displayed. The most surprising result is the striking difference between $^{5}J_{F10A,F7}$ and $^{5}J_{F9S,F12}$ SSCCs which could not be experimentally observed and their respective calculations are also close to 0 Hz, while $^{5}J_{F9A,F16}$ = 15 Hz and $^{5}J_{F10S,F5}$ = 17 Hz SSCCs were measured.

The transmission mechanisms of the $^{5}J_{FF}$ couplings cannot be rationalized on the same grounds as those operating for $^{4}J_{FF}$. Although the largest $^{5}J_{FF}$ couplings are also dominated by the FC term like $^{4}J_{FF}$ couplings, it is obvious that transmission mechanisms of the FC term for $^{4}J_{FF}$ are notably different than those for the FC term of

$^5J(F_mF_n)$ since for all four couplings the distances between the coupling nuclei are always larger than twice the van der Waals radius and, therefore, any direct ^5J(FC) through-space coupling should be ruled out.

Table 3-4. Calculated $^5J(F_mF_n)$ coupling constants and F-F distance for compound **51** (R=OMe).[a-c]

F_m	F_n	J^{FC}	J^{SD}	J^{PSO}	J^{DSO}	J_{total}	J_{exp}	$d(F_n\text{-}F_m)$
F9A	F16	14.99	2.1	-3.8	1.77	15.06	15	2.99
F10S	F5	15.06	2.21	-3.83	1.79	15.23	17	2.99
F9S	F12	0.22	0.85	-0.66	0.01	0.42	0	4.37
F10A	F7	0.20	0.86	-0.63	0.01	0.44	0	4.36

a. All Values are in Hz. b. Distances in Å. c. See Figure 3-2 for numbering of the atoms.

In order to rationalize the behavior of $^5J(F_mF_n)$ (FC), it must be recalled that it is known that the FC term can be transmitted by an intermediate moiety,[103,104] like that suggested by Mallory,[105] where a coupling $^6J_{F\text{-}F}$ = 6.4 Hz is transmitted through a phenyl ring (Figure 3-5).

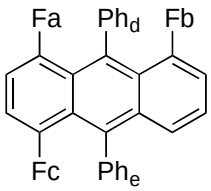

$^6J_{FaFb}$ = 6.4 Hz

Figure 3-5. Unusual through-space coupling transmitted by the electronic Ph_d system.

This TS coupling between fluorines **a** and **b** is due to overlapping interactions between the lone pair of each fluorine and the Π system of the phenyl group (**d**) with an anti-symmetric linear orbital combination (F-Ph-F). It should be noted that the phenyl group (d) is perpendicular to the anthracene plane.

It is also important to note that the appearance of the fragment defining $^5J_{FF}$ SSCCs shown in Table 3-4 can be represented by the fragment shown in Figure 3-6, where A, E and G represent fluorine atoms; here, $^5J_{FF}$ is represented by J_{AG}. It seems

that the D—E bond is playing the role of the Ph_d phenyl group in Figure 3-5. Therefore, this additional coupling pathway is of the through-space type, transmitted through the electric cloud corresponding to the fluorine atom occupying the E position.

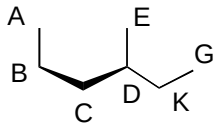

Figure 3-5. Representation of the unusual $^{5}J_{FF}$ SSCCs.

For instance, for ^{5}J(F9A-F16) and ^{5}J(F10S-F5) couplings the role of the intermediate is played by F10A and 9S, respectively. For example, the ^{5}J(F9A-F16) coupling pathway might operate like this: the overlap between the F10A and F16 lone-pairs yields ^{4}J(F10A-F16)(FC) = 26 Hz, which is transmitted through-space due to the overlap of their electronic clouds and “contaminates” the F10A lone-pairs with the F16 FC spin information and then F10A transmits the spin information to F9A by a second overlap. A similar path would apply for ^{5}J(F10S-F5).

In order to have an efficient coupling for the $^{5}J_{FF}$, the entire F<==>F<==>F mechanism should be connected at once. Now the question becomes why this mechanism is efficient for ^{5}J(F9A-F16) and ^{5}J(F10S-F5) and not for ^{5}J(F10A-F7) and ^{5}J(F9S-F12)? To answer this, it is important to consider two different aspects: 1) for one side of the molecule, one $^{5}J_{FF}$ is effective while the other is not; however, in both of them the $^{3}J_{FF}$ aliphatic vicinal coupling is common and the efficiency of the coupling is not coming from this connection, which take us to the second aspect, 2) the aromatic-aliphatic $^{4}J_{FF}$ connection. Interestingly, for the higher $^{4}J_{FF}$ SSCCs previously discussed, the $^{5}J_{FF}$ is ineffective, and for the smaller $^{4}J_{FF}$ SSCCs, the $^{5}J_{FF}$ is effective. These last

two statements mean that the effectiveness in the $^{5}J_{FF}$ SSCC is not due to the distances between all interacting fluorines.

It is believed at this point that there must be an orbital overlapping between all interacting fluorines that transmit the spin polarization mechanism in such a manner that it is effective in one way and not the other. Thus, as with any orbital overlapping, there is not only distance dependence, but also an angular dependence.

The calculated aromatic-aliphatic F-F dihedral angle for the effective $^{5}J_{FF}$ SSCCs is around 40°, while the ineffective $^{5}J_{FF}$ SSCCs the angles are all around 1°. Similar behavior is observed for analogous $^{5}J_{FF}$ SSCCs in **52** (R=NEt_2), but with the opposite trend (Table 3-5).

Table 3-5. Calculated $^{5}J(F_mF_n)$ coupling constants and F-F distance for compound **52** (R= NEt_2).[a-c]

F_m	F_n	J^{FC}	J^{SD}	J^{PSO}	J^{DSO}	J_{total}	J_{exp}	$d(F_n\text{-}F_m)$
F9A	F16	0.21	0.75	-0.55	0.01	0.42	0	4.29
F10S	F5	0.22	0.76	-0.52	0.01	0.47	0	4.29
F9S	F12	16.12	2.11	-3.87	1.79	16.15	11	3.08
F10A	F7	16.27	2.34	-3.91	1.81	16.51	11	3.05

a. All Values are in Hz. b. Distances in Å. c. See Figure 3-2 for numbering of the atoms.

In order to give further support to the previous hypothesis of having an intermediate moiety relaying the spin polarization from one fluorine to the other, three more calculations were done.

The first one was the replacement of the “connecting” fluorine by a chloride atom in one of the effective and one of the ineffective $^{5}J_{FF}$ SSCCs (separate calculations). The chlorine atom has a larger Van der Waals radii, which makes the interacting distances between the F<==>Cl<==>F couplings shorter; but, since the distance seems to not be as important as the angle in this coupling pathway, the coupling constants should not be affected significantly. The calculations were performed only with

compound **51**, using the ground state geometry previously calculated and only for the coupling constant in which the chloride atom might be part of. This is because the SSCC calculation requires significant amounts of memory and time. The new calculated coupling constants were only about 0.5 Hz higher than the ones without the chlorine, which supports the assumption that the distance is not as important as the dihedral angle might be.

The second calculation was the change of the dihedral angle between the aromatic-aliphatic fluorines. The calculation was performed only with compound **51**, using the ground state geometry previously calculated, except for the change of 15^{o} in the dihedral angle of one effective coupling constant (from 40.77^{o} to 25.77^{o}). The change in the dihedral angle for the ineffective coupling changes the vicinal aliphatic F-F distance to a significantly larger value ($^{3}J_{FF}$) and the results would not be as precise since this particular $^{3}J_{FF}$ coupling is distance dependent. The new calculated coupling constant changed from 15.06 Hz to 8.13 Hz, which supports the previously made assumption of angular dependence.

The third, final, and probably most accurate calculation was done using the Fermi Contact Coupling Pathway – Canonical Molecular Orbitals approach (FCCP-CMOs) that was explained previously. This method verified that the $^{5}J_{FF}$ SSCCs goes through an intermediate moiety. All of the calculations in this part were done using compound **51** as the model. The analysis of these calculations was done by Dr. Contreras (University of Buenos Aires, Buenos Aires, Argentina) and Dr. Tormena (University of Campinas, Sao Paulo, Brazil).

The occupied CMOs with an energy lower than - 0.679055 a.u. or higher than + 1 a.u. are not taken into account since they would involve a very large $\square_{a,i}\square\square\square(\square_a - \square_i)$ energy gap, and therefore their contributions to coupling constants relevant to this qualitative analysis should be too small to yield insight on the main factors determining the observed experimental trends. CMO expansions in terms of NBOs as given by the Weinhold et al.'s 5.0 NBO program are considered;[106] they are displayed using conventions used in the outputs of that program. Briefly they are, a) CMOs are numbered from lower to higher energy, indicating if they are occupied or vacant CMOs; CMO energies are given in atomic units, b) the first number, followed by an asterisk, when squared corresponds to each NBO contribution with a threshold of 5 %; c) the second number, in square brackets, corresponds to the NBO numbering, d) next, the NBO type is shown followed by the atom or atoms involved in it (numbered as in the Gaussian 03 program output), i.e. core, lone-pair; bonding, antibonding, or Rydberg orbitals, respectively.

In Table 3-6 only the relevant NBOs whose atoms participate explicitly in ^{5}J(F10S-F5), ^{5}J(F9S-F12), ^{4}J(F9A-F16) and ^{4}J(F10A-F7) coupling constants is shown for each CMO. Occupied CMOs are presented from highest to lowest orbital energies, while vacant CMOs are presented from lowest to highest energies to visualize easily the corresponding energy gaps. There are only five CMO(vir) containing NBOs that include more than one of the atoms involved in coupling constants mentioned above. It is observed that four of them include the F5 and F12 atoms, but neither F10S nor F9S atoms. These correspond to the transmission of the *pseudo-gem* ^{9}J(F12-F5) but not to the $^{5}J_{syn}$(F9S-F12) coupling. Therefore, the only virtual CMO that could be significant for

transmitting any of the $^{5}J_{syn}$(F10S-F5), $^{5}J_{syn}$(F9S-F12), $^{4}J_{syn}$(F9S-F5) and $^{4}J_{syn}$(F10S-F12) couplings is the CMO(vir) 130. The respective virtual transitions should be the following three, (I) CMO(occ)109→CMO(vir)130, (II) CMO(occ)108→CMO(vir)130 and (III) CMO(occ)98→CMO(vir)130.

Table 3-6. Expansion of relevant CMOs in terms of NBOs in compound **51**. Only NBOs involving F5, F9S, F10S and F12 are displayed.

Occupied CMOs	Vacant CMOs
CMO 109 (occ): □ = - 0.419280 a.u	CMO 129 (vir): □ = 0.024166 a.u.
0.370*[103]: LP (2) F5(lp)	-0.277*[437]: BD*(1) C12-F12*
-0.283*[114]: LP (2) F9S(lp)	-0.256*[471]: BD*(1) C5-F5*
0.240*[121]: LP (3) F10S(lp)	
CMO 108 (occ): □ = - 0.424528 a.u.	CMO 130 (vir): □ = 0.039066 a.u.
-0.247*[94]: LP (2) F12(lp)	-0.257*[451]: BD*(1) C10-F10S*
0.234*[103]: LP (2) F5(lp)	0.242*[471]: BD*(1) C5-F5*
0.233*[121]: LP (3) F10S(lp)	MO 131 (vir): □ = 0.050564 a.u.
CMO 106 (occ): □ = - 0.430080 a.u.	-0.300*[437]: BD*(1) C12-F12*
-0.268*[114]: LP (2) F9S(lp)	0.244*[471]: BD*(1) C5-F5*
-0.230*[103]: LP (2) F5(lp)	MO 136 (vir): □ = 0.099446 a.u.
CMO 103 (occ): □ = - 0.440928 a.u.	-0.235*[471]: BD*(1) C5-F5*
-0.381*[94]: LP (2) F12(lp)	0.225*[437]: BD*(1) C12-F12*
0.273*[120]: LP (2) F10S(lp)	MO 140 (vir): □ = 0.141878 a.u.
-0.268*[121]: LP (3) F10S(lp)	0.365*[471]: BD*(1) C5-F5*
CMO 100 (occ):□ = -0.456086 a.u.	0.257*[437]: BD*(1) C12- F12*
-0.373*[103]: LP (2) F5(lp)	
-0.366*[114]: LP (2) F10S(lp)	
-0.325*[94]: LP (2) F12(lp)	
CMO 98 (occ): □ = -0.471647 a.u.	
-0.326*[103]: LP (2) F5(lp)	
0.253*[121]: LP (3) F10S(lp)	
0.249*[94]: LP (2) F12(lp)	
0.225*[115]: LP (3) F9S(lp)	

Obviously, the virtual transition (I) corresponds to the coupling pathway mentioned in the working hypothesis: CMO(occ)109 contains these lone-pair orbitals: LP_2(F5), LP_3(F10S) and LP_2(F9S) where the F9S plays the role of the “intermediate F atom” for transmitting the FC term of $^{5}J_{syn}$(F10S-F5) coupling. It is highlighted the CMO(vir)130

does not include the □*(C9-F9S) antibonding orbital since ^{4}J(F9S-F5) coupling is transmitted by the overlap of LP(2) of F9S and LP(2) of F5. Virtual transition (II) contributes also to the ^{5}J(F10S-F5) coupling transmission but its energy gap is about 0.005 a.u. larger than in (I), The same can be said about the virtual transition (III). In this case the respective energy gap is about 0.062 a.u. larger than in (I), showing a notably smaller efficiency for transmitting the ^{5}J(F10S-F5) coupling.

There are not equivalent virtual transitions to transmit the FC term of ^{5}J(F9S-F12) since there is no virtual CMO containing the equivalent to CMO(vir)130, i.e. a CMO(vir) containing the NBOs □□(C9-F9S) and □□(C12-F12). Thus the 'towards' conformation of the upper deck for compound **4** leads to an important distortion of the F12-C12-C11-C10-F10S moiety, which inhibits the existence of a virtual CMO containing simultaneously those two NBO antibonding orbitals, rendering a very inefficient coupling pathway for ^{5}J(F9S-F12). This distortion renders also a much shorter F12---F10S distance, increasing notably the overlap between their electronic clouds, increasing the through space transmission of ^{4}J(F10S-F12).

It is highlighted that all three CMOs(occ)108, 103 and 98 contribute to the through-space via overlapping lone pairs the $^{4}J_{syn}$(F10S-F12) coupling, but they are not affected by the respective CMO orbital energies since they are transmitted by exchange interactions taking place in the lone-pair overlap region. Similarly, ^{4}J(F9S-F5) is transmitted by CMOs(occ) 109, 106, 100 and 98, *i.e.* such couplings do not require of antibonding orbitals for the transmission of their FC terms.

Preferred Conformations: Upper Deck Towards or Away

At this point it has been demonstrated experimentally and computationally that in fact the methoxy substituent has a different upper deck configuration (towards) than the

N,N-diethylamine substituent (away); however, the preference between one and the other has not been rationalized.

All the compounds that have been synthesized have shown to prefer the toward conformation as long as the substituent is not large. For those with a large substituent, such as N,N-dimethylamino, N,N-diethylamino and $(CH_2)_4N$ the away conformation is the preferred one. A potential energy scan around the aromatic C and the N bond in the N,N-dimethylamino-F8 compound indicated a highly repulsive interaction between the methyl group and the closest CF_2 in the bridge (Figure 3-7). This repulsive interaction causes the dimethylamino group to be out of the plane of the ring. The methyl groups push away the upper ring to minimize other repulsive interactions with the upper ring. Experimentally it was found that one methyl group from the Me_2N and one methylene group from Et_2N has splitting due to coupling with the fluorines of upper aromatic ring.

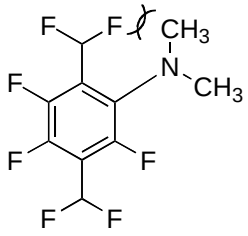

Upper ring omitted for simplicity

Figure 3-7. Repulsive interaction between the CH_3 and the closest CF_2 on the F8 bridge.

During the time of this computational study, different members of the group prepared other mono-substituted F8 derivatives that were included in this study, as they were needed. In particular, three new compounds help to fully understand the conformational preference: 1) NH_2 –F8, 2) NHEt-F8 and 3) H-F8.

The amino and the ethylamino- F8, both showed experimentally and computationally to have a toward conformation. The ground state calculations indicate

that both nitrogens are conjugated with the ring. The ethylamino group has the ethyl group pointing away from the CF_2 in the bridge avoiding any repulsive interaction and allowing the lone pair of the nitrogen to be conjugated with the ring. Lastly, we were all expecting the H-F8 compound to have a toward type conformation since the substituent is really small (smaller than methoxy or amino); however, both the NMR and the ground state calculation indicated that the away is the preferred conformation. The computational calculation showed that the away conformer is 2.3 kcal/mol lower in energy than the toward.

Taking into account that all the nucleophiles were heteroatoms, except for the hydride, then all the toward conformers have a substituent with a lone pair available. Previous reports have shown intermolecular attractive non-covalent interactions between electron lone pairs (LP) and the π system of a benzene ring. This LP→π intermolecular interaction is stronger when the ring is electron deficient, such a perfluorinated benzene ring.[107,108] The donating lone pair that is part of this non-covalent interface could also come from a halogen, as previously reported.[109] Then it is believed that one lone pair of the heteroatom substituent has a LP→π interaction with the upper ring, in addition to the other three coming from the fluorine lone pairs: One from the ortho fluorine to the substituent (with the upper ring), and two from the pseudo-meta and pseudo-para fluorines with the lower ring (LP(F) →π), for a total of 4 LP→π interactions. The away conformation in all heteroatom substituent cases would also have 4 LP→π interactions coming all from fluorines, which suggests that the one coming from the heteroatom might be stronger. When the substituent is a hydrogen the toward

conformation would have only 3 LP→π interactions, while away conformation would have 4, and in all cases the donating lone pairs come from the fluorines.

Interestingly, further support for the LP→π interactions in the towards conformation is seen in the ground state geometries. It was noticed that the lone pair of the nitrogen in the amino-F8 compound is pointing down in the away conformation, while it is pointing up in the towards conformation. Also, in all cases, the distances between the heteroatom (lower ring) and the closest carbon in the upper ring are less than the sum of the Van der Waals radii of both atoms. Both of these points support the possibility of non-covalent interaction between the lone pair and the pi system of the upper ring.

The final confirmation of this hypothesis was done calculating the ground state of the protonated version of the amino-F8 for both towards and away ($[NH_3\text{-F8}]^+$). In this case it was thought that by protonating the nitrogen, the bulkiness of the substituent is not affected, but the lone pair would not be available to do LP→π interaction. The results of the calculations indicated that the away conformer is 5 kcal/mol more stable than the toward conformer, supporting the possibility of the LP→π interaction with the upper ring.

CHAPTER 4
IMPACT OF FLUORINE SUBSTITUENTS ON THE RATES OF NUCLEOPHILIC ALIPHATIC SUBSTITUTION AND B-ELIMINATION

Introductory Remarks

The mechanism in which primary perfluoroalkyl substrates will undergo aliphatic substitution was introduced in Chapter 1. These types of substrates cannot experience bimolecular aliphatic substitution (S_N2) but instead are capable of undergoing nucleophilic substitution via the $S_{RN}1$ mechanism (Figure 1-21).[54]

Part of the “lore” of fluorine chemistry is that fluorine close to the site of nucleophilic substitution will *inhibit* such substitution; however, elimination reactions are accelerated by the presence of fluorine.

Although it is known that the presence of fluorine affects the reaction rates of both the S_N2 and the E2, limited information of a comprehensive and quantitative analysis can be found in the literature.

Haas was able to observe apparent S_N2 substitution reactions with benzylic, arylCF_2Br compounds (Scheme 4-1); however, the kinetic rate was not measured for this reaction.[110]

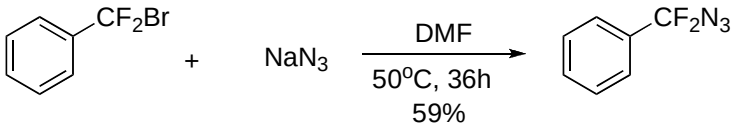

Scheme 4-1. S_N2 reaction of bromodifluoromethylbenzene.

It has been also reported that carrying out nucleophilic substitutions on β-fluorinated substrates such as CF_3CH_2X or R_FCH_2X requires rather harsh conditions, even with relatively good nucleophiles, such as azide, and good leaving groups, such as -OMs (Scheme 4-2).[111]

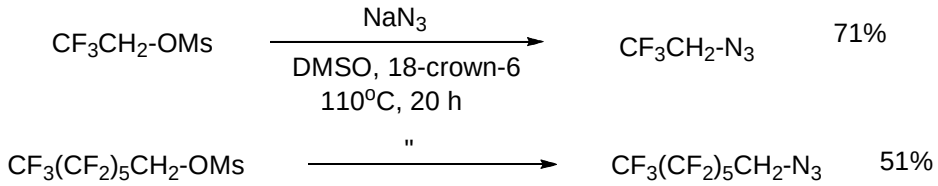

Scheme 4-2. Literature examples of S_N2 reactions of azide with β-fluorinated substrates.

When a substrate's fluorine substituents are two carbons or more from the leaving group they are considered to have S_N2 reactivities "similar" to those of simple *n*-alkyl halides, whereas γ-fluorinated substrates also have significantly enhanced E2 reactivities. Such considerations are important to recognize when one is designing syntheses of fluorous compounds using *n*-$R_FCH_2CH_2X$ substrates.

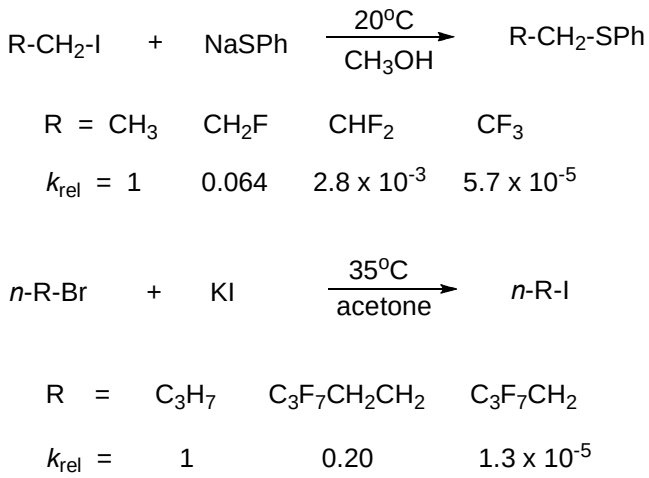

Scheme 4-3. Early Hine and McBee kinetic studies

There are two early papers that provide some quantitative insight into the effects of fluorine substitution at the β and γ positions of an alkyl halide on the rates of nucleophilic substitution, but to our knowledge there are no kinetic data available regarding the effect of fluorine on β-eliminations. Hine examined the reaction of phenyl thiolate with β-fluorinated ethyl iodide,[112] whereas McBee studied the reactions of iodide ion with β- and γ-fluorinated alkyl bromides (Scheme 4-3).[113]

Hine also provided the only data that is available on the effect of α-fluorine substitution with his study of the S_N2 reactivity of bromofluoromethane, which proved to be ~350 times less reactive than methylbromide in its reaction with iodide ion in acetone at 20^oC.[114]

The purpose of the present work is to provide comprehensive, hopefully definitive kinetic data for substitution and elimination reactions of α–, β–, and γ–fluorinated *n*-alkyl systems under a variety of solvent, nucleophilic and basic conditions, in order to provide synthetic organic chemists with sufficient understanding of the chemistry of such systems to allow them to plan successful syntheses when using partially fluorinated aliphatic substrates.

Comparative kinetic and reaction outcome data will be provided for the following partially fluorinated substrates: *n*-RBr, *n*-$R_fCH_2CH_2Br$, *n*-R_fCH_2Br, *n*-R-CHFBr, *n*-R-CF_2Br, and $PhCF_2Br$ in their reactions with two nucleophiles that have very different character, the strong base nucleophile, methoxide, and the weak base, strong nucleophile, azide; the kinetics of their reactions being examined in the protic solvent, methanol and the polar, aprotic solvent, DMSO.

Computational results will also be presented in order to provide a more complete understanding of the unusual kinetic effects of fluorine substituents.

Results and Discussion

The specific substrates that were included in this kinetic study are *n*-heptyl bromide (**53**), *n*-octyl iodide (**54**) and *n*-octyl tosylate (**55**), 1*H,*1*H*-perfluoro-*n*-butyl bromide (**56**), 1*H*,1*H*,2*H*,2*H*-perfluoro-*n*-hexyl bromide (**57**), 1-bromo-1-fluorononane (**58**), 1-bromo-1,1-difluorohexane (**59**), benzyl bromide (**60**), and

bromodifluoromethylbenzene (**61**). Substrates **53**, **54**, **56**, **57** and **60** were commercially available. Tosylate **55** was obtained from the alcohol in the usual manner.[115] 1-Bromo-1-fluorononane (**58**) was obtained essentially by the method of Garcia Martinez (Scheme 4-4).[116]

Interestingly, during the course of this study we attempted to synthetized 1-Iodo-1-fluorononane 1,1-diiodohexane was unreactive towards nucleophilic substitution by fluoride ion, when treated with CsF under various conditions and temperatures, or with commercial tetrabutyl ammonium fluoride. 1-Bromo-1,1-difluorohexane (**59**) was prepared as reported in our earlier study of its radical chemistry.[117]

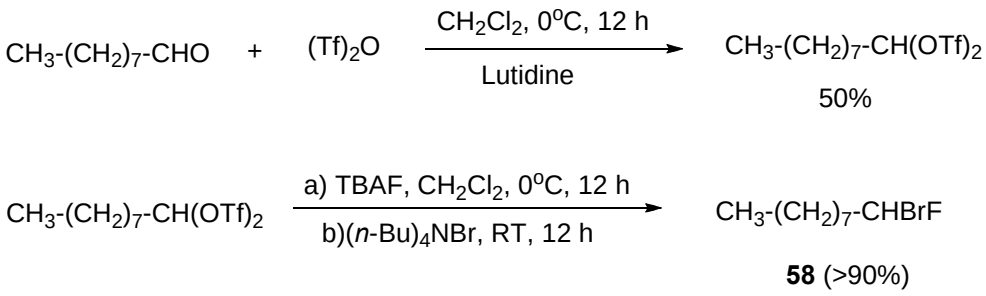

Scheme 4-4. Preparation of 1-bromo-1-fluorononane **58**.

All of the kinetic experiments were run under second-order reaction conditions, using two equivalents of nucleophile, and the rates were measured using either proton or fluorine NMR to follow the depletion of starting substrate and formation of substitution and elimination products. In all cases, the reactions, as studied, appeared to be quantitative, since no other products could be detected by proton or fluorine NMR. In order to be able to compare most of the reactions at the common temperature of 50°C, it was necessary to extrapolate the rate constants for very fast or very slow reactions of some of the substrates to this temperature through the use of the Eyring equation. Rates of such reactions at two temperatures were used for this purpose.

Kinetics

The second order character of bimolecular reactions such as S_N2 and E2 has long been recognized, since the rates of such reactions depend on the concentrations of both reactants (A + B → C), the rate is first order for each one (Equation 4-1). Integration of the rate expression results in a linear relationship between $\ln(A_oB/B_oA)$ and time *t* (Equation 4-2). A_o and B_o are the initial concentrations of both reactants, while A and B are the concentrations at time *t*.

$$\frac{dC}{dt} = -\frac{dA}{dt} = k[A][B] \quad (4\text{-}1)$$

$$\frac{1}{B_o - A_o} Ln \frac{A_o B}{B_o A} = kt \quad (4\text{-}2)$$

$$\frac{1}{A_o - B_o} Ln \frac{B_o(A_o - x)}{A_o(B_o - x)} = kt \quad (4\text{-}3)$$

Since experimentally it is usually easier to follow the reaction by the decrease in the concentration (x) of one of the reactants, Equation.4-2 can be expressed in terms of x and the initial concentrations, A_o and B_o (Equation 4-3). Given that the reaction is first order for each reactant, the amount of x is the same in both cases. The plot between $[1/(A_o - B_o)Ln((B_o(A_o-x))/(A_o(B_o-x))$ vs t gives the rate constant directly from the slope. This rate expression has been widely used for measuring the rate constants of second order reactions.[118]

Some of the reactions presented in this work undergo competitive substitution and elimination reactions. Since each reaction requires a 1:1 ratio between the substrate and the nucleophile/base, the rate constant (k_{obs}) derived from Equation 4-3 will be the *sum* of each of the individual rate constants, k_{SN2} and k_{E2}. The ratio between the two products can then be used to obtain the individual rate constants.

Because proton or fluorine NMR was being used to measure the changes in concentration of substrate, it was necessary that the particular starting material and product NMR signals be sufficiently resolved to allow accurate individual integrations. Figure 4-1 shows an example of how the reaction was followed by ^{1}H NMR. This method led to some limitations with respect to reactions that could be studied. For this reason, rates for the reactions of alkyl iodide with azide and reactions of alkyl tosylate in DMSO could not be measured.

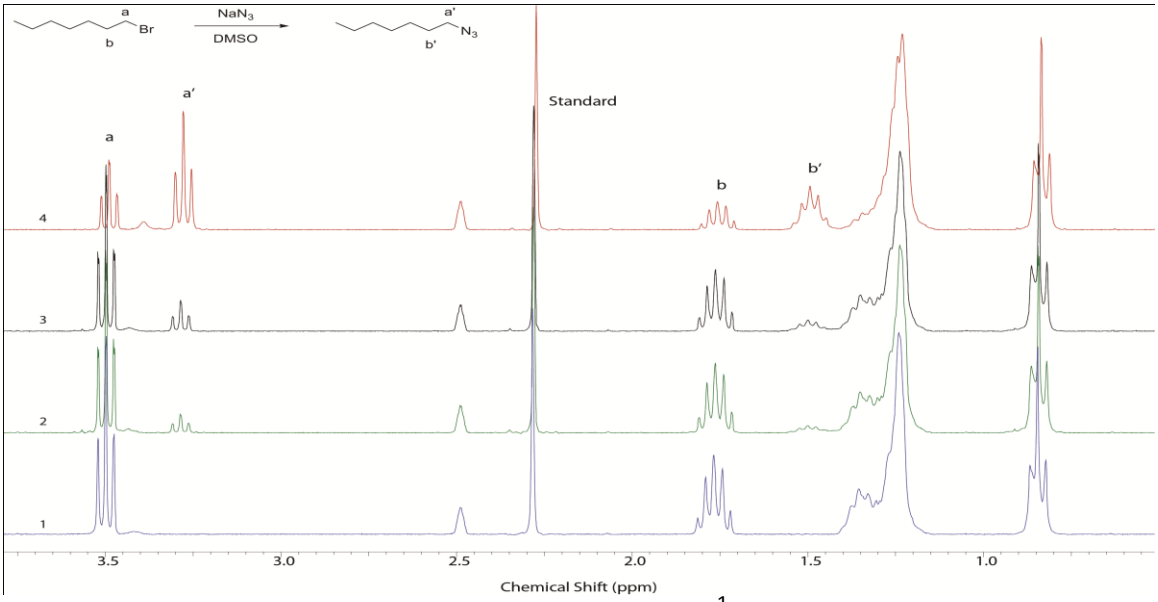

Figure 4-1. Example of a kinetic study followed by ^{1}H NMR. Spectra 1 (bottom) is the reaction at t=0, while 2,3 and 4 are the spectra at consecutive times.

Hydrocarbon Substrates

Kinetic data that directly compare leaving group abilities and nucleophilicities for S_N2 reactions of alkyl halides and tosylates in protic and aprotic solvents can, of course, be found in the old literature, but we believe that it is worthwhile to discuss these factors as they have revealed themselves in this study.

The observed overall results for reactions of methoxide with *n*-alkyl halides and tosylates are given in Scheme 4-5. As expected, elimination was found to compete with

substitution for reactions of *n*-octyl iodide and *n*-heptyl bromide with methoxide ion (pK_a = 15.5), but interestingly no elimination was observed when tosylate was the leaving group, either in methanol or DMSO.

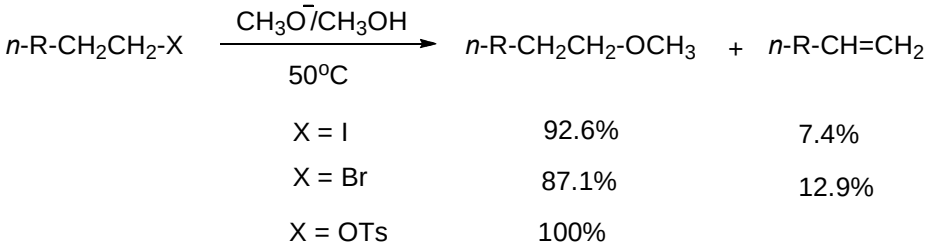

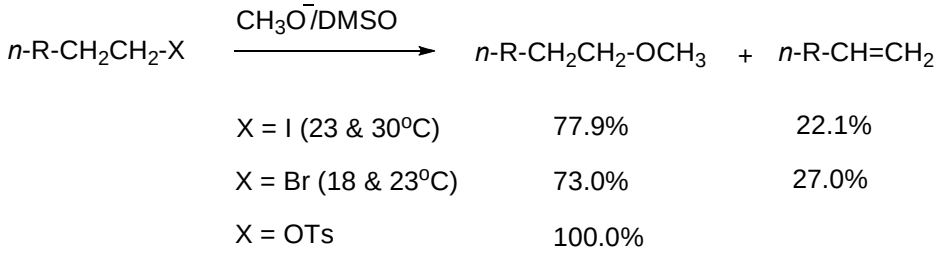

Scheme 4-5. Relative amounts of substitution versus elimination in reactions of *n*-alkyl iodide, bromide and tosylate with methoxide.

Thus, based upon our admittedly limited data, tosylate, rather than halide, would seem to be the preferred leaving group for carrying out Williamson synthesis of ethers. Such a conclusion does not appear to be part of the “lore” of the Williamson synthesis.[119] Although reports of effective use of tosylates can be found,[120,121] including one paper involving solvent-free alkylations that clearly showed that alkyl tosylates gave much less elimination in reactions with potassium *tert*-butoxide than alkyl halides.[122]

No trace of elimination products could be observed when using the much less basic azide ion (pK_a = 4.67). The kinetic data that were obtained for these reactions of non-fluorinated *n*-alkyl systems are given in Table 4-1 at 50°C. Some of the rate constants presented in Table 4-1 are the values obtained after extrapolation of two different temperatures. See appendix B for a complete set of experiments.

Table 4-1. 2nd order rate constants for *n*-alkyl iodide, bromide and and for benzyl bromide.

Expt. No	Substrate	Solvent	Nucleophile	T, °C	$10^5 k_2$ S_N2	$10^5 k_2$ E2
1	*n*-$C_8H_{17}I$ [a]	CH_3OH	CH_3O^-	50	6.19 ± 0.24	0.469 ± 0.016
4 [b]	*n*-$C_8H_{17}I$	DMSO	CH_3O^-	50	276 ± 41	76.8 ± 13
5	*n*-$C_7H_{15}Br$	CH_3OH	CH_3O^-	50	3.95 ± 0.24	0.566 ± 0.032
8 [b]	*n*-$C_7H_{15}Br$	DMSO	CH_3O^-	50	116 ± 15	40.4 ± 1.1
9	*n*-$C_7H_{15}Br$	CH_3OH	N_3^-	50	6.89 ± 0.064	*no* [c]
12 [b]	*n*-$C_7H_{15}Br$	DMSO	N_3^-	50	1590 ± 300	*no*
15 [b]	*n*-$C_7H_{15}Br$	DMSO	I^-	50	563 ± 140	*no*
16 [d]	*n*-$C_8H_{17}OTs$	CH_3OH	CH_3O^-	50	12.7 ± 0.70	*no*
17 [d]	*n*-$C_8H_{17}OTs$	CH_3OH	N_3^-	50	23.8 ± 1.0	*no*
18	Ph-CH_2Br	CH_3OH	CH_3O^-	15	13.5 ± 0.59	- [e]
20 [b]	Ph-CH_2Br	CH_3OH	CH_3O^-	50	188 ± 19	-
21	Ph-CH_2Br	DMSO	CH_3O^-	15	1020 ± 74	-
22	Ph-CH_2Br	CH_3OH	N_3^-	15	46.6 ± 0.64	-
24 [b]	Ph-CH_2Br	CH_3OH	N_3^-	50	606 ± 20	-
25 [f]	Ph-CH_2Br	DMSO	N_3^-	15	7480 ± 250	-

[a] The kinetics of reactions of *n*-$C_7H_{15}I$ with azide could not be studied because of overlap of relevant peaks in the proton NMR; [b]These 2nd order rate constants were approximated for comparison purposes using the Eyring equation; the given error was obtained by propagating that of the two data points; [c] *no* = not observed; [d] Reactions of *n*-$C_8H_{17}OTs$ in DMSO could not be studied kinetically because of overlap of relevant peaks in the proton NMR; [e] - (dash) means product not possible; [f] approximate, single point rate constant (56.8% of substrate consumed after 30 sec)

Leaving group abilities, bromide versus iodide and tosylate

The relative leaving group abilities of bromide, iodide and tosylate are compared in Table 4-2. As expected, iodide is a somewhat better leaving group than bromide in reactions with methoxide. Such results are consistent with a reported study of the reaction of hydroxide with methyl iodide versus methyl bromide, where the iodide reacted slightly faster (ratio = 1.1).[123] In studies of S_N1 reactions, the difference between iodide and bromide as leaving groups is considerably greater, an example being the solvolysis of phenylethyl iodide versus bromide in 80% ethanol at 75°C where the rate ratio was 6.5.[124] Tosylate was a better leaving group than bromide in the methoxide/methanol reaction. To our knowledge there is no literature comparison of tosylate with bromide in an S_N2 reaction. However, in the reaction of hydroxide with methyl bromide and mesylate in water, the mesylate was 3.6 faster.[123] In the phenylethyl solvolysis study mentioned just above, mesylate was found to be only

slightly poorer than tosylate (ratio = 1.2),[124] so the methanol results in Table 2.1 are more or less consistent with the literature.

Table 4-2. Relative leaving group abilities in S_N2 reactions at 50°C

Substrate	k_{rel} (CH_3O^-/ CH_3OH)	k_{rel} (CH_3O^-/DMSO)	k_{rel} (N_3^-/CH_3OH)	k_{rel} (N_3^-/DMSO)
n-$C_7H_{15}Br$	1.0	1.0	1.0	1.0
n-$C_8H_{17}I$	1.6	2.4	-	-
n-$C_8H_{17}OTs$	3.2	-	3.5	-

Effect of the nucleophile, methoxide versus azide

Azide is a better nucleophile than methoxide in both protic and aprotic solvents, but the difference is much greater in the aprotic solvent (DMSO) (Table 4-3). As expected, elimination competed with substitution when methoxide was the nucleophile (Scheme 4-5), but no elimination product was observed when azide was the nucleophile.

Table 4-3. Relative nucleophilicities of azide versus methoxide in S_N2 reactions.

Substrate	k_{rel} (CH_3OH)	k_{rel} (DMSO)
n-$C_7H_{15}Br$ (50°C)	1.7	13.7
n-$C_8H_{17}OTs$ (50°C)	1.9	-
$PhCH_2Br$ (15°C)	3.5	7.3

Rate of N_3^- / rate constant of MeO^-

Methoxide's greater basicity in DMSO than in methanol is reflected by the significantly greater amount of elimination observed in DMSO. Iodide was examined as a nucleophile in order to provide a comparison of our results with those of McBee.[113] It was a better nucleophile in DMSO than methoxide (k_{rel} = 4.9), but not as good as azide (k_{rel} = 0.35). Azide was not sufficiently soluble in acetone for rates to be measured, and then only DMSO was used for this evaluation. Comparing McBee's rate constants in acetone versus ours in DMSO, acetone appears to be a slightly better solvent for S_N2 reactions of iodide ion.

Solvent effect, methanol versus DMSO

Lastly, it is to be noted that the S_N2 reactions of both nucleophiles were much faster in DMSO than they were in methanol (Table 4-4), but rates for azide were affected more greatly than those of methoxide. Thus, as expected from previous literature reports,[125,126] the polar aprotic solvent DMSO facilitates S_N2 reactions better than does the polar protic solvent, methanol. Fuchs and Cole reported a rate ratio of 81 for the reaction of azide with *n*-hexyl tosylate at 40°C for DMSO versus methanol.[125] The ratio that we observed for the analogous reaction of azide with *n*-octyl tosylate at 50°C was 54.

Table 4-4. Relative rate constants for reactions in DMSO versus methanol

Substrate	Nucleophile	Temp, °C	k_{rel}
n-$C_8H_{17}I$	CH_3O^-	50	45
n-$C_7H_{15}Br$	CH_3O^-	50	29
n-$C_7H_{15}Br$	N_3^-	50	231
$PhCH_2Br$	CH_3O^-	15	76
$PhCH_2Br$	N_3^-	15	161

Rate of DMSO / rate constant of MeOH

Also observed was a significant difference on the substitution/elimination competition for the two solvents, with elimination being significantly more competitive in DMSO (7-13% elimination being observed in methanol as compared with 22-27% in DMSO). The rate of elimination for the reactions of methoxide with *n*-heptyl bromide and *n*-octyl iodide at 50°C were 71 and 164 times faster, respectively, in DMSO than in CH_3OH.

One last insight can be gleaned from the data in Table 4-4, by comparing the rates of benzyl bromide with those of *n*-heptyl bromide. Benzyl bromide is considerably more reactive than the primary alkyl bromide, 48 times faster in the reaction with methoxide in methanol and 88 times faster with azide the nucleophile in methanol, both at 50°C. This

can be compared with a value of 78 given by Streitwieser for the reaction of iodide in ethanol.[127]

Although similar comparative rate data can be found scattered throughout the early literature of nucleophilic substitution and elimination, the above data on S_N2 and E2 reactions of primary alkyl halides, to our knowledge, are not replicated in the literature, and they provide convenient access to quantitative information related to leaving group ability, nucleophilicity and solvent effects that can be useful for both teaching and research.

Fluorinated Substrates

γ-Fluorinated substrates

In terms of chemoselectivity, the γ-fluorine-substituted substrate, *n*-$C_6F_{13}CH_2CH_2Br$, exhibited completely different reactivity with the two nucleophiles, methoxide and azide, as seen in Scheme 4-6. In its reactions with the strong base nucleophile, methoxide, the $R_fCH_2CH_2Br$ substrate underwent exclusive elimination both in methanol and in DMSO, whereas when using weak base, strong nucleophile, azide, as the nucleophile, *only substitution* was observed. The rate data for this series of compounds are given in Table 4-5.

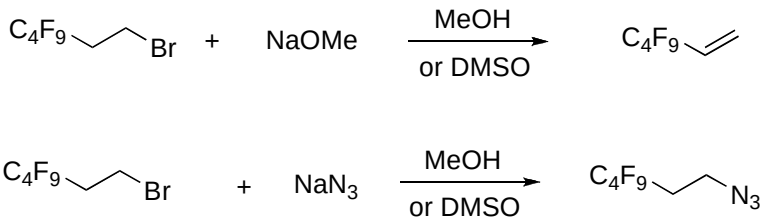

Scheme 4-6. Reactions of perfluoro-*n*-butylethyl bromide with methoxide and azide

This series of reactions allows us to make a direct comparison of substitution and elimination rates of *n*-alkyl versus perfluoro-*n*-alkylethyl bromides. The rate constants for elimination were much larger for methoxide reacting with perfluoro-*n*-butylethyl

bromide than for its reaction with *n*-heptyl bromide (k_{rel} = 1115 in methanol at 50°C, and 2466 in DMSO at 18°C). Comparing the rates of substitution for *n*-heptyl bromide with those of *n*-$C_4F_9CH_2CH_2Br$ at 50°C, in methanol the hydrocarbon bromide underwent substitution 8.4 times faster than the perfluoroalkylethyl bromide, whereas in DMSO the rate ratio was 7.0. This compares with McBee's ratio of 6.1 for the reaction of iodide in acetone at 35°C.[113] Thus, S_N2 chemistry can be observed relatively cleanly for perfluoroalkyethyl bromides when using a good nucleophile that is a weak base, although the presence of the perfluoroalkyl group has a significant damping effect upon the rates of substitution. On the other hand, if the good nucleophile is also a *strong base*, as in the case of methoxide, the rates of elimination are increased to such an extent that there appears to be little chance of observing any significant amount of substitution.

Table 4-5. 2nd order rate constants for perfluoro-*n*-butylethyl bromide.

Expt. No.	Substrate	Solvent	Nuc	T, °C	10^5k_2 S_N2	10^5k_2 E2
5	*n*-$C_7H_{15}Br$	CH_3OH	CH_3O^-	50	3.95 ± 0.24	0.566 ± 0.032
28 [c]	*n*-$C_4F_9CH_2CH_2Br$	CH_3OH	CH_3O^-	50	*no* [a]	631 ± 61
6	*n*-$C_7H_{15}Br$	DMSO	CH_3O^-	18	9.56 ± 0.20	3.48 ± 0.075
29	*n*-$C_4F_9CH_2CH_2Br$	DMSO	CH_3O^-	18	*no*	8,580 [b]
9	*n*-$C_7H_{15}Br$	CH_3OH	N_3^-	50	6.89 ± 0.064	*no* [a]
30	*n*-$C_4F_9CH_2CH_2Br$	CH_3OH	N_3^-	50	0.823 ± 0.056	*no*
12 [c]	*n*-$C_7H_{15}Br$	DMSO	N_3^-	50	1590	*no*
33 [c]	*n*-$C_4F_9CH_2CH_2Br$	DMSO	N_3^-	50	227 ± 71	*no*

[a] *no* = not observed; [b] calculated on the basis that 61% of starting material had reacted after 30 seconds of reaction; [c] These 2nd order rate constants were approximated for comparison purposes using the Eyring equation; the given error was obtained by propagating that of the two data points.

β-Fluorinated substrates

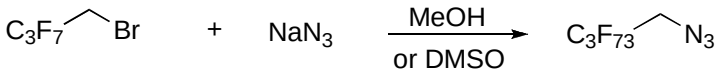

Scheme 4-7. Reactions of azide with perfluoro-*n*-propylmethyl bromide

Substitution was the only process observed for reactions of azide with perfluoro-*n*-propylmethyl bromide in either methanol or DMSO (Scheme 4-7). However, the

analogous reactions with methoxide did not lead to any observable products of substitution. No single product appeared to be formed in the methoxide reactions, which although not yet characterized, may involve some combination of α- and β-elimination processes. There is precedent for β-elimination of fluoride in a related system.[128] The comparative rate data for the azide reactions can be found in Table 4-6.

Table 4-6. 2nd order rate constants for perfluoro-*n*-propylmethyl bromide

Expt. No.	Substrate	Solvent	Nuc	T, °C	$10^5 k_2$
9	*n*-$C_7H_{15}Br$	CH_3OH	N_3^-	50	6.89 ± 0.064
34	*n*-$C_3F_7CH_2Br$	CH_3OH	N_3^-	50	6.90 ± 0.25 x 10^{-4}
12 [a]	*n*-$C_7H_{15}Br$	DMSO	N_3^-	50	1590 ± 300
35	*n*-$C_3F_7CH_2Br$	DMSO	N_3^-	50	4.23 ± 0.32 x 10^{-2}

[a] This 2nd order rate constant was approximated for comparison purposes using the Eyring equation; the given error was obtained by propagating that of the two data points.

The rates for S_N2 substitution of perfluoro-*n*-propylmethylbromide by azide were tremendously inhibited by the proximity of the perfluoroalkyl group, undergoing reaction at 50°C almost 10,000 times slower in methanol and more than 37,000 times slower in DMSO.

α-Fluoro substrate

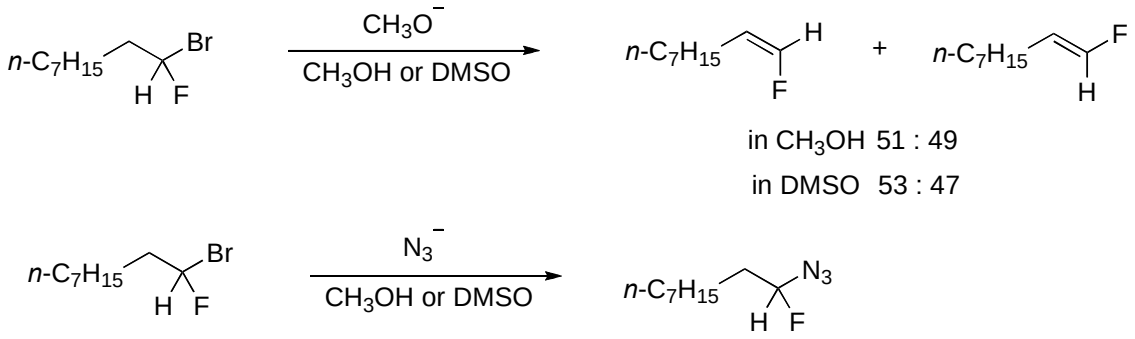

Scheme 4-8. Reactions of 1-bromo-1-fluorononane with methoxide and azide.

As indicated by the data given in Table 4-7, a *single* fluorine substituent at the α-position inhibits substitution while accelerating elimination, although both effects are

modest. These effects combine to give rise to exclusive elimination when MeO^- is used as nucleophile/base, and to exclusive substitution when N_3^- is used (Scheme 4-8).

Table 4-7. 2nd order rate constants for 1-bromo-1-fluorononane.

Expt. No.	Substrate	Solvent	Nuc	T, °C	10^5k_2 S_N2	10^5k_2 E2
5	*n*-$C_7H_{15}Br$	CH_3OH	CH_3O^-	50	3.95 ± 0.24	0.566 ± 0.032
36	*n*-$C_8H_{17}CHFBr$	CH_3OH	CH_3O^-	50	*no*[a]	1.10 ± 0.02
8[b]	*n*-$C_7H_{15}Br$	DMSO	CH_3O^-	50	116 ± 15	40.4 ± 1.1
37	*n*-$C_8H_{17}CHFBr$	DMSO	CH_3O^-	50	*no*	50.5 ± 2.6
9	*n*-$C_7H_{15}Br$	CH_3OH	N_3^-	50	6.89 ± 0.064	*no*
38	*n*-$C_8H_{17}CHFBr$	CH_3OH	N_3^-	50	1.42 ± 0.04	*no*
12[b]	*n*-$C_7H_{15}Br$	DMSO	N_3^-	50	1590 ± 300	*no*
41[b]	*n*-$C_8H_{17}CHFBr$	DMSO	N_3^-	50	226 ± 5.3	*no*

[a] *no* = not observed; [b] These 2nd order rate constants were approximated for comparison purposes using the Eyring equation; the given error was obtained by propagating that of the two data points.

Substitution of 1-bromo-1-fluorononane by azide ion, on the other hand, was modestly slower than of 1-bromoheptane, the non-fluorine-substituted compound undergoing reaction 4.9 times faster in methanol and 7.0 times faster in DMSO than its α-fluoro analog. The azide substitution reaction of the 1-bromo-1-fluoroalkane is 159 times faster in DMSO than it is in methanol. No product deriving from replacement of fluoride was observed for either the elimination or the substitution reactions.

α,α-Difluoro substrate

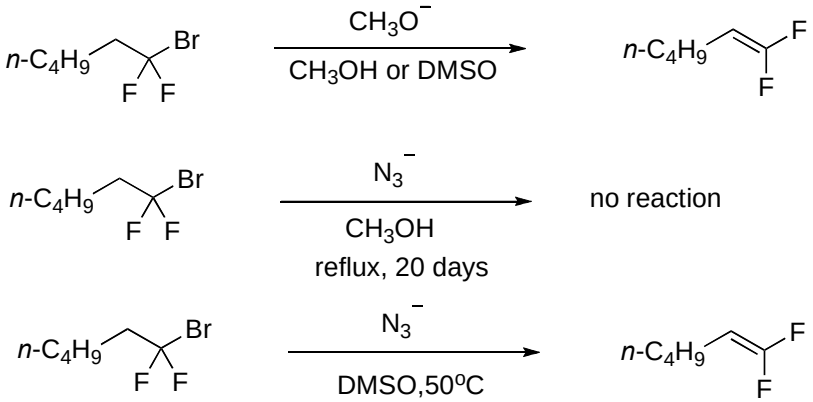

Scheme 4-9. Reactions of 1-bromo-1,1-difluorohexane with methoxide and azide.

No substitution involving displacement of bromide from the CF_2Br group of 1-bromo-1,1-difluorohexane by either methoxide or azide ion was observed in either

solvent, and for the first time, when the reaction was carried out in DMSO, azide was observed to give rise to exclusive elimination (Scheme 4-9).

Whereas substitution was strongly inhibited, elimination was enhanced. The rate of β-elimination of *n*-pentyl-CF_2Br was enhanced relative to that of *n*-alkyl bromide, loss of HBr occurring 4.4 times faster in methanol and 59 times faster in DMSO at 50°C. With no substitution being observed for the reaction of azide in methanol after 20 days at 50°C, it was possible to calculate a *maximum* rate for the S_N2 process if one assumed that one could detect a minimum of 0.5% of product in Expt. No. 47. Therefore the S_N2 reaction at a CF_2Br site is calculated to be at least 13,000 times slower than that at a CH_2Br site of a primary alkyl bromide.

Table 4-8. 2nd order rate constants for 1-bromo-1,1-difluorohexane.

Expt. No.	Substrate	Solvent	Nuc	T, °C	10^5k_2 S_N2	10^5k_2 E2
5	*n*-$C_7H_{15}Br$	CH_3OH	CH_3O^-	50.0	3.95 ± 0.24	0.566 ± 0.032
42	*n*-$C_5H_{11}CF_2Br$	CH_3OH	CH_3O^-	50.0	*no*a	2.50 ± 0.016
8 [b]	*n*-$C_7H_{15}Br$	DMSO	CH_3O^-	50.0	116	40.4
43	*n*-$C_5H_{11}CF_2Br$	DMSO	CH_3O^-	15.5	*no*	225 ± 6.7
44	*n*-$C_5H_{11}CF_2Br$	DMSO	CH_3O^-	20.5	*no*	328 ± 11
45 [b]	*n*-$C_5H_{11}CF_2Br$	DMSO	CH_3O^-	50.0	*no*	2380 ± 660
9	*n*-$C_7H_{15}Br$	CH_3OH	N_3^-	50.0	6.89 ± 0.064	*no*
46 [c]	*n*-$C_5H_{11}CF_2Br$	CH_3OH	N_3^-	50.0	<5.2 x 10-4	*no*
12 [b]	*n*-$C_7H_{15}Br$	DMSO	N_3^-	50.0	1590 ± 300	*no*
47	*n*-$C_5H_{11}CF_2Br$	DMSO	N_3^-	50.0	*no*	1.55 ± 0.037

[a] *no* = not observed; [b] These 2nd order rate constants were approximated for comparison purposes using the Eyring equation; the given error was obtained by propagating that of the two data points; [c] No reaction was observed after 20 days at 50°C; the *maximum* rate was approximated by assuming that 0.5% of product could have been detected.

Fluorinated benzylic bromides

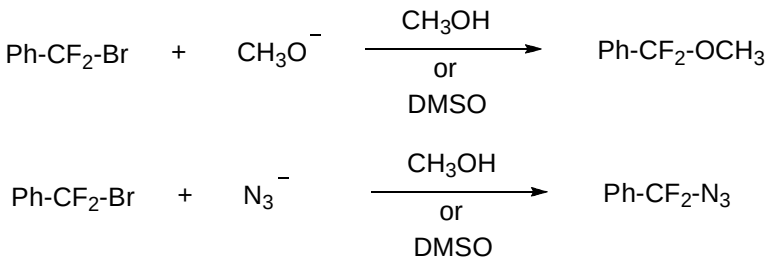

Scheme 4-10. Reactions of bromodifluoromethylbenzene with methoxide and azide.

The substitution of an α,α-difluoroalkyl compound was not possible, even with the weak base-strong nucleophile N_3^-. Only elimination was seen for this material. This demonstrates, so far, how big the effect of close-by fluorines is in an S_N2 reaction.

Nucleophilic substitution at the CF_2Br site of $PhCF_2Br$ has been reported,[110] and thus a study of this system where elimination cannot compete should be able to provide a more exact measure of the difference in S_N2 reactivity of a CF_2Br versus a CH_2Br site. In fact, both methoxide and azide were found to be effective nucleophiles in their reactions with $PhCF_2Br$ (Scheme 4-10).

Table 4-9. 2nd order rate constants for bromodifluoromethylbenzene.

Expt. No.	Substrate	Solvent	Nuc	T, °C	10^5k_2 S_N2
20 [a]	$PhCH_2Br$	CH_3OH	CH_3O^-	50	188 ± 46
48	$PhCF_2Br$	CH_3OH	CH_3O^-	50	4.29 ± 30 x 10-3
21	$PhCH_2Br$	DMSO	CH_3O^-	15	1020 ± 74
49	$PhCF_2Br$	DMSO	CH_3O^-	60	1.25 ± 0.045
50	$PhCF_2Br$	DMSO	CH_3O^-	50	0.549 ± 0.024
51[a]	$PhCF_2Br$	DMSO	CH_3O^-	15	1.96 ± 0.58 x 10-2
24 [a]	$PhCH_2Br$	CH_3OH	N_3^-	50	606 ± 20
52	$PhCF_2Br$	CH_3OH	N_3^-	50	8.88 ± 0.32 x 10-3
25[b]	$PhCH_2Br$	DMSO	N_3^-	15	7480 ± 250
53	$PhCF_2Br$	DMSO	N_3^-	60	2.34 ± 0.11
54	$PhCF_2Br$	DMSO	N_3^-	50	1.06 ± 0.058
55 [a]	$PhCF_2Br$	DMSO	N_3^-	15	4.35 ± 1.8 x 10-2

[a] These 2nd order rate constants were approximated for comparison purposes using the Eyring equation; the given error was obtained by propagating that of the two data points; [b] approximate, single point rate constant (56.8% of substrate consumed after 30 sec)

Table 4-10. Relative rates for S_N2 reactions of $PhCH_2Br$ versus $PhCF_2Br$.

Nucleophile	Solvent	Temp., °C	k_{rel} (CH_2Br/CF_2Br)
CH_3O^-	CH_3OH	50	43,800
CH_3O^-	DMSO	15	52,000
N_3^-	CH_3OH	50	68,200
N_3^-	DMSO	15	172,000

From the data in Table 4-10, as well as in Table 4-8, one can see that the presence of two α-fluorines provides a formidable inhibition of S_N2 chemistry, such that

E2 chemistry will exclusively dominate, except in those cases, such as in the benzyl system, where E2 is not possible.

Computational Results

In the experimental part of this paper, we have quantified the effect that near-by fluorines have on raising the S_N2 activation barrier, as well as their effect of lowering the E2 energy.

A recent computational paper by Liu et al. examined the effect of substituents on the S_N2 energy barrier.[129] Examining 54 different structures using CH_3Cl as a reference and fluoride as a nucleophile, Liu broke down the observed effects into three contributions (Equation 4-4), ΔE_s comprising the steric, ΔE_q the quantum, and $\Delta E_e$the electrostatic contribution. According to Liu's work, the steric effect is described by the Weizsacker kinetic energy, the quantum effect corresponds mainly to the exchange-correlation contribution, whereas the electrostatic effect is defined by a combination of a) nuclear-electron attraction, b) classical electron-electron Coulomb repulsion and c) nuclear-nuclear repulsion energies.

$$\Delta E \equiv \Delta E_s + \Delta E_q + \Delta E_e \qquad (4\text{-}4)$$

Consistent with general experimental observations, Lui's results show that the exchange of one hydrogen on the CH_3Cl by almost any other group leads to an increase in the energy barrier due to an increase in steric interactions, but that this is compensated by a decrease due to the quantum effect, with the result that the observed net overall increase in barrier is due largely to the impact of increasing electrostatic effect Liu finds that fluorine substituents do not fit this generalization. He does find that the substitution of hydrogens by one or more fluorines *increases* the energy barrier, but

the steric effect was found to decrease significantly for each hydrogen/fluorine replacement, with this decrease being compensated now by an equivalent *increase* in barrier from the quantum effect. Again, the net result was that the overall increase in energy barrier derived largely from the incremental increases in the electrostatic effect as one replaced hydrogen with fluorine, the largest contribution to this increase being the classical electron-electron Coulomb repulsive interaction.

In our computational study of the impact of fluorine on S_N2 and E2 transition state energies, we examined a series of model reactions involving hydroxide acting either as a nucleophile or a base (Scheme 4-11).

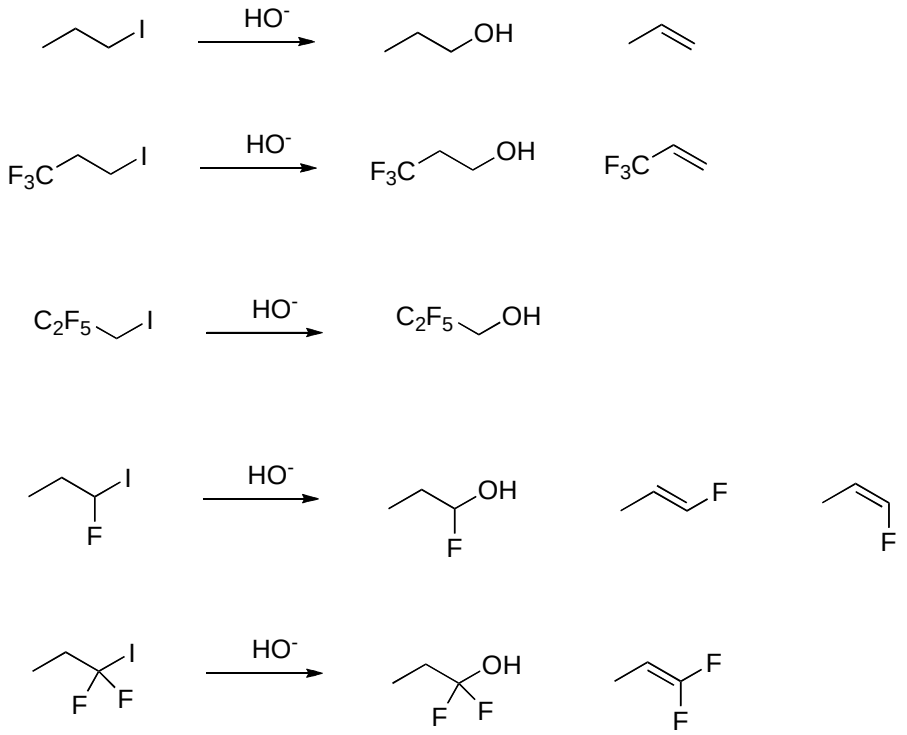

Scheme 4-11. Model structures used in the quantum chemical calculations.

The quantum chemical calculations were performed at MP2/6-31+G(d,p)-LANL2DZ level of theory using DMSO as a solvent, with the transition states being characterized by one and only one negative frequency and the Intrinsic Reaction Coordinate connecting both the starting material and the product. All the calculations

were performed using Gaussian 03 Software package.[92] Table 4-11 presents the enthalpy of reactions ΔH, energy barriers $\Delta G^{\ddagger}$ and some relevant geometrical data for the S_N2 transition state (TS) for the alkyl- iodide substrates with hydroxide as nucleophile.

Table 4-11. Relevant geometrical data and calculated energy barriers at the transition state for the S_N2 reaction between alkyl-iodide substrates and hydroxide.

Substrate	O-C (Å)[a]	C-I (Å)[b]	ΔH (Rx)	$\Delta G^{\ddagger}$[c]
n-C_3H_7I	2.22	2.54	-40.50	19.24
$CF_3C_2H_4I$	2.17	2.52	-43.03	19.65
$C_2F_5CH_2I$	2.13	2.50	-39.24	25.92
C_2H_5CHFI	2.24	2.58	-54.40	19.74
$C_2H_5CF_2I$	2.31	2.70	-62.20	29.17

[a] Oxygen - Carbon-center bond length; [b] Carbon-center – Iodide bond length; [c] Calculated energy barrier in kcal/mol

Looking at the last column of Table 4-11, it is seen that all of the substitution reactions are exothermic, as expected. Whereas the enthalpies of the β, γ, and non-fluorinated substrates do not differ greatly, those of the α-fluorinated substrates are considerably larger. This can be attributed to what has become known as "incremental geminal stabilization", wherein significant thermodynamic molecular stabilization derives from increased fluorine substitution on a carbon.[130] Similarly, it would be expected that the presence of an electronegative oxygen substituent on the same carbon as a fluorine or two fluorine substituents will provide significant stabilization to the molecule due to a hyperconjugative interaction of the type O(LP)→σ*(C-F).

Experimentally we found that the magnitude of the activation barrier for the S_N2 reaction using azide as a nucleophile had the following trend: *n*-$C_7H_{15}Br$ < *n*-$C_4F_9CH_2CH_2Br$ ~ *n*-$C_8H_{17}CHFBr$ << *n*-$C_3F_7CH_2Br$ < *n*-$C_5H_{11}CF_2Br$. The calculated activation barriers shown in Table 4-11 for hydroxide acting as a nucleophile follow the

same trend, which is consistent with the experimental observation that the presence of fluorines near the reactive site increases the energy barrier.

The incremental changes in the $\Delta G^{\ddagger}$ values found in the calculations can be understood in two ways. First, the partial positive charge that is generated at the carbon-center of an S_N2 transition state should be inductively destabilized by the presence of β or γ fluorines, resulting in an increase of the energy barrier. In the case of α-fluorines this partial positive charge might be partially stabilized (by electron donation by fluorine's lone pairs), which brings us to the second factor. Taking into account Liu's work, the electrostatic repulsive interactions between the incoming nucleophile and the electron clouds of the near-by fluorines should increase the activation energy, with this effect being largest for the gem-difluoro substrates.

As seen in Table 4-11, this repulsive effect due to the α-fluorines appears to give rise to larger distances between the nucleophile and the carbon-center at the TS for the α-fluorinated molecules than for the non-fluorinated standard: $C_2H_5CF_2I > C_2H_5CHFI >$ n-C_3H_7I. At the same time the length of the carbon- iodine leaving group bond is also larger than that for the non-fluorinated substrate, which is consistent with the loss of the Iodide being assisted by the α-fluorines, stabilizing the partial positive charge at the carbon-center. The net increase in barrier indicates that the repulsive effect outweighs the stabilizing effect, slightly for the mono-α-fluoro and greatly for the substrates with two α-fluorine substituents.

Evidence for the stabilization of the partial positive charge by α-fluorines in the transition state is seen by comparison of the bond lengths between the fluorine and the carbon center in the transition states of the α-fluoro substrates. They are shorter than

those in the respective ground states, i.e. C-F(Å) changes from 1.42 to 1.36 for the reaction of C_2H_5CHFI and from 1.38 to 1.32 for the reaction of $C_2H_5CF_2I$.

Further insight can be obtained by looking at the geometry of the transition state for the reaction of C_2H_5CHFI, where the OH nucleophile is seen to approach the carbon-center from an angle closer to the α-hydrogen than to the fluorine (Figure 4-2). This could be interpreted as the nucleophile *avoiding the repulsive interaction* with the α-fluorine.

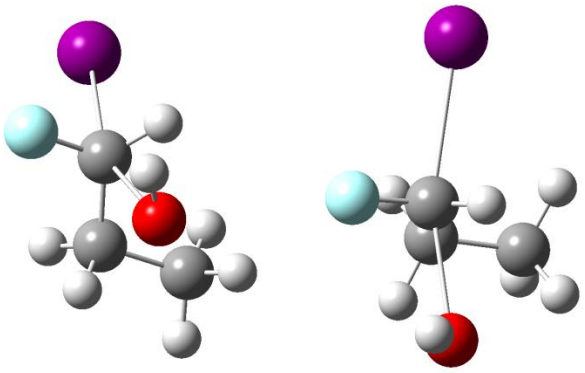

Figure 4-2. Two perspectives of the calculated transition state of the S_N2 reaction of hydroxide with CH_3CH_2CHFI.

Such avoidance would not be possible for the α,α-difluoro compound, with the result that it would have a much higher activation barrier, whereas the α-monofluoro compound would only be slightly less reactive than the fluorine-free compound.

During the experimental study, it was found that methoxide acted exclusively as a base in reactions with all of the fluoro compounds where E2 was possible. Such results undoubtedly derive from a combination of two effects. First, the barriers for the potentially competitive S_N2 reactions are increased when fluorine is present, and secondly, the acidities of those β-hydrogens that are vicinal to fluorines are increased, such that the activation barriers for their E2 processes are lowered. This combination of

slowing down the S_N2 and enhancing the E2 reactions can explain the experimental results.

Table 4-12. Relevant geometrical data and calculated energy barriers at the transition state for the E2 reaction between alkyl-iodide substrates and hydroxide as base.

Substrate	O-H (Å)[a]	H-C (Å)[b]	C-C (Å)[c]	C-I (Å)[d]	ΔH (Rx)	$\Delta G^{‡}$[e]
C_3H_7I	1.33	1.31	1.43	2.43	-36.41	19.87
$CF_3C_2H_4I$	1.27	1.35	1.48	2.24	-32.19	3.86
C_2H_5CHFI (E)	1.30	1.32	1.43	2.39	-33.33	11.56
C_2H_5CHFI (Z)	1.31	1.32	1.43	2.39	-33.63	11.67
$C_2H_5CF_2I$	1.28	1.34	1.43	2.32	-28.35	7.93

[a] Oxygen - Hydrogen bond length (new OH bond); [b] Hydrogen - Carbon bond length (Breaking bond); [c] Carbon-Carbon bond length (new double bond); [d] Carbon – Iodide bond length (Breaking bond); [e] Calculated energy barrier in kcal/mol

The quantum chemical calculations, as represented in Table 4-12, support these conclusions. Experimentally, the α,α-difluoroalkyl bromide has such a high energy barrier for the S_N2 reaction, that even azide would prefer to behave as a base, albeit at a slow rate. The highest calculated energy barrier, $\Delta G^{‡}$, for substitution was 29.17 kcal/mol, which was for the 1,1-difluoro compound. Even with such a relatively high barrier, it seems reasonable that this reaction would have occurred were it not for the relative ease of the elimination reaction. Comparing values from Tables 4-11 and 4-12 one can see that for each of the reactions of fluorinated compounds where β-elimination is possible, the energy barrier for the E2 process is much lower than that for S_N2.

The calculated trend for the activation barrier in the E2 reaction decreases as follows: $C_3H_7I > C_2H_5CHFI > C_2H_5CF_2I > CF_3C_2H_4I$, which is consistent with the observed experimental trend. From the data in Table 4-12 it is possible to glean other interesting insight. Although both $CF_3C_2H_4I$ and $C_2H_5CF_2I$ have multiple fluorines in the β-position with respect to the abstracted hydrogen, the barrier to elimination of the CF_2I compound is double that of $CF_3C_2H_4I$. We believe that this is due to the fact that in the

transition state for the elimination of $CF_3C_2H_4I$, one of the fluorines from the CF_3 group have a dihedral angle of almost 180^o with respect to the hydrogen that is being removed. Thus, in addition to the inductive stabilization that the CF_3 group provides, there is hyperconjugative stabilization of this transition state, with interaction of the partial negative forming charge and the σ* orbital of the *anti* C-F bond. In contrast, looking at the transition state for elimination from $C_2H_5CF_2I$, both fluorines are skewed at a dihedral angle of about 60^o from the breaking C-H bond, which means that these fluorines can only provide inductive stabilization of the developing negative charge on this carbon.

All of the elimination transition states were characterized computationally as E2 processes. However, one can see that the lowest $\Delta G^{\ddagger}$ values have the longest C-H bond lengths, and least C-C double bond character based on bond length of the forming double bond, and the shortest C-I bond length. These results suggest a highly unsymmetrical bimolecular elimination consistent with E_1cb character.

The elimination of HI from the mono-fluoro, C_2H_5CHFI can result in formation of either cis (*Z*) and trans (*E*) products. The calculated energy barriers for these reactions were found to be very similar, and this correlates with the almost 1:1 ratio observed experimentally.

Finally, the enthalpy of reactions presented on Table 10-2 help to support the proposed hyperconjugative interaction of the type O(LP)→σ*(C-F) since there is not an OMe group attached in any of products, the enthalpy of the reaction does not change as much as in Table 4-11. The data presented in Table 4-12 clearly supports that the Elimination vs Substitution is dominated by the transition state since all substituted

products are more stable than the eliminated ones. The Z product is slightly more stable than the E product for the C_2H_5CHFI compound, which is known due to the slightly larger antiperiplanar hyperconjugation σ(CH)→σ*(CF).

Experimental Section

Synthesis of 1-bromo-1-fluorononane (58): In the following order 170 mL of anhydrous CH_2Cl_2, 5.1 mL (28.1 mmol, 1 equiv., 95%) of nonanal and 3.9 mL (33.7 mmol, 1.2 equiv.) of 2,6-lutidine were placed into a 250 mL round bottomed flask. The mixture was then cooled down to -5 ˚C and 9.5 mL (56.2 mmol, 2 equiv.) of triflic anhydride in 20 mL of anhydrous CH_2Cl_2 were added dropwise to the reaction mixture over a period of 45 min. The reaction was stirred for 7h at 0 ˚C and was then placed in the refrigerator (0 ˚C) for an extra 17 hours. The relatively dilute nonanal solution, the presence of the base and the slow addition of triflic anhydride were important in order to obtain good yield in this reaction; otherwise a polymer is obtained as a major product. The solvent was removed and the dark remaining mixture was extracted with pentane (4 x 100 mL). The polymer is insoluble in pentane. The organic layer was washed with aqueous HCl 1.2 M (2 x 100 mL), followed by concentrated aqueous $NaHCO_3$ (2 x 100 mL) and then brine (1 x 100 mL). The solution was dried over $MgSO_4$, filtered, and the solvent removed to give a dark yellow oil, 9.5 g, 80% yield of the geminal, bis-triflate (by NMR). This material was used without further purification for the following step. Once the solvent is removed, the product should be kept in the refrigerator, since it not stable neat at room temperature

The bis-triflate (9.5 g, 22.5 mmol, 1 equiv.) along with 150 mL of anhydrous CH_2Cl_2 were placed in a 250 mL round bottomed flask. The mixture was then cooled to 0 ˚C, and 22.5 mL of TBAF 1M solution in THF (22.5 mmol, 1 equiv.) were added and

stirred for 12 h at 0 ˚C. Subsequently 14.5 g (45 mmol, 2 equiv.) of tetrabutylammonium bromide were added and stirred at room temperature for 16 hours more.

The solvent was then removed and the remaining oily material was filtered through silica gel using pentane as a solvent. The solvent was removed and a second column in pentane was run to obtain 68% of product. The result is a mixture of 88% 1-bromo-1-fluorononane (**58**) and 12% 1,1-difluorononane, which was used for the kinetic experiments as is. ^{1}H NMR ($CDCl_3$) δ 6.36-6.53 (dt, $^{2}J_{HF}$ = 50.7 Hz , $^{3}J_{HH}$ = 5.3 Hz, 1H, C**H**F), 2.00 - 2.45 (m, 2H, CH_2), 1.20 – 1.75 (m, 14H, CH_2), 0.89 (t, 3H, CH_3); ^{19}F NMR ($CDCl_3$) δ -130.65 (ddd, $^{2}J_{HF}$ = 50.3 Hz, $^{3}J_{HH}$ = 20.5 Hz, $^{3}J_{HH}$ = 18.2 Hz, 1F); ^{13}C NMR ($CDCl_3$) δ 95.9 (d, $^{1}J_{CF}$=252.5 Hz, **C**HF), 40.9 (d, $^{2}J_{CF}$=18.7 Hz, CH_2(**C**HF)), 32.02 (CH_2), 29.56 (CH_2), 29.33 (CH_2), 28.91 (CH_2), 25.30 (CH_2), 22.86 (CH_2), 14.29 (CH_3); HRMS: Calc. 223.0503 ($(M-H)^+$). Found. 223.0489 ($(M-H)^+$).

1-Octyl Tosylate (55) was prepared according to the literature.[115] It's NMR spectra were consistent with those in the literature.[131]

General Procedure for the Kinetic Experiments

Stock solutions of NaN_3, NaOMe and NaI (0.6 M in MeOH-d_4 and DMSO-d_6) were prepared prior to the kinetics experiments. For kinetic experiments below room temperature, 0.75 mL of the required 0.6M stock solution, and 5-10 mg of internal standard (toluene for ^{1}H NMR and trifluorotoluene for ^{19}F NMR) were placed into an NMR tube and the tube cooled to the desired temperature inside the NMR instrument. Then, 0.22 mmols of substrate previously dissolved in 0.25 mL of deuterated solvent were added to the NMR tube. The reaction was then followed by measurement of the decrease of one particular NMR signal with respect to the internal standard up to 30%

of the reaction. For kinetic experiments above room temperature, 0.22 mmol of substrate in 0.25 mL of deuterated solvent were placed into an NMR tube, and then 0.75 mL of the corresponding 0.6M stock solution and 5-10 mg of internal standard were added. The NMR tube was warmed to the desired temperature and the reaction followed by NMR up to 30% of the reaction.

Computational Methods

The quantum chemical calculations were performed with a hybrid basis set at MP2/6-31+G(d,p)- LANL2DZ level of theory. The effective core potential (ECP) of iodide was included in the calculations in order to minimize the time in the optimization. DMSO was used as a solvent in all calculations using the Polarizable Continuum Model (PCM). The transition states were characterized by one and only one negative frequency and the Intrinsic Reaction Coordinate (IRC) connecting both the starting material and the product. All the calculations were performed using Gaussian 03 Rev. E01 Software package.[92]

CHAPTER 5
CONCLUSIONS

The role of fluorine in three areas has been evaluated. All three fields are consistent with the fact that fluorine brings very interesting chemistry and behavior to the molecules it is part of. We had the opportunity to work with fluorine synthetically, theoretically and kinetically, and the conclusions have been divided into each individual area.

Fluorine as Pentafluorosulfanyl Group in Furazan Energetic Materials

The role of fluorine as pentafluorosulfanyl group in furazan energetic material was evaluated. Ten new energetic materials have been synthesized and characterized by the usual spectroscopic methods. An SF_5-acetyl building block was chosen, and the best reaction conditions to incorporate this group into aminofurazans were established. Eight of these materials are SF_5-furazan-based, one being tetrazole-based and the last one does not contain an SF_5 group. The chemical and physical properties of the SF_5 and furazan groups, such as high density and good thermal and chemical stability, have been combined with good results. Good thermal stabilities and high densities are the two most important properties possessed by the SF_5-furazan-based energetic materials. Their general level of performance was better than that of the baseline compound and of other previously synthesized SF_5-containing energetic materials.

During the course of this project small scale reactions were utilized, and there were no issues or accidents encountered while working with the final products. They proved to be stable under the laboratory conditions that were used. The SF_5 group proved to be very stable under strong oxidizing conditions, but the electron-withdrawing

ability of the furazan group makes the SF_5-acetyl or SF_5-urea functionalities good leaving groups, which sometimes limited one's ability to isolate such derivatives.

The lack of nucleophilicity of the aminofurazans was the most serious problem that we encountered within this project. The electron-withdrawing ability of the furazan ring made the functionalization of the amino groups very challenging, and at times impossible. Solubility issues also presented a serious synthetic obstacle when trying to make many of the furazan derivatives.

Based on their high density, good thermal and chemical stability, and the performance results of these compounds, as calculated by Cheetah, we believe that this new class of high density energetic materials creates much potential for future benefit to the field of high energy, high density materials. For these reasons we think is important to continue research on this new class of materials. Although the SF_5-acetyl building blocks are reactive enough for the functionalization of the aminofurazans, it is important to redesign the aminofurazans in such a way that the amino group (or alcohol) is separated by at least one carbon from the furazan group. This should help with both types of problems that we encountered, the nucleophilicity of the amino group and the stability of the new derivatives (amides, ureas, esters or carbamates).

Finally, the high fluorine content, along with the low hydrogen content of these new compounds, as well as the presence of sulfur, allow these materials the possibility of releasing "free fluorine" upon detonation. Further experimental results must be obtained in order to determine quantitatively which gases are actually released when the materials are detonated.

Fluorine and Its Impact on Long Range Coupling Constants

The results presented in this work show the important structural information that can be obtained by performing a detailed analysis of long-range J_{FF} coupling constants in mono-substituted perfluoro[2.2]paracyclophanes. In particular, OMe and Et_2N substituents were taken as a model compounds to study, from a theoretical point of view, the influence of a skewed geometry on the $^4J_{FF}$ and $^5J_{FF}$ couplings. It was found that the $^4J_{FF}$ Spin-Spin Coupling Constants (SSCCs) are due to the through space transmission of the FC term by the contact of the orbital clouds of the interacting fluorines, and they are strictly distance dependent.

On the other hand, the $^5J_{FF}$ SSCCs are also transmitted through the space but with the help of an intermediate moiety. To this end, the FCCP-CMO approach was applied to rationalize the unusual trends observed for the FC term of such couplings. The angle by which the orbitals interact seemed to be in this case the most important factor in determining the coupling transmission.

When the substituent on F8 was H, it was found that the preferential conformation is ‘away’ indicating that the size of the substituent is not the only interaction determining the conformation of the type of monosubstituted perfluoroparacyclophanes studied in this work. Apparently, an important role determining such conformation is played by an attractive interaction between the available lone pairs on the heteroatoms and fluorines on one ring with the electron deficient π system of the other benzene ring.

Fluorine and Its Impact on S_N2 and E2 Reactions

An experimental measure of the quantitative effect of proximate fluorine substituents on the rates of S_N2 and E_2 reactions has been obtained. The study was comprised mainly of reactions of fluorinated *n*-alkyl bromides with weak base, strong

nucleophile azide ion and strongly basic nucleophile methoxide ion in the protic solvent methanol and the aprotic solvent, DMSO.

The order of reactivity for S_N2 reactions of azide in methanol at 50^oC was *n*-alkyl-Br > *n*-alkyl-CHFBr > *n*-perfluoroalkyl-CH_2CH_2Br >> *n*-perfluoroalkyl-CH_2Br > *n*-alkyl-CF_2Br, with approximate relative rates of reaction being: 1, 0.20, 0.12, 1×10^{-4}, 7.7×10^{-5}. The order of reactivity for E_2 reactions was *n*-perfluoroalkyl-CH_2CH_2Br >> *n*-alkyl-CF_2Br > *n*-alkyl-CHFBr > *n*-alkyl-Br, with the approximate relative rates for reaction of methoxide in methanol at 50^oC being: 1100, 4.4, 1.9, 1. It appears that the detrimental effect of fluorine substituents on S_N2 reactions derive from two main effects: their electron withdrawing inductive effect, which destabilizes the partial positive charge that develops at the carbon center undergoing substitution, and the electrostatic repulsive influence of (particularly α-substituted) fluorine lone pairs on the approaching nucleophile. The rate-enhancing effect of fluorine substituents on E_2 reactions appears to be largely due to their C-H acidifying influence, which derives from two factors: their aforementioned inductive effect, and when geometry allows, their powerful hyperconjugative stabilization of developing β-negative charge.

APPENDIX A
SF_5-ENERGETIC MATERIALS

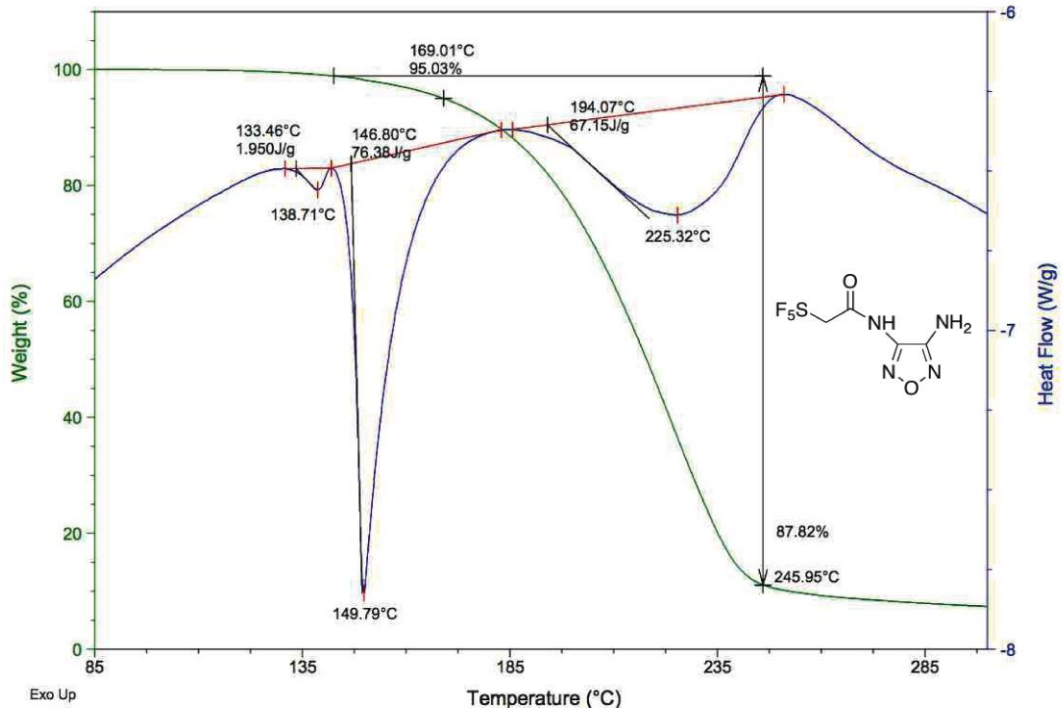

Figure A-1. TGA-DSC compound **27**

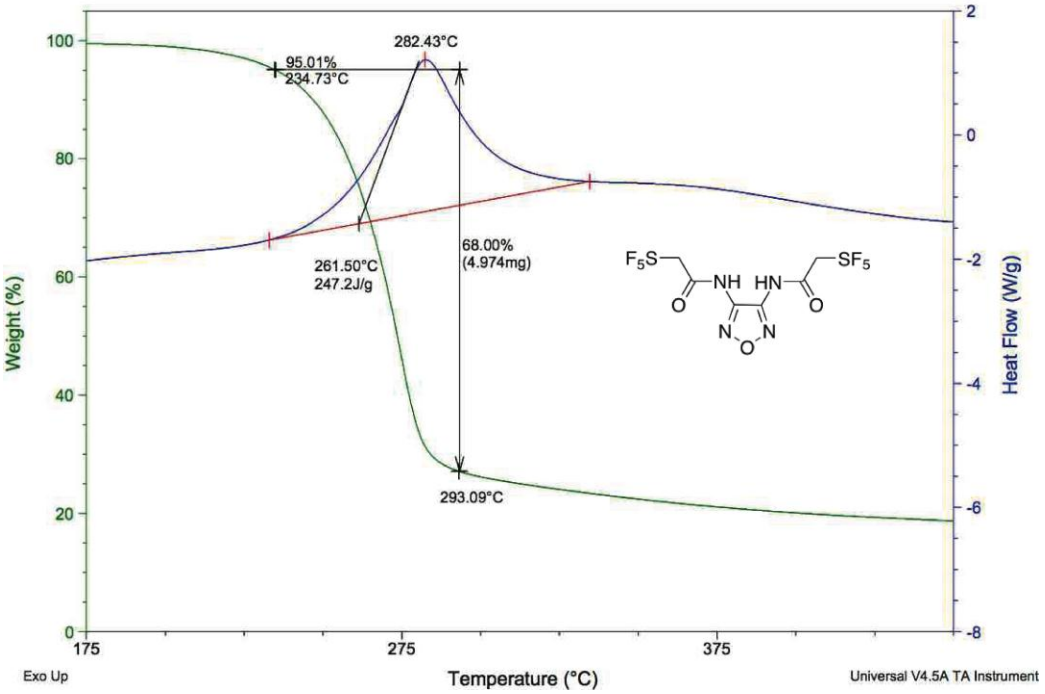

Figure A-2. TGA-DSC compound **28**

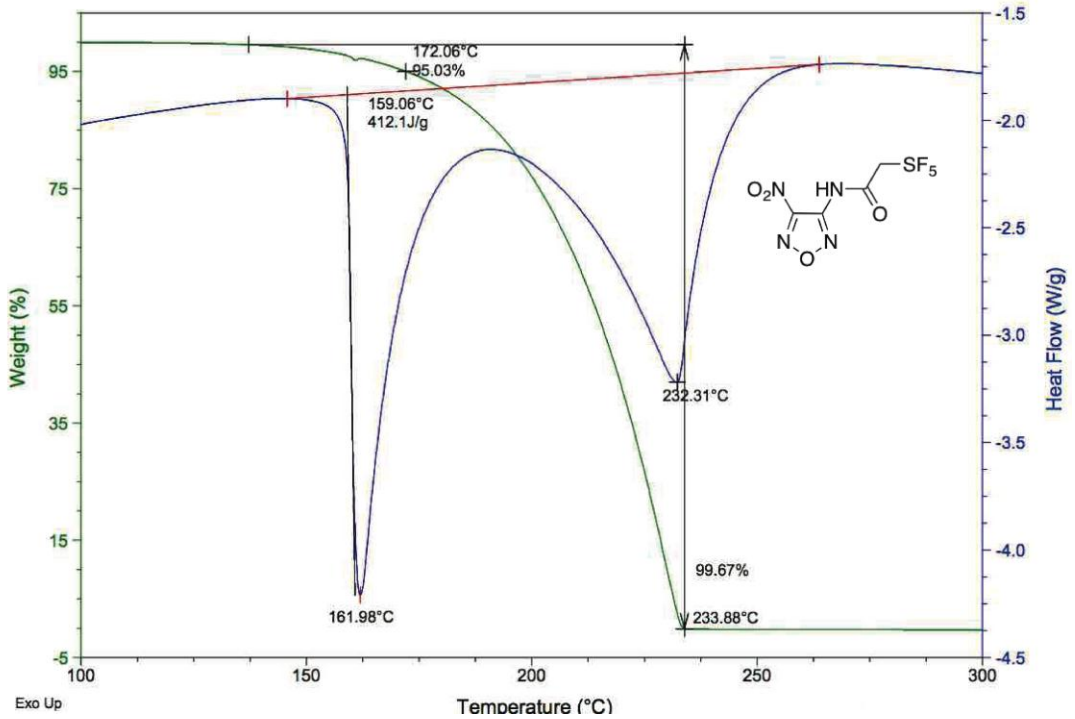

Figure A-3. TGA-DSC compound **50**

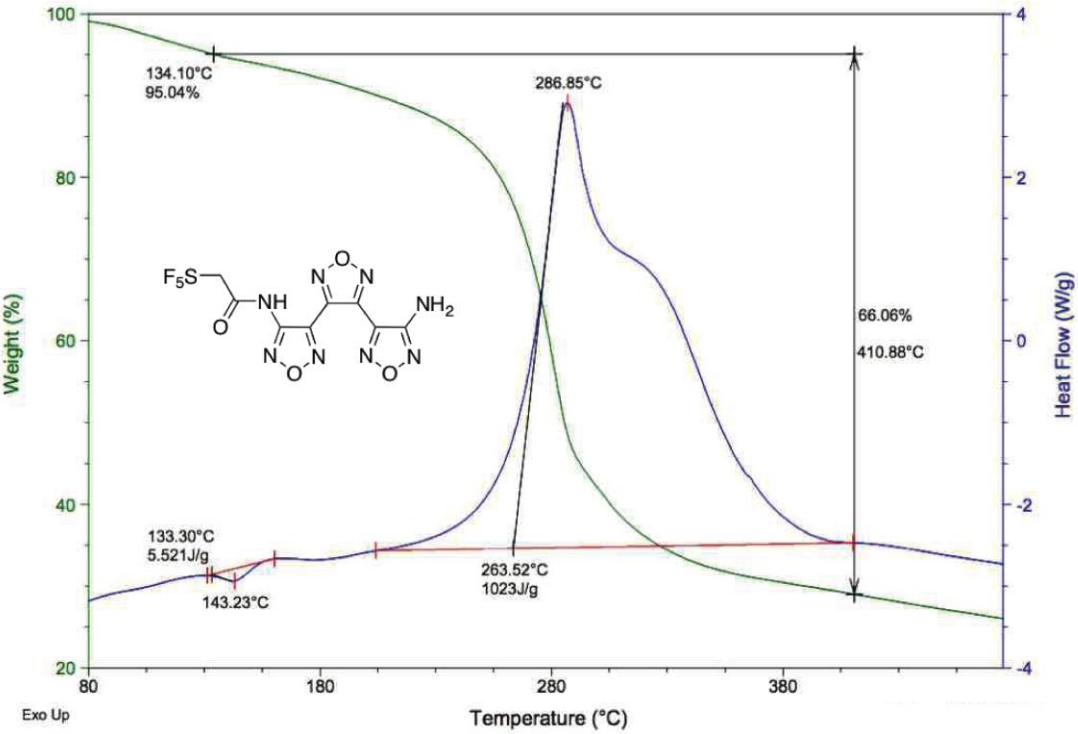

Figure A-4. TGA-DSC compound **29**

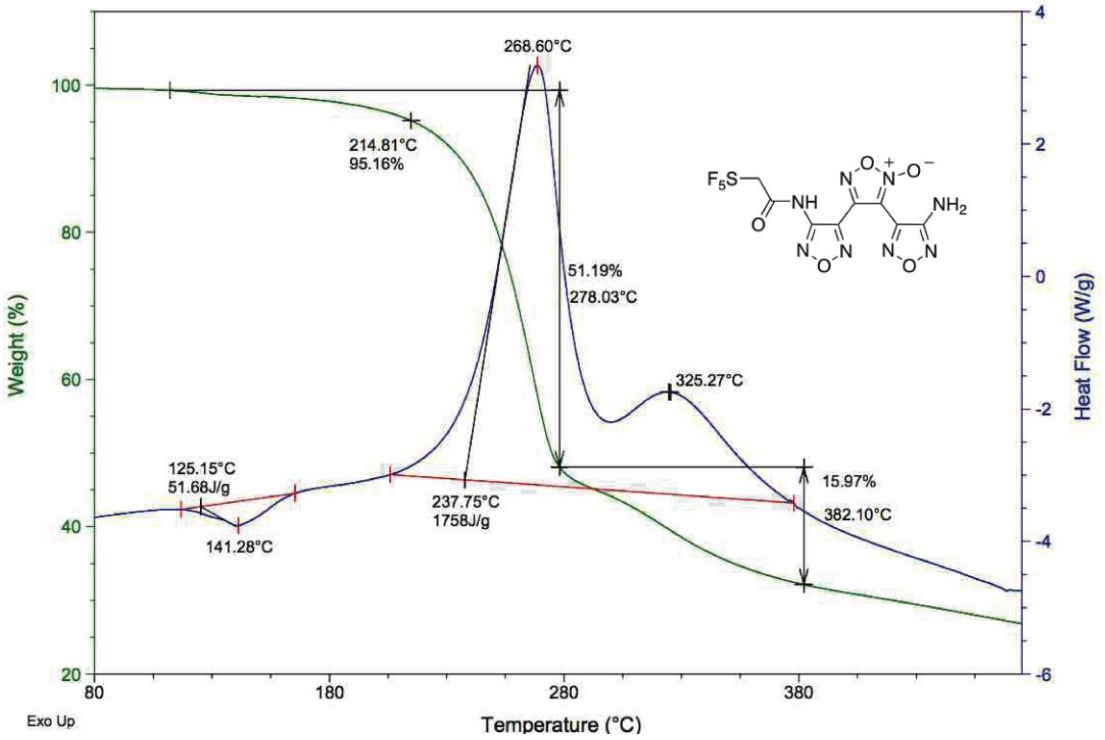

Figure A-5. TGA-DSC compound **30**

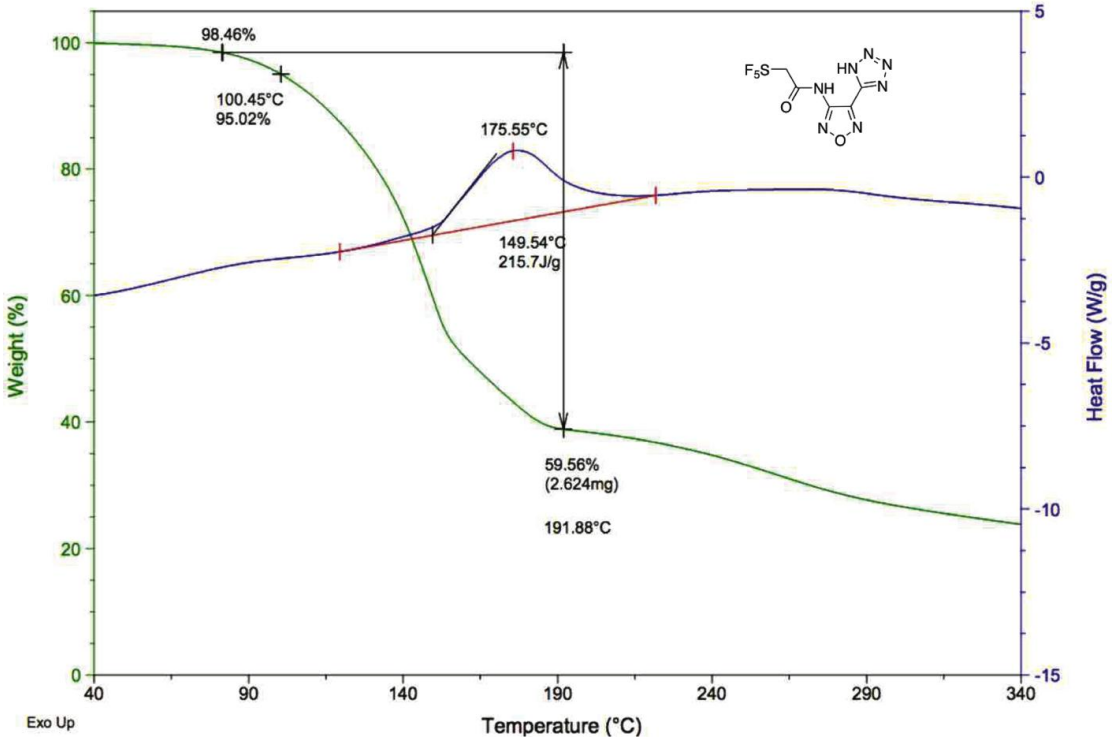

Figure A-6. TGA-DSC compound **31**

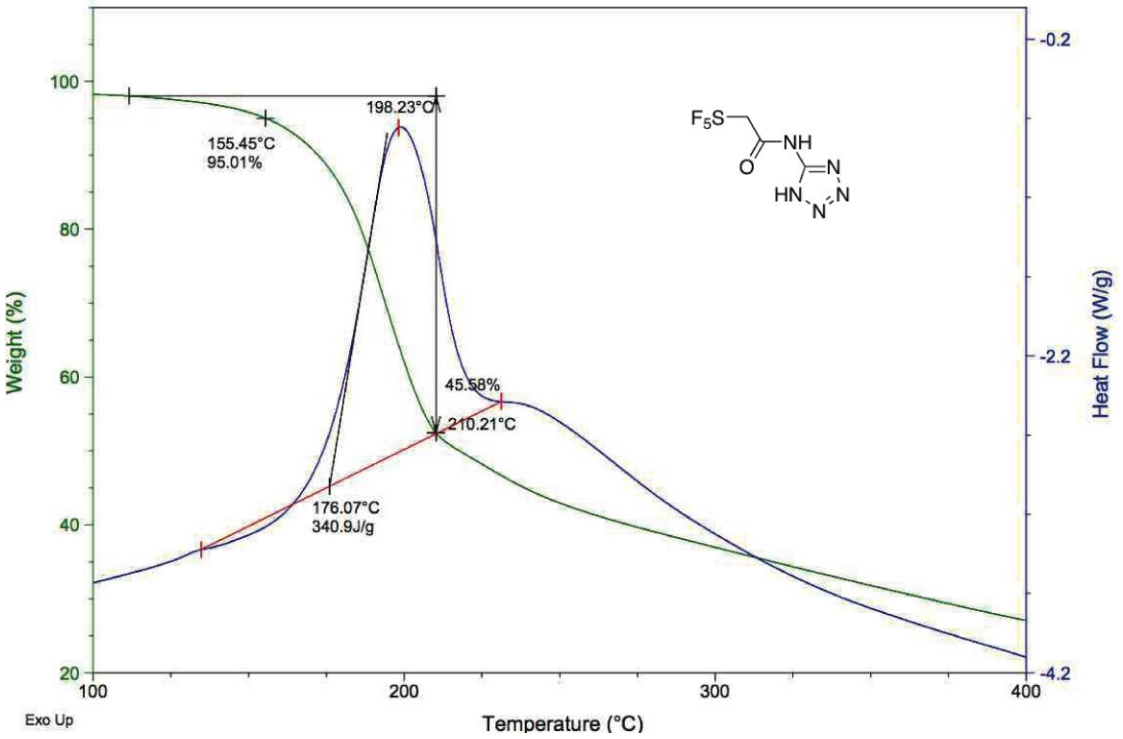

Figure A-7. TGA-DSC compound **32**

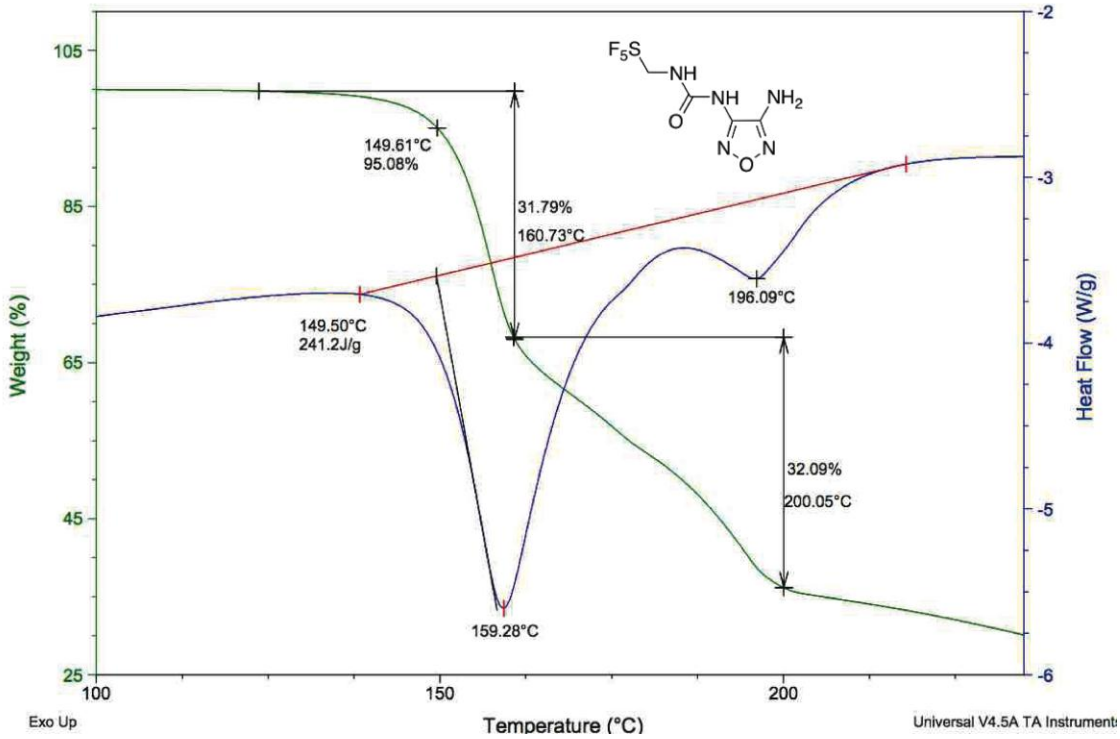

Figure A-8. TGA-DSC compound **48**

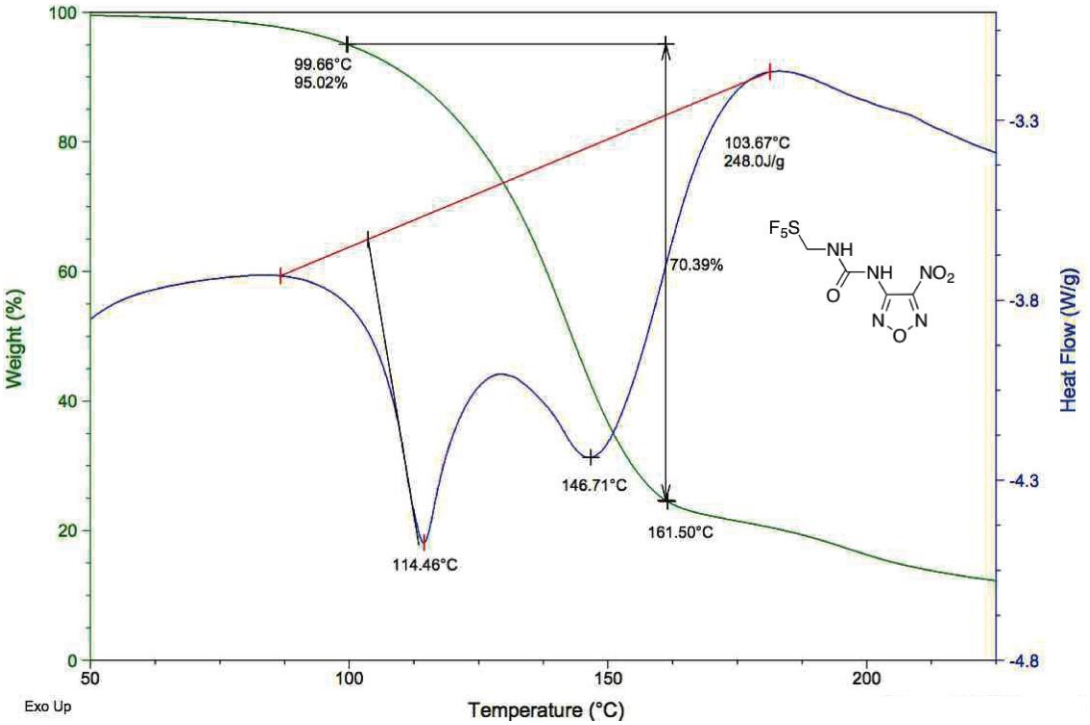

Figure A-9. TGA-DSC compound **49**

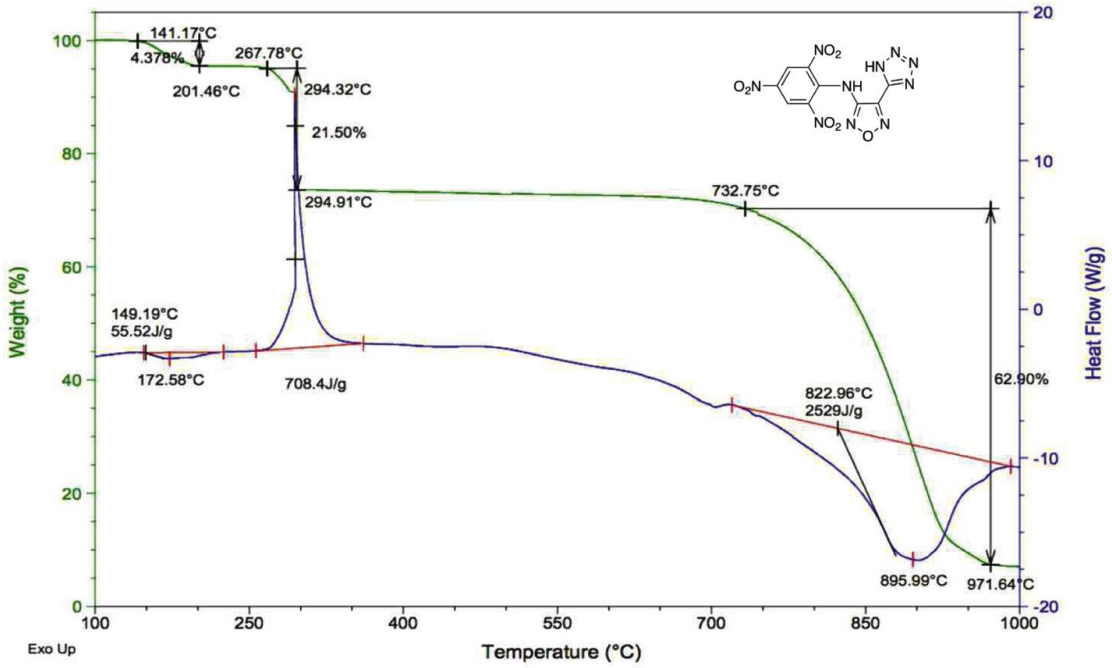

Figure A-10. TGA-DSC compound **41**

APPENDIX B
FLUORINE ON S_N2 AND E2 REACTIONS

Table B-1. Complete data for the 2nd order rate constants for *n*-alkyl iodide, bromide and tosylate and for benzyl bromide

Expt. No	Substrate	Solvent	Nucleophile	T, °C	10^5k_2 S_N2	10^5k_2 E2
1	*n*-$C_8H_{17}I$ [a]	CH_3OH	CH_3O^-	50	6.19 ± 0.24	0.469 ± 0.016
2	*n*-$C_8H_{17}I$	DMSO	CH_3O^-	23	35.7 ± 1.4	9.53 ± 0.42
3	*n*-$C_8H_{17}I$	DMSO	CH_3O^-	33	79.3 ± 3.7	21.5 ± 1.1
4 [b]	*n*-$C_8H_{17}I$	DMSO	CH_3O^-	50	276 ± 41	76.8 ± 13
5	*n*-$C_7H_{15}Br$	CH_3OH	CH_3O^-	50	3.95 ± 0.24	0.566 ± 0.032
6	*n*-$C_7H_{15}Br$	DMSO	CH_3O^-	18	9.56 ± 0.20	3.48 ± 0.075
7	*n*-$C_7H_{15}Br$	DMSO	CH_3O^-	23	14.6 ± 0.064	5.29 ± 0.009
8 [b]	*n*-$C_7H_{15}Br$	DMSO	CH_3O^-	50	116 ± 15	40.4 ± 1.1
9	*n*-$C_7H_{15}Br$	CH_3OH	N_3^-	50	6.89 ± 0.064	*no* [c]
10	*n*-$C_7H_{15}Br$	DMSO	N_3^-	18	101 ± 3.4	*no*
11	*n*-$C_7H_{15}Br$	DMSO	N_3^-	23	162 ± 3.5	*no*
12 [b]	*n*-$C_7H_{15}Br$	DMSO	N_3^-	50	1590 ± 300	*no*
13	*n*-$C_7H_{15}Br$	DMSO	I^-	25	61.8 ± 2.6	*no*
14	*n*-$C_7H_{15}Br$	DMSO	I^-	30	99.0 ± 3.7	*no*
15 [b]	*n*-$C_7H_{15}Br$	DMSO	I^-	50	563 ± 140	*no*
16 [d]	*n*-$C_8H_{17}OTs$	CH_3OH	CH_3O^-	50	12.7 ± 0.70	*no*
17 [d]	*n*-$C_8H_{17}OTs$	CH_3OH	N_3^-	50	23.8 ± 1.0	*no*
18	Ph-CH_2Br	CH_3OH	CH_3O^-	15	13.5 ± 0.59	- [e]
19	Ph-CH_2Br	CH_3OH	CH_3O^-	25	30.5 ± 1.8	-
20 [b]	Ph-CH_2Br	CH_3OH	CH_3O^-	50	188 ± 19	-
21	Ph-CH_2Br	DMSO	CH_3O^-	15	1020 ± 74	-
22	Ph-CH_2Br	CH_3OH	N_3^-	15	46.6 ± 0.64	-
23	Ph-CH_2Br	CH_3OH	N_3^-	25	103 ± 1.4	-
24 [b]	Ph-CH_2Br	CH_3OH	N_3^-	50	606 ± 20	-
25 [f]	Ph-CH_2Br	DMSO	N_3^-	15	7480 ± 250	-

[a] The kinetics of reactions of *n*-$C_7H_{15}I$ with azide could not be studied because of overlap of relevant peaks in the proton NMR; [b]These 2nd order rate constants were approximated for comparison purposes using the Eyring Equation; the given error was obtained by propagating that of the two data points; [c] *no* = not observed; [d] Reactions of *n*-$C_8H_{17}OTs$ in DMSO could not be studied kinetically because of overlap of relevant peaks in the proton NMR; [e] - (dash) means product not possible; [f] approximate, single point rate constant (56.8% of substrate consumed after 30 sec)

Table B-2. Complete data for the 2nd order rate constants for perfluoro-*n*-butylethyl bromide.

Expt. No.	Substrate	Solvent	Nuc	T, °C	10^5k_2 S_N2	10^5k_2 E2
5	*n*-$C_7H_{15}Br$	CH_3OH	CH_3O^-	50	3.95 ± 0.24	0.566 ± 0.032
26	*n*-$C_4F_9CH_2CH_2Br$	CH_3OH	CH_3O^-	10	*no* [a]	45.3 ± 1.0
27	*n*-$C_4F_9CH_2CH_2Br$	CH_3OH	CH_3O^-	20	*no*	93.5 ± 2.2
28 [c]	*n*-$C_4F_9CH_2CH_2Br$	CH_3OH	CH_3O^-	50	*no*	631 ± 61
6	*n*-$C_7H_{15}Br$	DMSO	CH_3O^-	18	9.56 ± 0.20	3.48 ± 0.075
29	*n*-$C_4F_9CH_2CH_2Br$	DMSO	CH_3O^-	18	*no*	8,580 [b]
9	*n*-$C_7H_{15}Br$	CH_3OH	N_3^-	50	6.89 ± 0.064	*no* [a]
30	*n*-$C_4F_9CH_2CH_2Br$	CH_3OH	N_3^-	50	0.823 ± 0.056	*no*
12 [c]	*n*-$C_7H_{15}Br$	DMSO	N_3^-	50	1590	*no*
31	*n*-$C_4F_9CH_2CH_2Br$	DMSO	N_3^-	18	8.530 ±.31	*no*
32	*n*-$C_4F_9CH_2CH_2Br$	DMSO	N_3^-	23	14.9 ± 0.64	*no*
33 [c]	*n*-$C_4F_9CH_2CH_2Br$	DMSO	N_3^-	50	227 ± 71	*no*

[a] *no* = not observed; [b] calculated on the basis that 61% of starting material had reacted after 30 seconds of reaction; [c] These 2nd order rate constants were approximated for comparison purposes using the Eyring Equation; the given error was obtained by propagating that of the two data points.

LIST OF REFERENCES

(1) Kitazume, T.; Yamazaki, T. Experimental Methods in Organic Fluorine Chemistry; 1 ed.; Kodansha: Tokyo-Japan, 1998.

(2) Chambers, R. D. Fluorine in Organic Chemistry; 1st ed.; Blackwell Publishing: USA, 2004.

(3) Singh, R. P.; Shereeve, J. M. Acc. Chem. Res. 2004, 37, 31.

(4) Sun, H.; DiMagno, S. G. J. Am. Chem. Soc. 2005, 127, 2050.

(5) Sun, H.; DiMagno, S. G. Chem. Commun. 2007, 528.

(6) Furuya, T.; Klein, J.; Ritter, T. Synthesis 2010, 11, 1804.

(7) Wang, X.; Mei, T.; Yu, J. J. Am. Chem. Soc. 2009, 131, 7520.

(8) Grushin, V. V.; Marshall, E. J. Organometallics. 2007, 26, 4997.

(9) Watson, D. A.; Su, M.; Teverovskiy, G.; Zhang, Y.; Garcia, J.; Kinzel, T.; Buchwald, S. Science. 2009, 325, 1661.

(10) Umemoto, T.; Singh, R. P.; Xu, Y.; Saito, N. J. Am. Chem. Soc. 2010, 132, 18199.

(11) Akiba, K.-y.; Lentz, D.; Seppelt, K. Chemistry of Hypervalent Compounds.; Wiley-VHC, Inc.: USA, 1999.

(12) Stump, B.; Eberle, C.; Schweizer, W. B.; Kaiser, M.; Brun, R.; Krauth-Siegel, R. L.; Lentz, D.; Diederich, F. ChemBioChem 2009, 10, 79.

(13) Sheppard, W. A. J. Am. Chem. Soc. 1962, 3064.

(14) Ye, C.; Gard, G. L.; Winter, R. W.; Syvret, R. G.; Twamley, B.; Shreeve, J. n. M. Org. Lett. 2007, 9, 3841.

(15) Kirsch, P.; Hahn, A. Eur. J. Org. Chem. 2005, 3095.

(16) Lim, D. S.; Choi, J. S.; Pak, C. C.; Welch, J. T. J. Pestic. Sci. 2007, 32, 255.

(17) Welch, J. T.; Lim, D. S. Bioorg. Med. Chem. 2007, 6659.

(18) Garg, S.; Shreeve, J. M. J. Mater. Chem. 2011, 21, 4787.

(19) R., C. J.; Ray, N. H.; Roberts, H. L. J. Chem. Soc. 1961.

(20) AttMohand, S.; Dolbier, W. R. Org. Lett. 2002, 4, 3013.

(21) Dolbier, W. R.; Ait-Mohand, S.; Schertz, T. D.; Sergeeva, T. A.; Cradlebaugh, J. A.; Mitani, A.; Gard, G. L.; Winter, R. W.; Thrasher, J. S. J. Fluorine Chem. 2006, 127, 1302.

(22) Sergeeva, T. A.; Dolbier, W. R. Org. Lett. 2004, 6, 2417.

(23) Dolbier, W. R.; Zheng, Z. J. Org. Chem. 2009, 74, 5626.

(24) Agrawal, J. P.; Hodgson, R. Organic Chemistry of Explosives; John Wiley & Sons: West Sussex, 2007.

(25) Fried, L. E.; Manaa, R.; Pagoria, P. F.; Simpson, R. L. Annu. Rev. Mater. Res. 2001, 31, 291.

(26) Kazandjian, L.; Danel, J. Propellants Explos. Pyrotech. 2006, 31, 20.

(27) Agrawal, J. P. Prog. Energy Combust. Sci. 1998, 24, 1.

(28) Sitzmann, M. E.; Gilligan, W. H.; Ornellas, D. L.; Thrasher, J. S. J. Energetic Mat. 1990, 8, 352.

(29) Sitzmann, M. E. J. Fluorine Chem. 1991, 195.

(30) Gao, H.; Ye, C.; Winter, R. W.; Gard, G. L.; Sitzmann, M. E.; Shreeve, J. M. Eur. J. Inorg. Chem. 2006, 3221.

(31) Ornellas, D. L. Propellants, Explosives, Pyrotechnics 1989, 14, 122.

(32) Dolbier, W. R.; Asghar, M. A.; Pan, H.; Celewicz, L. J. Org. Chem. 1993, 58, 1827.

(33) Dolbier, W. R.; Beach, W. F. J. Fluorine Chem. 2003, 122, 99.

(34) Ziegert, R. E.; Brase, S. Synlett. 2006, 13, 2119.

(35) Brase, S.; Dahmen, S.; Hofener, S.; Lauterwasser, F.; Kreis, M.; Ziegert, R. E. Synlett. 2004, 15, 2647.

(36) Dahmen, S.; Brase, S. Org. Lett. 2001, 3, 4119.

(37) Skultety, M.; Hubner, H.; Lober, S.; Gmeiner, P. J. Med. Chem. 2010, 53, 7219.

(38) Morisaki, Y.; Chujo, Y. Polym. Chem. 2011, 2, 1949.

(39) Valentini, L.; Mengoni, A.; Land, S.; Minuti, L.; Kenny, J. M. New J. Chem. 2006, 30, 939.

(40) Valentini, L.; Marrochi, A.; Seri, M.; Mengoni, A.; Meloni, F.; Tatichi, A.; Kenny, J. M. Thin Solid Films. 2008, 7193.

(41) Roche, A. J.; Dolbier, W. R. J. Org. Chem. 2000, 65, 5282.

(42) Dyson, P. J.; Humphrey, D. G.; McGradt, J. E.; Mingos, D. M.; Wilson, D. J. J. Chem. Soc., Dalton trans. 1995, 4039.

(43) Reich, H. J.; Cram, D. J. J. Am. Chem. Soc. 1969, 91, 3517.

(44) Dolbier, W. R.; Xie, P.; Zhang, L.; Xu, W.; Chang, Y.; Abboud, K. A. J. Org. Chem. 2008, 73, 2469.

(45) Zhang, L.; Ogawa, K.; Ghiviriga, I.; Dolbier, W. R. J. Org. Chem. 2009, 74, 6831.

(46) Battiste, M. A.; Duan, J.-X.; Zhai, Y.-A.; Ghiviriga, I.; Abboud, K. A.; Roitberg, A.; Shelton, G. R.; Dolbier, W. R. Tetrahedron Lett. 2002, 43, 7047.

(47) Roche, A. J.; Dolbier, W. R. J. Org. Chem. 1999, 64, 9137.

(48) Roche, A. J.; Canturk, B. J. Fluorine Chem. 2005, 126, 483.

(49) Wu, K.; Dolbier, W. R.; Battiste, M. A.; Zhai, Y. Mendeleev Commun. 2006, 16, 146.

(50) Hansch, C.; Leo, A.; Taft, R. W. Chem. Rev. 1991, 91, 165.

(51) Fruttero, R.; Boschi, D.; Fornatto, E.; Serafino, E.; Gasco, A.; Exner, O. J. Chem. Research (M). 1998, 2545.

(52) Dolbier, W. R. Guide to fluorine NMR for Organic Chemist.; John Wiley & Sons, Inc.: USA, 2009.

(53) Ernst, L.; Ibrom, K. Magn. Reson. Chem. 1997, 35, 868.

(54) Feiring, A. E. J. Org. Chem. 1983, 48, 347.

(55) Sheremetev, A. B.; Kulagina, V. O.; Aleksandrova, N. S.; Dmitriev, D. E.; Strelenko, Y. A. Propellants Explos. Pyrotech. 1998, 23, 142.

(56) Pagoria, P. F.; Lee, G. S.; Mitchell, A. R.; Schimidt, R. D. Thermochim. Acta. 2002, 187.

(57) Cannizzo, L. F.; Hamilton, S.; Highsmith, T. K.; Sanderson, A. J.; Zentner, B. A. Furazan-Based Energetic Ingredients., Thiokol propulsion, 1999.

(58) Zhang, C. J. Mol. Struct. THEOCHEM. 2006, 77.

(59) Kohsari, I.; Pourmortazavi, S. M.; Hajimirsadeghi, S. S. J. Therm. Anal. Calorim. 2007, 89, 543.

(60) Sheremetev, A. B.; Aleksandrova, N. S. Russ. Chem. Bull. International Ed. 2005, 54, 1715.

(61) Talawar, M. B.; Sivabalan, R.; Senthilkumar, N.; Prabhu, G.; Asthana, S. N. J. Hazard. Mater. 2004, 113, 11.

(62) Chavez, D.; Hill, L.; Hiskey, M.; Kinkead, S. J. Energetic Mat. 2000, 18, 219.

(63) Lim, C. H.; Kim, T. K.; Kim, K. H.; Chung, K. H.; Kim, J. S. Bull. Korean Chem. Soc. 2010, 31, 1400.

(64) Talawar, M. B.; Nair, J. K.; Pundalik, S. M.; Satput, R. S.; Venugopalan, S. J. Hazard. Mater. 2006, 136, 978.

(65) Beal, R. W.; Brill, T. B. Propellants Explos. Pyrotech. 2000, 25, 241.

(66) Coburn, M. D. J. Heterocycl. Chem. 1968, 5, 83.

(67) Sheremetev, A. B.; Makhova, N. N.; Friedrichsen, W. Adv. Heterocycl. Chem. 2001, 78, 67.

(68) Tselinskii, I. V.; Mel'nikova, S. F.; Vergisov, S. N. Chem. Heterocycl. Compd.(Engls. Transl.) 1981, 17, 228.

(69) Brill, T. B.; Williams, G. K. Combust. Flame. 1998, 114, 569.

(70) Sinditskii, V. P.; Sheremetev, A. B.; Aleksandrova, N. S. Thermochim. Acta 2008, 473, 25.

(71) Kiselev, V. G.; Gritsan, N. P. J. Phys. Chem. A. 2009, 113, 3677.

(72) Lesnikovich, A. I.; Ivashkevich, O. A.; Levchilk, S. V.; Balabanovich, A. I.; Gaponik, P. N.; Kulak, A. A. Thermochim. Acta. 2002, 388, 233.

(73) Paletsky, A. A.; Budachev, N. V.; Korobeinichev, O. P. Kinet. Catal. 2009, 50, 627.

(74) Silva, G.; Bozzelli, J. J. Org. Chem. 2008, 73, 1343.

(75) Paul, K. W.; Hurley, M. M.; Irikura, K. K. J. Phys. Chem. A 2009, 113, 2483.

(76) Andrianov, V. G.; Eremeev, A. V. Chem. Heterocycl. Compd. 1994, 30, 608.

(77) Wang, R.; Guo, Y.; Zeng, Z.; Twamley, B.; Shreeve, J. M. Chem. Eur. J. 2009, 15, 2625.

(78) Zelenin, A. K.; Trudell, M. L. J. Heterocycl. Chem. 1997, 34, 1057.

(79) Zelenin, A. K.; Trudell, M. L. J. Heterocycl. Chem. 1998, 35, 151.

(80) Kakanejadifard, A.; Saniei, A.; Delfani, F.; Farnia, M.; Najafi, G. R. J. Heterocycl. Chem. 2007, 44, 717.

(81) Willer, R. L.; Moore, D. W. J. Org. Chem. 1985, 50, 5123.

(82) Huttunen, K. M.; Leppanen, J.; Kemppainen, E.; Palonen, P.; Rautio, J.; Jarvinen, T.; Vepsalainen, J. Synthesis 2008, 3619.

(83) Sitzmann, M. E. J. Fluorine Chem. 1995, 70, 31.

(84) Katritzky, A. R.; Zhang, Y.; Singh, S. K. Synthesis. 2003, 18, 2795.

(85) Bowman, R. J. Chem. Soc. Perkin Trans. 1. 1982, 1897.

(86) Zhang, L.; Duan, J.; Xu, Y.; Dolbier, W. R. Tetrahedron Lett. 1998, 39, 9621.

(87) Clifford, A. F.; Shanzer, A. J. Fluorine Chem. 1976, 7, 65.

(88) Trasher, J. S.; Howell, J. L.; Clifford, A. F. Chem. Ber. 1984, 117, 1707.

(89) Sitzmann, M. E.; Gilligan, W. H.; US4,231,186 - 07/213,038: United States, 1989.

(90) Kleemann, G.; Seppelt, K. Chemische Berichte 1979, 112, 1140.

(91) Ray, N. H. J. Chem. Soc. 1963, 1440.

(92) Frisch, M. J. T., G. W.; Schlegel, H. B.; Scuseria, G. E.; Robb, M. A.; Cheeseman, J. R.; Montgomery, Jr., J. A.; Vreven, T.; Kudin, K. N.; Burant, J. C.; Millam, J. M.; Iyengar, S. S.; Tomasi, J.; Barone, V.; Mennucci, B.; Cossi, M.; Scalmani, G.; Rega, N.; Petersson, G. A.; Nakatsuji, H.; Hada, M.; Ehara, M.; Toyota, K.; Fukuda, R.; Hasegawa, J.; Ishida, M.; Nakajima, T.; Honda, Y.; Kitao, O.; Nakai, H.; Klene, M.; Li, X.; Knox, J. E.; Hratchian, H. P.; Cross, J. B.; Bakken, V.; Adamo, C.; Jaramillo, J.; Gomperts, R.; Stratmann, R. E.; Yazyev, O.; Austin, A. J.; Cammi, R.; Pomelli, C.; Ochterski, J. W.; Ayala, P. Y.; Morokuma, K.; Voth, G. A.; Salvador, P.; Dannenberg, J. J.; Zakrzewski, V. G.; Dapprich, S.; Daniels, A. D.; Strain, M. C.; Farkas, O.; Malick, D. K.; Rabuck, A. D.; Raghavachari, K.; Foresman, J. B.; Ortiz, J. V.; Cui, Q.; Baboul, A. G.; Clifford, S.; Cioslowski, J.; Stefanov, B. B.; Liu, G.; Liashenko, A.; Piskorz, P.; Komaromi, I.; Martin, R. L.; Fox, D. J.; Keith, T.; Al-Laham, M. A.; Peng, C. Y.; Nanayakkara, A.; Challacombe, M.; Gill, P. M. W.; Johnson, B.; Chen, W.; Wong, M. W.; Gonzalez, C.; and Pople, J. A.; Gaussian, In: Wallingford C, 2004.

(93) Putis, S. M.; Zubarev, V. Y.; Poplavskii, V. S.; Ostrovskii, V. A. Chem. Heterocycl. Compd. 2004, 40, 854.

(94) Autschbach, J.; Le-Guennic, B. J. Chem. Educ. 2007, 84, 156.

(95) Contreras, R. H.; Gotelli, G.; Ducati, L. C.; Barbosa, T. M.; Tormena, C. F. J. Phys. Chem. A. 2010, 114, 1044.

(96) Contreras, R. H.; Natiello, M. A.; Scuseria, G. E. Magn. Reson. Rev. 1985, 9, 239.

(97) Rae, I. D.; Staffa, A.; Diz, A. C.; Giribet, C. G.; Ruiz, M. C.; Contreras, R. H. 1987, 40, 1923.

(98) Krivdin, L. B.; Contreras, R. H. Annu. Rep. NMR Spectrosc. 2007, 61, 133.

(99) Soncini, A.; Lazzeretti, P. J. Chem. Phys. 2003, 119, 1343.

(100) Castillo, N.; Matta, C. F.; Boyd, R. J. J. Chem. Inf. Model. 2005, 45, 354.

(101) Contreras, R. H.; Ruiz, M. C.; Giribet, C. G.; Aucar, G. A.; Lobayan, R. J. Mol. Struct. THEOCHEM. 1993, 284, 249.

(102) Arnold, W. D.; Mao, J.; Sun, H.; Oldfield, E. J. Am. Chem. Soc. 2000, 122, 12164.

(103) Natiello, M. A.; Contreras, R. H. Chem. Phys. Lett. 1984, 104, 568.

(104) Contreras, R. H.; Peralta, J. E. Prog. Nucl. Mag. Res. Sp. 2000, 37, 321.

(105) Mallory, F. B.; Mallory, C. W.; Baker, M. B. J. Am. Chem. Soc. 1990, 112, 2577.

(106) Glendening, E. D.; Badenhoop, J. K.; Reed, A. E.; Carpenter, J. E.; Bohmann, J. A.; Morales, C. M.; Weinhold, F. NBO 5.0. Theoretical Chemistry Institute, University of Wisconsin, Madison. 2001.

(107) Gung, B. W.; Amicangelo, J. C. J. Org. Chem. 2006, 71, 9261.

(108) Gallivan, J. P.; Dougherty, D. A. Org. Lett. 1999, 1, 103.

(109) Lu, Y.; Zou, J.; Wang, Y.; Yu, Q. Int. J. Quantum Chem. 2007, 107, 1479.

(110) Haas, A.; Spitzer, M.; Lieb, M. Chem. Ber. 1988, 121, 1329.

(111) Wu, Y.-Z.; Deng, J.; Fang, X.; Chen, Q.-Y. J. Fluorine Chem. 2004, 125, 1415.

(112) Hine, J.; Ghirardelli, R. G. J. Org. Chem. 1958, 23, 1550.

(113) McBee, E. T.; Battershell, R. D.; Braendlin, H. P. J. Am. Chem. Soc. 1962, 84, 3157.

(114) Hine, J.; Thomas, C. H.; Ehrenson, S. J. J. Am. Chem. Soc. 1955, 77, 3886.

(115) Kabalka, G. W.; Varma, M.; Varma, R. S. J. Org. Chem. 1986, 51, 2386.

(116) Garcia-Martinez, A.; Osio-Barcina, J.; Rys, A. Z.; Subramanian, L. R. Synlett. 1993, 587.

(117) Bartberger, M. D.; Dolbier, W. R.; Lusztyk, J.; Ingold, K. U. Tetrahedron. 1997, 53, 9857.

(118) Moore, J. W.; Pearson, R. G. Kinetics and Mechanism; Jhon Wiley & Sons, Inc., 1981.

(119) Feuer, H.; Hooz, J. In the Chemistry of the Ether Linkage; Wiley: New York, 1967.

(120) Sekera, V. V.; Marvel, C. S. J. Am. Chem. Soc. 1933, 55, 345.

(121) Shirley, D. A.; Zietz, J. R.; Reedy, W. H. J. Org. Chem. 1953, 18, 378.

(122) Barry, J.; Bram, G.; Decodts, G.; Loupy, A.; Pigeon, P.; Sansoulet, J. Tetrahedron. 1984, 40, 2945.

(123) Hartman, S.; Roberson, R. E. Can. J. Chem. 1960, 38, 2033.

(124) Noyce, D. S.; Virgilio, J. A. J. Org. Chem. 1972, 37, 2643.

(125) Fuchs, R. L.; Cole, L. L. J. Am. Chem. Soc. 1973, 95, 3194.

(126) Alexander, R.; Ko, E. C.; Parker, A. J.; Broxton, T. J. J. Am. Chem. Soc. 1968, 90, 5049.

(127) Streitwieser, A. Chem. Rev. 1956, 56, 371.

(128) Patel, S. T.; Percy, J. M.; Wilkes, R. D. Tetrahedron. 1995, 51, 9201.

(129) Liu, S.; Hu, H.; Pedersen, L. G. J. Phys. Chem. A. 2010, 114, 5913.

(130) Dolbier, W. R.; Medinger, K. S.; Greenberg, A.; Liebman, J. F. Tetrahedron. 1982, 38, 2415.

(131) Kazemi, F.; Massah, A. R.; Javaherian, M. Tetrahedron. 2007, 63, 5083.

BIOGRAPHICAL SKETCH

Henry Martinez was born in Cali, Colombia. He received his B.S. in chemistry from Universidad del Valle in 2006 with an outstanding undergraduate research award. He came to study his Ph.D. in chemistry at the University of Florida under the supervision of Professor William R. Dolbier, Jr. in 2007, and will receive his Ph.D. in December 2011. Henry married his lovely wife, Paula, in Church in December of 2009.